

Impact of sorbitan esters and topical formulation containing sorbitan monostearate on the skin barrier function

Dissertation

der Mathematisch-Naturwissenschaftlichen Fakultät
der Eberhard Karls Universität Tübingen
zur Erlangung des Grades eines
Doktors der Naturwissenschaften
(Dr. rer. nat.)

vorgelegt von
Mag. Pharm. Hans Schönfelder
aus Chemnitz

Tübingen
2024

Gedruckt mit Genehmigung der Mathematisch-Naturwissenschaftlichen Fakultät der
Eberhard Karls Universität Tübingen.

Tag der mündlichen Qualifikation:

19.12.2024

Dekan:

Prof. Dr. Thilo Stehle

1. Berichterstatter/-in:

Prof. Dr. Dominique Jasmin Lunter

2. Berichterstatter/-in:

Prof. Dr. Rolf Daniels

Acknowledgments

First of all, I would like to thank Prof. Lunter, my supervisor, who made it possible for me to do this dissertation in the first place. Countless discussions and ideas led to this thesis in the end. However, people often forget the tasks alongside the dissertation that really help you move forward. I would like to thank you for the many trips in Germany and Europe, which I will remember forever. In addition, the intensive time together supervising and organizing the Praktikum.

I would also like to thank Prof. Daniels for his open ear and for reviewing my work. I will very much miss the various small conversations and discussions during the years.

Special thanks go to the hard-working helpers behind the scenes, especially Klaus and Irina, who made a significant contribution to this thesis. In addition, Bogu, Jutta, and Ingrid, were always supportive.

Many thanks go to my colleagues, who provided moral support throughout the entire dissertation and who supported me in difficult times, as well as some becoming co-authors.

My final thanks go to my family and fiancée, who have always believed in me and made it possible for me, both financially and in terms of content, to continue my education after graduation. My fiancée's tireless support and belief in me deserve special mention.

>> TUN – LEIDEN – LERNEN ! << aus Orestie (Όρέστεια) von Aischylos 458 v. Chr.

Table of Contents

Acknowledgments	I
Table of Contents.....	III
Abbreviations.....	IV
Zusammenfassung	IX
Summary	X
List of publications	XI
Personal contribution.....	XII
List of poster presentations.....	XIII
1. Introduction.....	1
1.1. Skin.....	1
1.1.1. SC	3
1.1.2. In-vitro/in-vivo skin analysis	4
1.1.3. Human and porcine skin.....	5
1.2. Trans-epidermal water loss (TEWL).....	5
1.3. CRS	8
1.4. Liquid chromatography-mass spectrometry (LC-MS).....	10
1.5. Ceramides.....	11
1.6. Sorbitan esters/emulsifiers	13
1.7. Basic therapy and cutaneous treatment.....	15
1.8. References.....	16
2. Objectives.....	25
3. Systematic investigation of factors, such as the impact of emulsifiers, which influence the measurement of skin barrier integrity by in-vitro trans-epidermal water loss (TEWL).....	26
4. Development and characterization of topical formulation for maintenance therapy containing sorbitan monostearate with and without PEG-100-stearate	34
5. Ceramides profiling of porcine skin and systematic investigation of the impact of sorbitan esters (SEs) on the barrier function of the skin	46

Abbreviations

%	Percentage
°C	Celsius degree
δ	Scissoring mode (Raman)
$\mu\text{g/mL}$	Microgram per milliliter
μl	Microliter
μm	Micrometer
μM	Micromole
ν	Stretching mode (Raman)
ω	Angular frequency
ANOVA	Analysis of variance
APCI	Atmospheric pressure chemical ionization
API	Active pharmaceutical ingredient
APPI	Atmospheric pressure photoionization
AUC	Area under the curve
CCD	Charge-coupled device
CER	Ceramide
CHOL	Cholesterol
CoA	Certificate of Analysis
cm	Centimeter
cm^{-1}	Per centimeters
CRR	Cosmic ray removal
CRS	Confocal Raman spectroscopy
CRM	Confocal Raman microscopy

e.g.	exempli gratia (for example)
et al.	Et alia, and others
EMA	European Medicines Agency
ESI	Electrospray ionization
FDA	Food and Drug Administration
FFA	Free fatty acid
FOD	factors of difference
FWHM	Full width of half maximum
g	Gram
G	Gauge
G'	Storage modulus
G''	Loss modulus
g/cm ²	Gram per square centimeter
g/cm ³	Gram per cubic centimeter
g · m ² · h ⁻¹	Gram times square meter per hour (TEWL unit)
g/mL	Gram per milliliter
g/mm	Grooves per milliliter
h	Hour
HCl	Hydrochloric acid
HEK	Human embryonic kidney
HLB	Hydrophilic lipophilic balance
HPLC	High performance liquid chromatography
HWN	High wavenumber
i.e.	id est (in other words)
in.	Inch

kg	Kilogram
LC-MS	Liquid chromatography-mass spectrometry
LD ₅₀	Lethal dose 50
LOD	Limit of detection
LOQ	Limit of quantification
LPP	Long periodicity phase
LVE	Linear viscoelastic
MCT	Middle chain triglycerides
min	Minute
min.	Minimum
mL	Milliliter
mm	Millimeter
m/m %	Percentage by mass
mM	Millimole
mg	Milligram
MRM	Multiple reaction monitoring
MS	Mass spectrometry
mW	Milliwatt
m/z	Mass-to-charge ratio
n	Number
NA	Numerical aperture
NHEK	Normal human-derived epidermal keratinocytes
nm	Nanometer
o/w	Oil in water
p	p-value

PBS	Phosphate buffer saline
PCA	Principal component analysis
PEG	Polyethylene glycol
PEGylated	Polyoxyethylated
pH	Negative log of activity of hydrogen ions
Pharm. Eur.	European Pharmacopoeia
po.	Pouce French inch
R ²	Correlation coefficients
rad · s ⁻¹	Radiant per second
ref.	Reference
RH	Relative humidity
RHE	Reconstructed human epidermis
RP	Reversed phase
rpm	Revolutions per minute
RSD	Relative standard deviation
s	Second
SC	Stratum corneum
SD	Standard deviation
SE	Sorbitan ester
SLS	Sodium lauryl sulfate
SPP	Short periodicity phase
SRM	Selected reaction monitoring
SubBG	Background subtraction
SV	Saponification value
t	Time

TAG	Triacyl glycerides
TEWL	Trans-epidermal water loss
USP	United States Pharmacopoeia
v/v %	Percentage by volume
w/o	Water in oil

Zusammenfassung

Die Hautforschung bietet ein breites Spektrum an Methoden mit vielen Herausforderungen. In der folgenden Arbeit lag der Schwerpunkt auf der Wirkung von Emulgatoren auf die Schweinehaut.

Die Möglichkeiten der TEWL-Messung (trans-epidermalen Wasserverlust) wurden untersucht. Es wurde ein Protokoll für In-vitro-Messungen in Schweinehaut entwickelt. Einige Emulgatoren wie S20 (PEG-20 Stearylether) und C20 (PEG-20 Cetylether) zeigten nachteilige Auswirkungen, während S40 (PEG-40 Stearylether), S100 (PEG-100 Stearylether), SE 60 (Sorbitanmonostearat), SE 80 (Sorbitanmonooleat), Cholesterin und Lecithin keine zeigten.

Es wurde ein multimodaler Ansatz entwickelt, um die Auswirkungen von Emulgatoren auf die Hautbarrierefunktion zu analysieren. TEWL, CRS (konfokale Raman-Spektroskopie) und LC-MS (Flüssigchromatographie-Massenspektrometrie) wurden kombiniert, um die Auswirkungen von Sorbitan-Estern auf das Stratum corneum von Schweinen zu analysieren. Die Bestimmung der Lipide mit CRS und LC-MS bot die Möglichkeit, die Ceramide des SC einzeln zu analysieren und ein spezifisches Ceramidprofil für jede Probe zu erhalten. Sorbitanester zeigten keine nachteiligen Auswirkungen auf die Hautbarrierefunktion, SLS hingegen schon.

Formulierungen für die Basistherapie, die Sorbitanmonostearat und PEG-(Polyethylenglykol) 100 Stearylether enthalten, wurden entwickelt und auf Schweinehaut in-vitro getestet. Zunächst wurden die Formulierungen mittels Rheologie und polarisierter Lichtmikroskopie auf ihre Stabilität geprüft. Anschließend wurden die Auswirkungen auf die Barrierefunktion der Schweinehaut durch TEWL und Pyraninfärbung analysiert, um die Lipidaufnahme durch Fluoreszenzlichtmikroskopie darzustellen. Es zeigte sich, dass die entwickelten Formulierungen Lipide an die SC lieferten, die vor der Untersuchung teilweise extrahiert worden waren. Dies unterstreicht, wie wichtig es ist, topische Formulierungen im Hinblick auf ihre tatsächliche Wirkung auf der Haut zu testen. Die Wirksamkeit dieser Formulierungen zur Behandlung von Hautkrankheiten ist ein wichtiger Parameter für die Basistherapie.

Summary

Skin research offers a wide range of methods with many challenges. In the following thesis, the main focus was the effect of emulsifiers on porcine skin.

The opportunities provided by TEWL (trans-epidermal water loss) measurements were investigated. A protocol was developed for measuring in-vitro in porcine skin. Some emulsifiers, like S20 (PEG-20 stearyl ether) and C20 (PEG-20 cetyl ether) showed adverse effects, while S40 (PEG-40 stearyl ether), S100 (PEG-100 stearyl ether), SE 60 (Sorbitan monostearate), SE 80 (Sorbitan monooleate), cholesterol and lecithin showed none.

A multimodal approach was developed to analyze the impact of emulsifiers on the skin barrier function. TEWL, CRS (confocal Raman spectroscopy), and LC-MS (liquid chromatography-mass spectrometry) were combined to analyze sorbitan esters effects on porcine SC (stratum corneum). The determination of lipids with CRS and LC-MS offered the possibility to analyze the SC's ceramides individually and to obtain a specific ceramide profile for each sample. Sorbitan esters showed no adverse effects on the skin barrier function whereas SLS did.

Formulations for basic therapy containing sorbitan monostearate and PEG—(polyethylene glycol) 100 stearyl ether were developed and tested on porcine skin in-vitro. Initially, the formulations were tested for its stability by rheology and polarized light microscopy. Afterward, the effects on porcine skin barrier function were analyzed by TEWL and pyranine staining to image the lipids uptake by fluorescent light microscopy. It was shown that the developed formulations delivered lipids to the SC that had been partially lipid extracted prior to the investigation. This underlines the importance of testing topical formulations with respect to their real effects on the skin. The effectiveness of these formulations for treatment of skin diseases is an important parameter for basic therapy.

List of publications

The work presented in the thesis has been published in international peer-reviewed journals. Three research papers were published to fulfill the requirement of this cumulative dissertation.

Publications related to the dissertation

Publication 1

Schoenfelder, H., Liu, Y., Lunter*, D.J., 2023. Systematic investigation of factors, such as the impact of emulsifiers, which influence the measurement of skin barrier integrity by in-vitro trans-epidermal water loss (TEWL). *Int J Pharm* 638, 122930. <https://doi.org/10.1016/J.IJPHARM.2023.122930>

Publication 2

Schoenfelder, H., Wiedemann, Y., Lunter*, D.J., 2024. Development and characterization of topical formulation for maintenance therapy containing sorbitan monostearate with and without PEG-100-stearate. *Int J Cosmet Sci* 00, 1–11. <https://doi.org/10.1111/ics.13023>

Publication 3

Schoenfelder, H., Reuter, M., Evers, D.-H., Herbig, M.E., Lunter*, D.J., 2024. Ceramides profiling of porcine skin and systematic investigation of the impact of sorbitan esters (SEs) on the barrier function of the skin. *Mol. Pharmaceutics*, submitted

* Corresponding author

Personal contribution

Publications related to the thesis

Publication 1

Schoenfelder, H., Liu, Y., Lunter, D.J., 2023. Systematic investigation of factors, such as the impact of emulsifiers, which influence the measurement of skin barrier integrity by in-vitro trans-epidermal water loss (TEWL). *Int J Pharm* 638, 122930. <https://doi.org/10.1016/J.IJPHARM.2023.122930>

Idea: Dominique Jasmin Lunter and Hans Schönfelder

Study design: Hans Schönfelder and Dominique Jasmin Lunter

Experiment: Hans Schönfelder, Yali Liu

Evaluation: Hans Schönfelder and Dominique Jasmin Lunter

Manuscript: Hans Schönfelder and Dominique Jasmin Lunter

Publication 2

Schoenfelder, H., Wiedemann, Y., Lunter, D.J., 2024. Development and characterization of topical formulation for maintenance therapy containing sorbitan monostearate with and without PEG-100-stearate. *Int J Cosmet Sci* 00, 1–11. <https://doi.org/10.1111/ics.13023>

Idea: Dominique Jasmin Lunter and Hans Schönfelder

Study design: Hans Schönfelder and Dominique Jasmin Lunter

Experiment: Hans Schönfelder, Yvonne Wiedmann

Evaluation: Hans Schönfelder and Dominique Jasmin Lunter

Manuscript: Hans Schönfelder and Dominique Jasmin Lunter

Publication 3

Schoenfelder, H., Reuter, M., Evers, D.-H., Herbig, M.E., Lunter*, D.J., 2024. Ceramides profiling of porcine skin and systematic investigation of the impact of sorbitan esters (SEs) on the barrier function of the skin. *Mol. Pharmaceutics*, submitted

Idea: Dominique Jasmin Lunter and Hans Schönfelder

Study design: Hans Schönfelder and Dominique Jasmin Lunter

Experiment: Hans Schönfelder, Moritz Reuter, Dirk-Heinrich Evers, Michael E. Herbig

Evaluation: Hans Schönfelder and Dominique Jasmin Lunter

Manuscript: Hans Schönfelder, Moritz Reuter, Dirk-Heinrich Evers, Miachel E. Herbig, Dominique Jasmin Lunter

List of poster presentations

Poster presentations in academic conferences during the period of this thesis are listed as follows.

Poster presentation 1

14th World Meeting on Pharmaceutics, Biopharmaceutics and Pharmaceutical Technology (PBP), March 2024, Vienna.

In-vitro and in-vivo analysis of skin barrier function as affected by pharmaceutical emulsifiers

Hans Schönfelder, Moritz Reuter, Annette Gaiser, Sebastian Volc, Dominique Jasmin Lunter*

Poster presentation 2

Gesellschaft für Dermopharmazie Annual Meeting, November 2023, Wiesbaden.

Impact of pharmaceutically-used emulsifiers on in-vitro and in-vivo skin barrier function by trans-epidermal water loss (TEWL), confocal Raman spectroscopy (CRS), and ceramide profiling by liquid chromatography-mass spectrometry (LC-MS)

Hans Schönfelder, Moritz Reuter, Annette Gaiser, Sebastian Volc, Dominique Jasmin Lunter*

Poster presentation 3

Deutsche Pharmazeutische Gesellschaft (DPhG) Annual Meeting, October 2023, Tübingen.

Characterization of trans-epidermal water loss (TEWL), skin hydration, erythema index, and skin-pH in in-vivo human skin after exposure to pharmaceutical emulsifiers

Hans Schönfelder, Moritz Reuter, Annette Gaiser, Sebastian Volc, Dominique Jasmin Lunter*

Poster presentation 4

APGI Skin and Formulation 6th Symposium, October 2023, Nantes.

Systematic investigation of sorbitan esters on in-vitro porcine skin measured by trans-epidermal water loss (TEWL) and confocal Raman spectroscopy (CRS)

Hans Schönfelder, Moritz Reuter, Dominique Jasmin Lunter*

Poster presentation 5

Deutsche Pharmazeutische Gesellschaft (DPhG) Annual Meeting, September 2022, Marburg.

Impact of pharmaceutical emulsifiers on ex-vivo trans-epidermal water loss (TEWL)

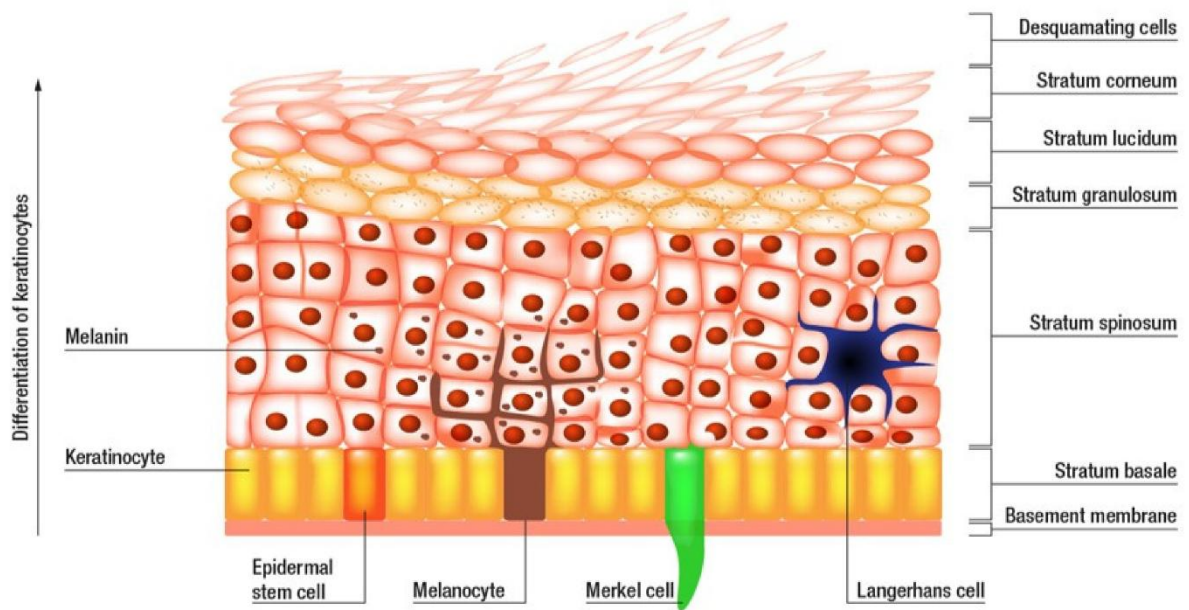
Hans Schönfelder, Yali Liu, Dominique Jasmin Lunter*

* Corresponding author

1. Introduction

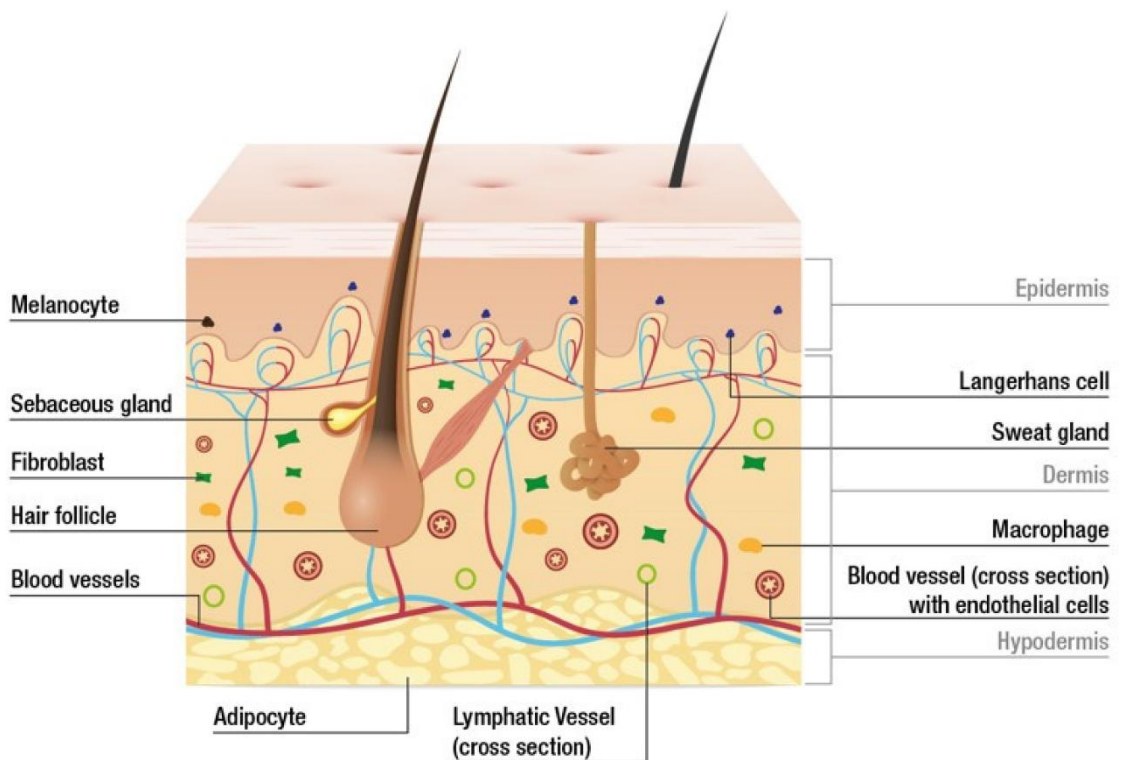
1.1. Skin

The skin is the largest human organ and is constructed from the outer layer of the epidermis over the dermis to the subcutis (Byrd et al., 2018). It is the interface between the body and the environment. The mechanical border restricts water loss and protects the body from external xenobiotics or microorganisms (Pasparakis et al., 2014). The epidermis is subdivided into the stratum corneum, stratum granulosum, spinous cell, and basal layers, as seen in Figure 1. It mainly comprises sheets of keratinocytes but also contains non-epithelial cells, including antigen-presenting dendritic Langerhans cells, melanocytes, and Merkel cells (Abdo et al., 2020). There are three distinct layers of nucleated cells. Every 28 days, fully differentiated cuboidal basal keratinocytes with large nuclei and phospholipid membrane migrate apically from the basal layer through the spinous and granular layers (Abdo et al., 2020; Usui et al., 2008). Among their functions, keratinocytes proliferate to heal wounds, transport urea, and water through aquaporins, receive melanin from melanocytes, control water permeability, and participate in congenital and flexible immunity through antimicrobial peptide secretion and the presence of Langerhans cells (Abdo et al., 2020; ter Horst et al., 2018). The dermis contains fibroblasts, fibrocytes, and structural cells of blood and lymph vessels (Pasparakis et al., 2014). It assures the flexibility of the skin and temperature maintenance of the body. It consists mainly of collagen fibers, blood vessels, sensory nerves, and lymphatic channels, as seen in Hofmann et al. (Hofmann et al., 2023).



Credit: iStock/Itz
Edited by JOHANNELM RESEARCH

Figure 1 shows human skin stratum layers, such as stratum corneum, lucidum, granulosum, spinosum, and basale, containing Langerhans cells, Merkel cells, melanocytes, stem cells, keratinocytes, and melanin (Hofmann et al., 2023).



Credit: iStock/Paladaj
Edited by JOHANNELM RESEARCH

Figure 2 shows the structural details of human skin. It consists of three layers: epidermis, dermis, and hypodermis. The epidermis acts as a barrier to invasion and regulates water leaving the body. The dermis mainly consists of an extracellular matrix produced by fibroblasts (Hofmann et al., 2023).

1.1.1. SC

The stratum corneum (SC) is part of the epidermis and connects the skin surface with the environment (Das and Olmsted, 2016). It is the skin's barrier and is built up by corneocytes and a lipid matrix measuring about 20 μm (Das and Olmsted, 2016). The lipid matrix is essential for trespassing of xenobiotics. Every dermal product, with or without active pharmaceutical ingredient (API), aims to pass through this first layer. Therefore, the knowledge of the structure of the SC is helpful in understanding this process (Van Smeden et al., 2014). Corneocytes contain eighty percent keratin, the primary protein structure in keratinocytes. Keratins are arranged in clusters, are fibrous, and are products of the intermediate filament gene family (Jiao et al., 2022). Corneocytes are a product of the proliferation of keratinocytes. The keratinocytes undergo sequential differentiation with death by cornification. The cornification starts with forming an intracellular keratin network, continues with the cornified envelopes' assembly with the cornified lipid envelope, and ends with the selective degradation of corneodesmosomes (Évora et al., 2021). Cornified envelopes and corneodesmosomes are responsible for the mechanical strength and resistance of the SC. The filaments are aligned into disulfide cross-linked macrofibres under the influence of filaggrin (Abdo et al., 2020; Pekny and Lane, 2007). The SC contains lipids from the classes ceramides (CERs), cholesterol (CHOL), and free fatty acids (FFAs) (Bouwstra et al., 2021). The intercellular lipids are arranged in layers with two coexisting lamellar phases: a 13 nm long-periodicity phase (LPP) and a 6 nm short-periodicity phase (SPP) (Beddoes et al., 2018). The possible arrangements of lateral organization shown in Figure 3 are very dense as an orthorhombic structure, less dense as a hexagonal structure, and disordered as a liquid state (Janssens et al., 2012). The SC lipids are the pivotal part of the SC, forming the skin's barrier to the environment. Ceramides regulate proliferation, differentiation, and apoptosis. They form multilamellar lipid membranes between corneocytes and the SC (Vavrova et al., 2017). All lipids prevent water loss from the body and penetration of undesirable substances, allergens, and microbes from the environment (Bouwstra et al., 2002). When SC-lipids are extracted by substances or reduced by diseases, the natural barrier function is compromised. Consequently, the skin loses water and is more susceptible to damage (Bouwstra et al., 2021; Machado et al., 2010). Van Smeden et al. documented an overview of different skin diseases that affect the SC and its lipid

composition and structural changes. Lamellar ichthyosis, psoriasis, Netherton (ichthyosis congenita), and atopic dermatitis show changes to the lipid structure and altered LPP, shorter lamellar periodicities, and with the exception of psoriasis, a reduction in orthorhombicity. Chanarin-Dorfman (Excessive accumulation of triglyceride) showed the presence of non-lamellar lipid domains. In the case of lipid composition, lamellar ichthyosis had a reduction of ceramides NP and EOS, psoriasis had a reduction of ceramides EOP, NP, and AP and an increase in ceramides AS and NS. Netherton showed a reduction of ceramides EOS, EOP, EOH, EOdS, and NP and an increase in short-chain lipids and unsaturated lipids. Atopic dermatitis reduced ceramides EOS, EOP, EOH, and EOdS and increased ceramides AS, AH, AP, AdS, short-chain lipids, and unsaturated FFAs. Chanarin-Dorfmann showed a reduction in Acyl-Ceramides and increased TAGs (Triacylglycerides) (Van Smeden et al., 2014).

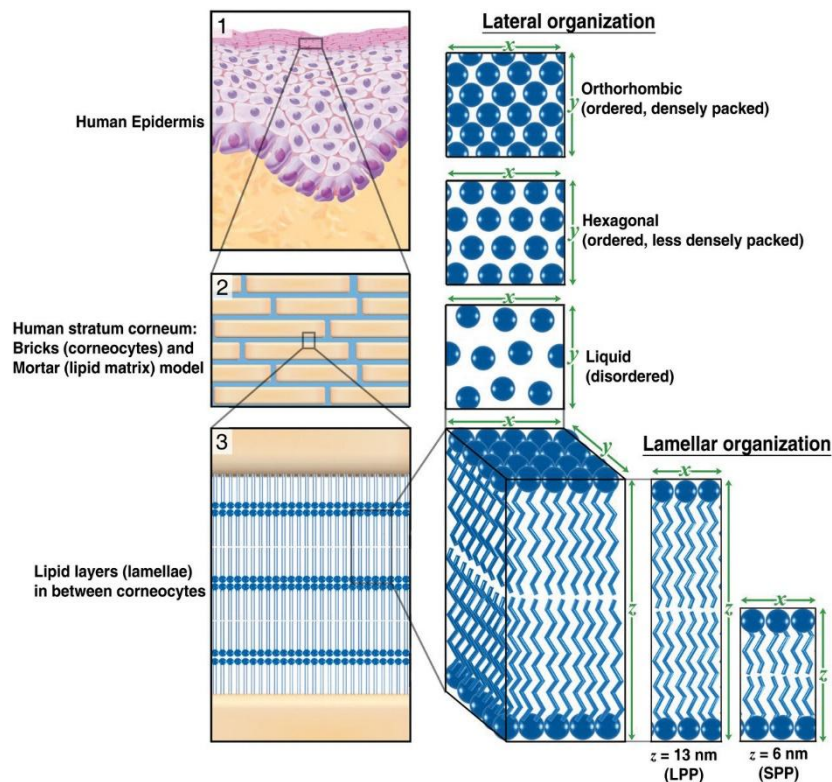


Figure 3 Lateral structure in SC: ordered and densely packed as orthorhombic, ordered and less densely packed as hexagonal, and disordered as liquid. The lamellar structure is divided into the long-periodicity phase (LPP) and the short-periodicity phase (SPP) (Janssens et al., 2012).

1.1.2. In-vitro/in-vivo skin analysis

In-vitro skin analysis is an easy way to analyze skin or SC. Ex-vivo skin samples are often accessible and can be stored in a frozen state. Ex-vivo samples themselves are not entirely equivalent to live humans or animals. With respect to prolonged treatment or incubation times, the samples need to be considered carefully as they lack blood or

lymphatic flow, and skin regeneration processes are also absent (Schoenfelder et al., 2023). In-vivo skin analysis is more challenging because of ethical issues, government regulations, and higher costs. The analysis in living animals is problematic, even for small mammals like rodents. Ethical aspects should also be considered. In contrast to in-vitro studies, the results are more transferrable, because of the characteristics of living skin such as temperature control, e.g., sweating. Rodents are excluded, because their skin is different from human skin.

1.1.3. Human and porcine skin

Human and porcine skin are primarily utilized for different in-vitro and in-vivo skin analysis methods. For in-vitro skin tests, porcine skin is used mainly for skin analysis because it can be delivered quickly and the skin is not heat treated from butchers (Hopf et al., 2020). The skin of porcine ears is comparable in thickness, e.g., SC, hairiness, e.g., hair follicles, hair growth, structure, and histology. Other areas of porcine skin differ more from human skin (Jacobi et al., 2007). Ex-vivo human studies are also possible, but they also lack living skin characteristics in the same way as porcine skin. The purchase of human tissues depends on the availability and is more difficult because of higher ethical restrictions. In-vivo porcine studies are rare and expensive. In-vivo human studies are performed in dermatological clinics or must be accompanied by dermatologists which makes them expensive as well. Nevertheless, data collection is more accessible after managing the ethical protocols. Human and porcine skin equivalence is proven and accepted (Barbero and Frasch, 2009; Jacobi et al., 2007; Tfaili et al., 2012). Barbero and Frasch compared porcine skin with human skin for in-vitro percutaneous penetration using the factors of difference (FOD). They considered that most of the porcine results were comparable to the human results. Jacobi et al. compared the different donors histologically and suggested using porcine skin, e.g., for percutaneous penetration. Tfaili et al. examined the difference of skin by Raman microscopy and suggested porcine skin as equivalent, with only minor differences in deep depth measurements.

1.2. Trans-epidermal water loss (TEWL)

Spontaneous water exchange between skin and ambient atmosphere is known as trans-epidermal water loss. The barrier to water loss is the SC (Endo et al., 2007). Water constantly leaves the body via the skin pathway from the dermis and epidermis through the SC to the skin surface (Akdeniz et al., 2018; Kottner et al., 2013).

Functional and healthy skin only evaporates tiny amounts, e.g., approx. $9.5 \text{ g}\cdot\text{m}^{-2}\cdot\text{h}^{-1}$ on the forearm (Akdeniz et al., 2018). Diseased skin loses much more water; thus, higher TEWL values indicate skin barrier impairment. Montero-Vilchez et al. showed in a cross-sectional study that, for example, in psoriatic skin, TEWL rises from 11.86 to $20.75 \text{ g}\cdot\text{m}^{-2}\cdot\text{h}^{-1}$, and in atopic dermatitis, TEWL rises from 13.75 to $31.67 \text{ g}\cdot\text{m}^{-2}\cdot\text{h}^{-1}$ (Montero-Vilchez et al., 2021).

TEWL is a standard method in dermatology for investigating skin diseases. The principle is based on Fick's law (Argatov et al., 2022; Endo et al., 2007; Schwindt et al., 1998). The calculations are based on measuring the water vapor pressure gradient at the skin surface by the difference of two distinct points aligned perpendicularly to the skin surface. The vapor pressure is calculated as the product of relative humidity and saturated vapor pressure depending on the temperature. Capacitive sensors measure the relative humidity, and fast thermistors measure the temperature (Du Plessis et al., 2013). When the skin barrier function is negatively affected, water loss from the body increases, and more water flows through the probe. The consequence is an increasing TEWL value. Multiple market instruments exist for in-vitro and in-vivo examinations (Du Plessis et al., 2013). For in-vitro measurements, two central systems exist: open-chamber and closed-chamber systems (Du Plessis et al., 2013; Pinnagoda et al., 1990). According to Steiner et al., open-chamber systems are restricted to measuring high values, and closed-chamber systems are less sensitive to differences in the lower range (Steiner et al., 2011). For the investigations in this thesis, an open-chamber system was used with a specially designed probe for Franz diffusion cells. The probe represents the donor chamber of a typical Franz diffusion cell; the setup is shown in Figure 4. The TEWL itself is commonly used for skin analysis, for example, to measure one of the porcine in-vitro macroscopic barrier properties that have an impact on the API flux which is influenced by different solvent systems or penetration enhancers (Levang et al., 1999), in-vitro microneedle influences (Gomaa et al., 2010), hair removal methods (Pany et al., 2018) or in-vivo for analysis of, for example o/w emulsions with different emollients (Gore et al., 2020), nanoparticles (Pereira-Leite et al., 2023), in-vivo microneedle arrays (Daugimont et al., 2010), the different relationship to skin temperature and TEWL in patients with psoriatic and eczematic skin in contrast to healthy skin (Grice et al., 1975), or topical oil application in infants (Nangia et al., 2015).



Figure 4 Franz diffusion cell with open-chamber probe for TEWL measurements.

For in-vivo testing, there is a probe with 30 sensors available, which detects the TEWL of human beings (Courage & Khazaka electronic GmbH, 2022a).

Regarding skin characterization by medical practitioners, other parameters can also be detected in humans (Gonzalez-Bravo et al., 2022; Herrero-Fernandez et al., 2022). For example, skin hydration is another parameter that the capacitive measurement principle can be applied to, which enables the amount of water in the skin to be calculated. The measuring principle is based on the capacitance measurement of a dielectric medium, the SC. With water having a higher dielectric constant, the dielectric properties change with increasing hydration (Courage & Khazaka electronic GmbH, 2022b). The erythema index can show skin irritations, such as red skin. Low values represent intact skin, whereas high values indicate skin irritation. The measurement is based on absorption and reflection. The probe emits three specific light wavelengths. A receiver detects the light reflected by the SC. The wavelengths of hemoglobin (558 nm and 660 nm) are used to see the erythema index (Courage & Khazaka electronic GmbH, 2022c). The third wavelength is used to investigate the melanin content of the skin. A pH probe also measures the skin's pH. Healthy skin pH on human forearms is between 4.5 and 5.5 (Lambers et al., 2006). Generally, diseased skin tends to have a neutral or basic pH (Ali and Yosipovitch, 2013). The sebum of the skin is

another factor of skin health. It lubricates the skin and controls the physiological acid skin milieu with resistance to pathogens (Schmid-Wendtner and Korting, 2006). It can be sampled on the forehead or scalp by a parchment-like film and then photometrically measured (Crowther, 2016).

1.3. CRS

Confocal Raman spectroscopy (CRS) is a non-destructive method for skin analysis (Orlando et al., 2021). Raman spectroscopy is based on the Raman effect. The wavelength of a small fraction of scattered radiation differs from that of monochromatic incident radiation. Its basis is the inelastic scattering of incident radiation due to molecules vibrating under its influence. Raman spectroscopy is a scattering technique (Bumrah and Sharma, 2016). A confocal Raman spectroscope has a microscope objective, focusing a laser beam to a small focal volume. Raman-scattered photons are collected by the same objective and pass through a confocal aperture, letting only those photons generated near the beam focus pass and guiding them to the detector via an optical fiber (Everall, 2010). Different objectives, like metallurgic or immersion, are available (Everall et al., 2007; Liu and Lunter, 2021; Lunter, 2017). For the resolution of CRS, the laser wavelength and the objective numerical aperture (NA) determine the size of the laser focus, and the spectrometer's pinhole diameter determines the degree of confocality by directing scattered light into the spectrometer (Lunter, 2016). This thesis used a 100x objective with 0.9 NA with a laser power of 10 mW and a theoretical resolution of 1 μm . In CRS, green (532 nm) and near-infrared (785 nm) lasers are often used (Liu and Lunter, 2022). The green laser was used in this thesis due to the higher intensity of the Raman spectrum at the SC surface, whereas the near-infrared laser has a higher penetration depth into the SC.

From the Raman spectrum it is possible to detect the amount of lipids in the SC, in addition the lipid conformation can also be examined (Choe et al., 2016). These are two critical parameters that characterize skin physiology after exposure to emulsifiers or other substances. The switch from orthorhombic to hexagonal lipid conformation which is detectable by CRS reveals specific information about the skin barrier's functionality. The thickness of the SC is also measurable by CRS (Böhling et al., 2014; Lee et al., 2018). Reduced SC thickness indicates lipid loss and impaired skin barrier function. These three main pieces of information obtained from CRS measurements are essential and a promising way to characterize skin.

Additionally, using CRS for skin penetration studies of APIs or model drugs is widespread (Jung et al., 2022; Vukosavljevic et al., 2017). This method offers the opportunity to detect the analyzed molecule spatially resolved over the depth of the SC. In chromatographic methods, the samples are often obtained by tape stripping. The amount of SC sticking on the tape strips varies. The detected amount of lipids differs and depends to some extent on the tape stripping. For CRS, it is possible to detect an API throughout the first layers of the SC and calculate a penetration profile of the API (Kourbaj et al., 2023; Krombholz et al., 2022a, 2022b).

The Raman spectrum is presented as an intensity-versus-wavelength shift and is mainly divided into the high wavenumber (HWN) region and the fingerprint region shown in Figure 5. The HWN region, around 2800 to 3030 cm^{-1} , is one area where it is possible to calculate the lipid content at 2830 - 2910 cm^{-1} . The lipid content is then normalized to the signal of the homogeneously distributed keratin to account for inter- and intra-sample variability. The so-called keratin peak is located at 2920 - 2960 cm^{-1} . In the fingerprint region the lipids occur around 1425 to 1490 cm^{-1} and gives the opportunity to calculate them. The amide-1-mode derived from keratin located at 1630 to 1710 cm^{-1} is used for normalization. For lipid conformation, the trans-gauche-trans ratio is analyzed. Two peaks of trans conformation (1060 around 1057 to 1063 and 1130 around 1127 to 1133 cm^{-1}) represent the ordered state, and one peak of gauche conformation (1080 around 1074 to 1086 cm^{-1}) represents the disordered state; all three are used to build the ratio by the division of gauche over the addition of both trans values. A high value shows a disordered state, whereas low values show an ordered state (Choe et al., 2016; Snyder et al., 1978; Williams et al., 1994).

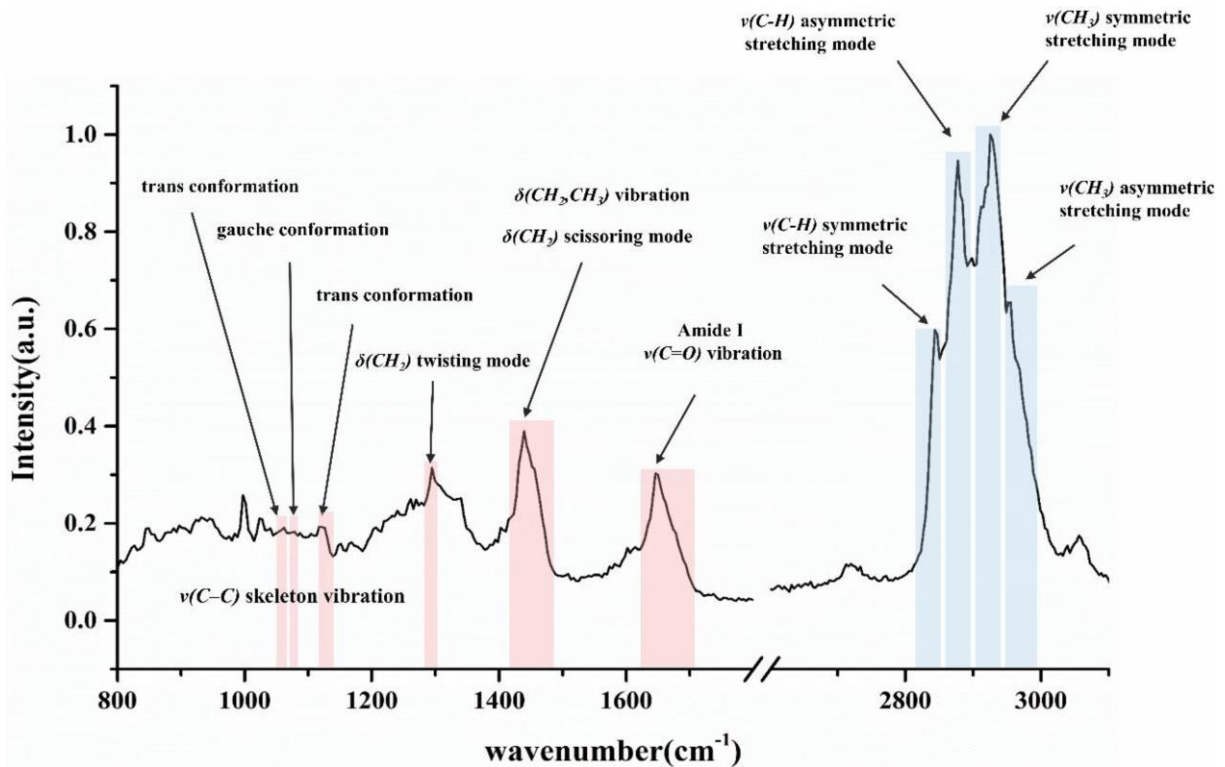


Figure 5 CRS spectrum of porcine skin with fingerprint (left) and high wavenumber region (right) (Liu and Lunter, 2020).

1.4. Liquid chromatography-mass spectrometry (LC-MS)

Chromatography is often used in skin analytics. Recently, methods have been developed to investigate the SC, from either humans or animals, investigating its chemical compounds, such as ceramides, fatty acids, and cholesterol (Bakar et al., 2022; Groen et al., 2011; Morris et al., 2022). From an overall view of total ceramide contents (Van Smeden et al., 2014) to detailed analyses of every single ceramide class and chain lengths of fatty and sphingoid side chains (Kawana et al., 2020; Łuczaj et al., 2021, 2020). Additionally, cholesterol and fatty acids were detected and quantified. These methods can supplement, for example, TEWL or CRS measurements or can be used independently.

The LC-MS analysis offers several technical variants regarding LC or MS systems. In the LC section, many columns are available, where the regular phase (Boiten et al., 2016; Janssens et al., 2012) and reversed-phase (RP) (Kawana et al., 2020) with C8 or C18 (carbon atoms) are the most prominent. The MS compartment can be equipped with an atmospheric pressure chemical ionization (APCI), electrospray ionization (ESI) source, or atmospheric pressure photoionization (APPI) as an ion source. The ion source ionizes the sample gas and focuses the beam into the analyzer (Thomas et al., 2022). The central part of the MS can be equipped with a triple quadrupole system,

which allows the use of a tandem MS, also called MS/MS or MS². With the tandem MS, it is possible to analyze selected reaction monitoring (SRM), also called multiple reaction monitoring (MRM) runs. The first MS system searches for precursor ions, and the second MS system for product ions (Thomas et al., 2022). This helps to identify and quantify, e.g., ceramides more precisely (Kawana et al., 2020). The following thesis used a C8 reversed-phase column with an ESI ion source and triple quadrupole system, as shown in Figure 6.

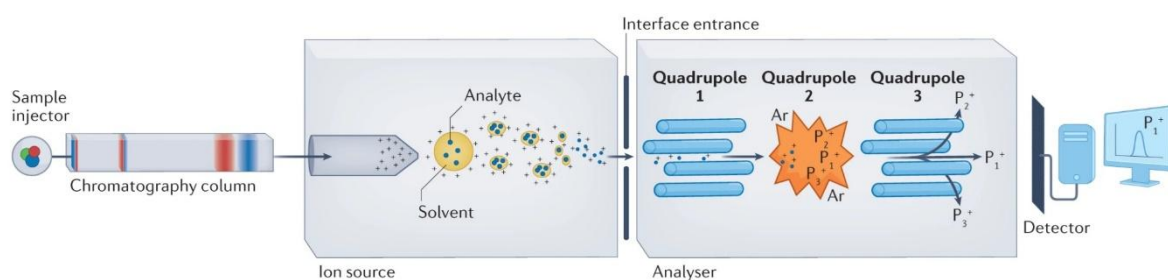


Figure 6 LC-MS with ESI as ion source and triple quad as analyzer (Thomas et al., 2022)

1.5. Ceramides

Ceramides form the major component of the SC lipid matrix by weight (Das and Olmsted, 2016). They consist of an amide bond with a sphingoid base and a fatty acid part, as shown in Figure 7. The sphingoid base and fatty acid part have different chain lengths. The combination of sphingosines (dS, S, P, H) and fatty acids (N, A, EO) leads to a double letter code or referenced Cer + number code shown in Table 1. The double-letter code was chosen here because it quickly reveals the ceramide's chemical structure. Secondly, a number describing the chain length is added (Bouwstra et al., 2021; Cha et al., 2016; Suzuki et al., 2022). For example, NS24: N stands for the non-hydroxyl fatty acid, S for sphingosine, and 24 for the fatty acid moiety. The ceramide composition is different in each species. Kawana et al. investigated the difference between humans and mice and synthesized in-vitro ceramides of BS (beta hydroxy sphingosine, dominant in mice, not detectable in humans) in HEK 293T (human embryonic kidney) cells to analyze the R/S configuration of the hydroxylated β -carbon BS (Kawana et al., 2020). The difference between human and porcine ceramides (Wertz and Downing, 1983) and human and artificial skin or RHE (reconstructed human epidermis) from Episkin® (NHEK, normal human-derived epidermal

keratinocytes, on polycarbonate filters) (Bakar et al., 2022) has already been investigated and showed some differences to take into consideration. Some ceramides exist in humans (EOH), and others only exist in pigs (ADS, EODS), or the quantities are entirely different: e.g., in porcine skin the most abundant is NDS and in human is NP. Furthermore, various chain lengths must be adjusted to obtain LC-MS signals with associated calculations. Ceramides can also be analyzed as protein-bound ones. They are covalently bound to corneocyte surface proteins and are essential for the skin barrier function (Kawana et al., 2020; Ohno et al., 2023). In this thesis, the most abundant ceramides of porcine skin were analyzed: NDS, NS, NP, NH, AS, ADS, AP, AH, EOS, EOP, EODS, and their fatty acid moiety from C20 to C30, with some shifts below C20 for NS and above C30 for EO ceramides.

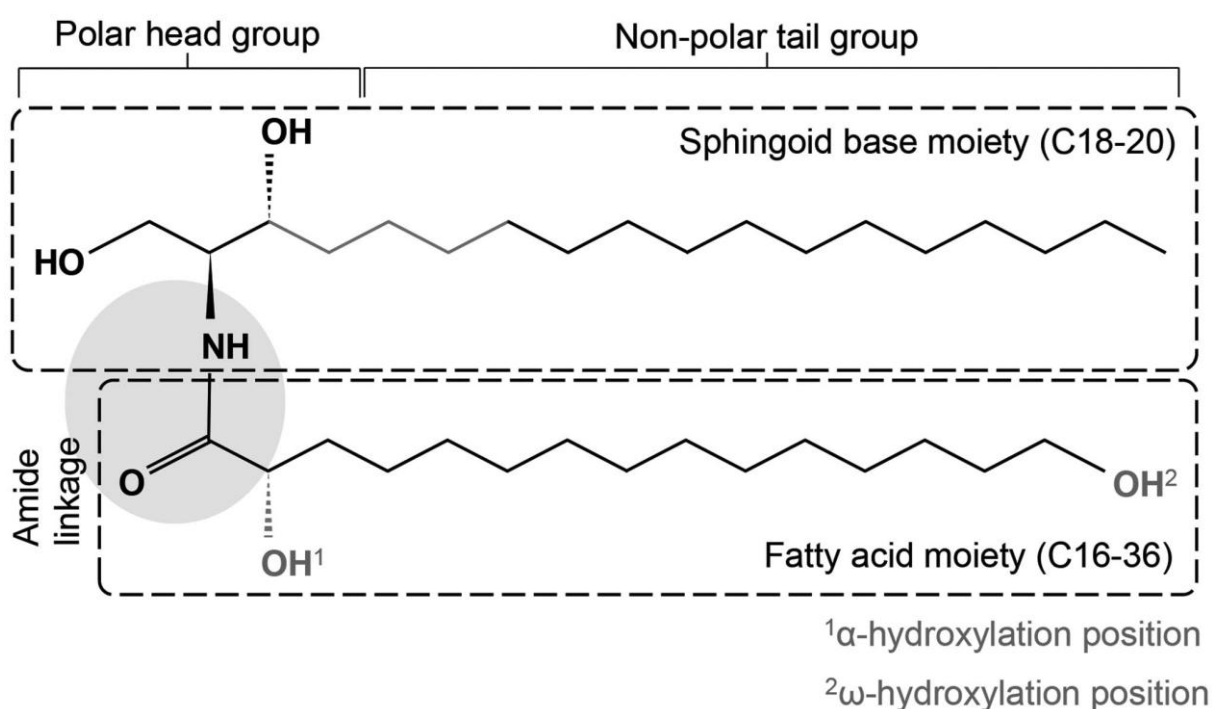
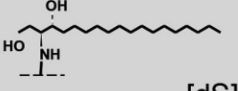
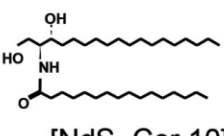
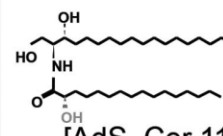
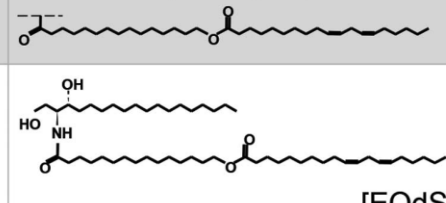
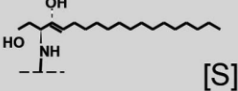
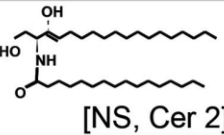
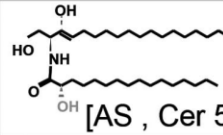
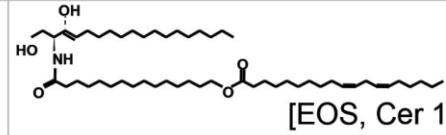
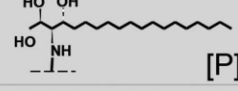
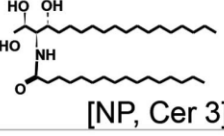
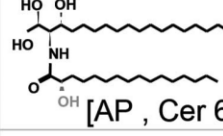
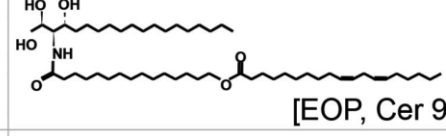
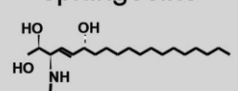
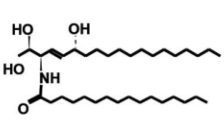
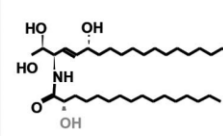
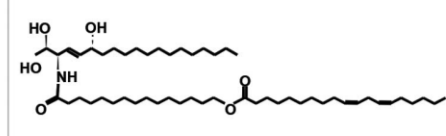


Figure 7 Chemical structure of ceramides: amide linkage of sphingoid base and fatty acid. The non-polar tail groups differ in chain length (Cha et al., 2016).

Table 1 Ceramides Overview: The nomenclature combines sphingoid base and fatty acid in a double-letter code or Cer + number (Cha et al., 2016).

Fatty acid moiety Sphingoid base moiety	Non-hydroxyl fatty acid [N]	α -hydroxyl fatty acid [A]	Esterified ω -hydroxyl fatty acid [EO]
Dihydroshingosine  [dS]	 [NdS, Cer 10]	 [AdS, Cer 11]	 [EOdS]
Sphingosine  [S]	 [NS, Cer 2]	 [AS, Cer 5]	 [EOS, Cer 1]
Phytosphingosine  [P]	 [NP, Cer 3]	 [AP, Cer 6]	 [EOP, Cer 9]
6-hydroxy sphingosine  [H]	 [NH, Cer 8]	 [AH, Cer 7]	 [EOH], Cer 4

1.6. Sorbitan esters/emulsifiers

The variety of emulsifiers offers plenty of opportunities to develop skin care products for clinical or cosmetic purposes. One commonly used emulsifier is sodium lauryl sulfate (SLS). However, research has found that SLS can be disruptive for diseased skin (Lemery et al., 2015; Mao et al., 2012; Törmä et al., 2008). Because of the published results, analyzing other emulsifiers is necessary. In the laboratory of Lunter, Zhang et al. and Liu et al. attempted to characterize different commonly used pharmaceutically emulsifiers primarily by CRS measurements. The main focus was on pegylated emulsifiers. Sorbitan esters are another class of emulsifiers often used in products, alone or in combination with other emulsifiers. They are biodegradable nonionic surfactants with sorbitan as the hydrophilic headgroup and fatty acid chains as the hydrophobic groups (Liu and Binks, 2022). Their physical appearance varies because of the different fatty acid chains. Sorbitan monopalmitate and monostearate are solid, whereas sorbitan monooleate and monoisostearate are liquids. Some preliminary investigations were made to analyze these compounds: Fiume et al. listed several sorbitan esters, where sorbitan palmitate and stearate showed no irritating effects on human skin and rabbit oculars (Fiume et al., 2019). Wang and Fingas

developed an HPLC method to separate and identify different sorbitan esters (Wang and Fingas, 1994). In this thesis, sorbitan esters are the main focus.

Cholesterol and lecithin were also selected for investigation. Cholesterol is mainly used as an active compound in products to supplement the naturally embedded cholesterol of the SC. Cholesterol is also a weak emulsifier (Di Nardo et al., 1998; Groen et al., 2011). Lecithin is often used in the food and cosmetics industry as an emulsifier and is a constituent of cell membranes (Latifi et al., 2016). However, it is also established in pharmaceuticals, such as nanoemulsions (Vater et al., 2022, 2020).

In our laboratory in-vitro investigations also of other emulsifiers had previously been performed and some of them are thus also part of this thesis. Polyethylene glycol (PEG)-20 cetyl ether (C20), PEG-2 stearyl ether (S2), PEG-20 stearyl ether (S20), and PEG-100 stearyl ether (S100) were investigated by Liu and Lunter (Liu and Lunter, 2021, 2020) and hydroxypropyl methylcellulose (HPMC) by Zhang and Lunter (Zhang and Lunter, 2018). C20 showed adverse effects on in-vitro porcine skin lipids, like SLS, and should be avoided in skin care products. PEG-2 and 100 stearyl ethers showed limited or no in-vitro porcine skin impairment. PEG-emulsifiers are a remarkable group of emulsifiers with a very wide range of properties and functionality. However, most were only briefly cataloged due to their safety assessment, like lethal dose 50 (LD₅₀) in rats or rabbits or cataloged as components in cosmetics (Fiume et al., 2012; Fruijtjer-Pölloth, 2005). Table 2 shows an overview of the emulsifiers that were investigated with abbreviations and types.

Table 2 Emulsifiers Overview

Abbreviation	Chemical Name	Type
SE 40	Sorbitan monopalmitate	w/o
SE 60	Sorbitan monostearate	w/o
SE 80	Sorbitan monooleate	w/o
SE 120	Sorbitan monoisostearate	w/o
C20	PEG-20 cetyl ether	o/w
S2	PEG-2 stearyl ether	w/o
S20	PEG-20 stearyl ether	o/w
S100	PEG-100 stearyl ether	o/w
HPMC	Hydroxypropyl methylcellulose	o/w

1.7. Basic therapy and cutaneous treatment

Basic therapy involves applying nourishing topical products with or without special additives (Daniels, 2017). Using active ingredient-free basic preparations, authorized medicinal products, or dermocosmetics is an efficient way to avoid or reduce the frequency/severity of relapses (Staubach and Lunter, 2014). Basic therapy is recommended for every skin disease and, of course, combined with API-containing pharmaceuticals. In addition to the ingredients of the applied product, the galenic type is another factor to consider and is also essential for the patient's compliance. Two central systems are commonly used: fluid formulations and semisolid formulations. Fluid formulations are liquids, emulsions, and shaking mixtures. Semisolid formulations have many possibilities, the most common being creams and ointments. In Figure 8, the overview of formulations is supplemented with their effects and degree of severity of the skin disease they can be used for. For example, lipogel has high oil and no water content and increases drug penetration, hydration, and maceration, but has no antiexudative, drying, or cooling effect and is thus suitable for the chronic stage. Daniels points out that basic therapy must always be adjusted according to the changes in skin condition over time. Typical actives in basic therapy are glycerol, urea, linoleic acid, and γ -linoleic acid. Glycerol and urea have hydrating properties, whereas linoleic acid and its precursors are helpful for lipid synthesis in the skin, especially for ceramides (Chylla et al., 2018; Daniels and Knie, 2007).

Type of base	Properties of base		Effect of base on skin						Severity of skin disease
	Water content	Oil content	Drug penetration	Antiexudative	Drying	Cooling	Hydrating	Macerating	
Moist dressing									Acute, oozing
Liquid									Acute
Shake lotion									Subacute
O/W emulsion									Subchronic
W/O emulsion									Subchronic
Paste									Subchronic
Rich ointment									Chronic
Lipogel									Chronic
Hydrocarbon gel									Chronic, hyperkeratotic

Figure 8 Overview of cutaneous skin care products regarding properties of the base, effects on the skin, and severity of skin disease (Daniels and Knie, 2007)

1.8. References

- Abdo, J.M., Sopko, N.A., Milner, S.M., 2020. The applied anatomy of human skin: A model for regeneration. *Wound Medicine*.
<https://doi.org/10.1016/j.wndm.2020.100179>
- Akdeniz, M., Gabriel, S., Lichterfeld-Kottner, A., Blume-Peytavi, U., Kottner, J., 2018. Transepidermal water loss in healthy adults: a systematic review and meta-analysis update. *British Journal of Dermatology*. <https://doi.org/10.1111/bjd.17025>
- Ali, S.M., Yosipovitch, G., 2013. Skin pH: From basic science to basic skin care. *Acta Derm Venereol*. <https://doi.org/10.2340/00015555-1531>
- Argatov, I., Roosen-Runge, F., Kocherbitov, V., 2022. Dynamics of post-occlusion water diffusion in stratum corneum. *Sci Rep* 12. <https://doi.org/10.1038/s41598-022-22529-x>
- Bakar, J., Michael-Jubeli, R., Libong, D., Baillet-Guffroy, A., Tfayli, A., 2022. Stratum corneum ceramide profiles in vitro, ex vivo, and in vivo: characterization of the α -hydroxy double esterified ceramides. *Anal Bioanal Chem* 414, 3675–3685.
<https://doi.org/10.1007/s00216-022-04011-9>
- Barbero, A.M., Frasch, H.F., 2009. Pig and guinea pig skin as surrogates for human in vitro penetration studies: A quantitative review. *Toxicology in Vitro*.
<https://doi.org/10.1016/j.tiv.2008.10.008>
- Beddoes, C.M., Gooris, G.S., Bouwstra, J.A., 2018. Preferential arrangement of lipids in the long-periodicity phase of a stratum corneum matrix model. *J Lipid Res* 59, 2329–2338. <https://doi.org/10.1194/jlr.M087106>
- Böhling, A., Bielfeldt, S., Himmelmann, A., Keskin, M., Wilhelm, K.P., 2014. Comparison of the stratum corneum thickness measured in vivo with confocal Raman spectroscopy and confocal reflectance microscopy. *Skin Research and Technology* 20, 50–57. <https://doi.org/10.1111/srt.12082>
- Boiten, W., Absalah, S., Vreeken, R., Van Smeden, J., 2016. Quantitative analysis of ceramides using a novel lipidomics approach with three dimensional response modelling. *Biochim Biophys Acta* 1861, 1652–1661.
<https://doi.org/10.1016/j.bbalip.2016.07.004>
- Bouwstra, J., Gooris, G., Ponc, M., 2002. The Lipid Organisation of the Skin Barrier: Liquid and Crystalline Domains Coexist in Lamellar Phases, *Journal of Biological Physics*.
- Bouwstra, J.A., Helder, R.W.J., El Ghalbzouri, A., 2021. Human skin equivalents: Impaired barrier function in relation to the lipid and protein properties of the stratum corneum. *Adv Drug Deliv Rev*. <https://doi.org/10.1016/j.addr.2021.05.012>
- Bumrah, G.S., Sharma, R.M., 2016. Raman spectroscopy – Basic principle, instrumentation and selected applications for the characterization of drugs of abuse. *Egypt J Forensic Sci*. <https://doi.org/10.1016/j.ejfs.2015.06.001>

- Byrd, A.L., Belkaid, Y., Segre, J.A., 2018. The human skin microbiome. *Nat Rev Microbiol.* <https://doi.org/10.1038/nrmicro.2017.157>
- Cha, H.J., He, C., Zhao, H., Dong, Y., An, I.S., An, S., 2016. Intercellular and intracellular functions of ceramides and their metabolites in skin (Review). *Int J Mol Med.* <https://doi.org/10.3892/ijmm.2016.2600>
- Choe, C., Lademann, J., Darvin, M.E., 2016. A depth-dependent profile of the lipid conformation and lateral packing order of the stratum corneum in vivo measured using Raman microscopy. *Analyst* 141, 1981–1987. <https://doi.org/10.1039/c5an02373d>
- Chylla, R., Schnopp, C., Volz, T., 2018. Basic skin care in atopic dermatitis – New and established treatment options. *JDDG - Journal of the German Society of Dermatology.* <https://doi.org/10.1111/ddg.13594>
- Courage & Khazaka electronic GmbH, 2022a. Brochure_Tewameter TMHex.
- Courage & Khazaka electronic GmbH, 2022b. Brochure_Corneometer.
- Courage & Khazaka electronic GmbH, 2022c. Brochure_Mexameter.
- Crowther, J.M., 2016. Method for quantification of oils and sebum levels on skin using the Sebumeter®. *Int J Cosmet Sci* 38, 210–216. <https://doi.org/10.1111/ics.12258>
- Daniels, R., 2017. Basistherapeutika: Was zeichnet moderne Pflegeprodukte zum Schutz und zur Wiederherstellung der Hautbarriere aus? *Hautarzt.* <https://doi.org/10.1007/s00105-017-4044-y>
- Daniels, R., Knie, U., 2007. Galenik der Dermatika - Grundlagen, Eigenschaften, Freisetzung. *JDDG - Journal of the German Society of Dermatology.* <https://doi.org/10.1111/j.1610-0387.2007.06321.x>
- Das, C., Olmsted, P.D., 2016. The physics of stratum corneum lipid membranes. *Philosophical Transactions of the Royal Society A: Mathematical, Physical and Engineering Sciences* 374. <https://doi.org/10.1098/rsta.2015.0126>
- Daugimont, L., Baron, N., Vandermeulen, G., Pavselj, N., Miklavcic, D., Jullien, M.C., Cabodevila, G., Mir, L.M., Pr eat, V., 2010. Hollow microneedle arrays for intradermal drug delivery and DNA electroporation. *Journal of Membrane Biology* 236, 117–125. <https://doi.org/10.1007/s00232-010-9283-0>
- Di Nardo, Wertz, Giannetti, Seidenari, 1998. Ceramide and Cholesterol Composition of the Skin of Patients with Atopic Dermatitis, *Acta Derm Venereol (Stockh).* <https://doi.org/10.1080/00015559850135788>
- Du Plessis, J., Stefaniak, A., Eloff, F., John, S., Agner, T., Chou, T.C., Nixon, R., Steiner, M., Franken, A., Kudla, I., Holness, L., 2013. International guidelines for the in vivo assessment of skin properties in non-clinical settings: Part 2. transepidermal water loss and skin hydration. *Skin Research and Technology* 19, 265–278. <https://doi.org/10.1111/srt.12037>

- Endo, K., Suzuki, N., Yoshida, O., Sato, H., Fujikura, Y., 2007. The barrier component and the driving force component of transepidermal water loss and their application to skin irritant tests. *Skin Research and Technology* 13, 425–435. <https://doi.org/10.1111/j.1600-0846.2007.00247.x>
- Everall, N., Lapham, J., Adar, F., Whitley, A., Lee, E., Mamedov, S., 2007. Optimizing Depth Resolution in Confocal Raman Microscopy: A Comparison of Metallurgical, Dry Corrected, and Oil Immersion Objectives. *Appl Spectrosc* 61.
- Everall, N.J., 2010. Confocal Raman microscopy: Common errors and artefacts. *Analyst*. <https://doi.org/10.1039/c0an00371a>
- Évora, A.S., Adams, M.J., Johnson, S.A., Zhang, Z., 2021. Corneocytes: Relationship between structural and biomechanical properties. *Skin Pharmacol Physiol*. <https://doi.org/10.1159/000513054>
- Fiume, M.M., Bergfeld, W.F., Belsito, D. V., Hill, R.A., Klaassen, C.D., Liebler, D.C., Marks, J.G., Shank, R.C., Slaga, T.J., Snyder, P.W., Gill, L.J., Heldreth, B., 2019. Safety Assessment of Sorbitan Esters as Used in Cosmetics. *Int J Toxicol* 38, 60S-80S. <https://doi.org/10.1177/1091581819871877>
- Fiume, M.M., Heldreth, B., Bergfeld, W.F., Belsito, D. V., Hill, R.A., Klaassen, C.D., Liebler, D., Marks, J.G., Shank, R.C., Slaga, T.J., Snyder, P.W., Andersen, F.A., 2012. Safety Assessment of Alkyl PEG Ethers as Used in Cosmetics. *Int J Toxicol* 31, 169S-244S. <https://doi.org/10.1177/1091581812444141>
- Fruijtjer-Pölloth, C., 2005. Safety assessment on polyethylene glycols (PEGs) and their derivatives as used in cosmetic products. *Toxicology* 214, 1–38. <https://doi.org/10.1016/J.TOX.2005.06.001>
- Gomaa, Y.A., Morrow, D.I.J., Garland, M.J., Donnelly, R.F., El-Khordagui, L.K., Meidan, V.M., 2010. Effects of microneedle length, density, insertion time and multiple applications on human skin barrier function: Assessments by transepidermal water loss. *Toxicology in Vitro* 24, 1971–1978. <https://doi.org/10.1016/j.tiv.2010.08.012>
- Gonzalez-Bravo, A., Montero-Vilchez, T., Arias-Santiago, S., Buendia-Eisman, A., 2022. The Effect of Sunscreens on the Skin Barrier. *Life* 12. <https://doi.org/10.3390/life12122083>
- Gore, E., Picard, C., Savary, G., 2020. Complementary approaches to understand the spreading behavior on skin of O/W emulsions containing different emollientss. *Colloids Surf B Biointerfaces* 193. <https://doi.org/10.1016/j.colsurfb.2020.111132>
- Grice, K., Sattar, H., Baker, H., Sharratt, M., 1975. The relationship of transepidermal water loss to skin temperature in psoriasis and eczema. *Journal of Investigative Dermatology* 64, 313–315. <https://doi.org/10.1111/1523-1747.ep12512258>
- Groen, D., Poole, D.S., Gooris, G.S., Bouwstra, J.A., 2011. Investigating the barrier function of skin lipid models with varying compositions. *European Journal of*

- Pharmaceutics and Biopharmaceutics 79, 334–342.
<https://doi.org/10.1016/j.ejpb.2011.05.007>
- Herrero-Fernandez, M., Montero-Vilchez, T., Diaz-Calvillo, P., Romera-Vilchez, M., Buendia-Eisman, A., Arias-Santiago, S., 2022. Impact of Water Exposure and Temperature Changes on Skin Barrier Function. *J Clin Med* 11.
<https://doi.org/10.3390/jcm11020298>
- Hofmann, E., Schwarz, A., Fink, J., Kamolz, L.P., Kotzbeck, P., 2023. Modelling the Complexity of Human Skin In Vitro. *Biomedicines*.
<https://doi.org/10.3390/biomedicines11030794>
- Hopf, N.B., Champmartin, C., Schenk, L., Berthet, A., Chedik, L., Du Plessis, J.L., Franken, A., Frasch, F., Gaskin, S., Johanson, G., Julander, A., Kasting, G., Kilo, S., Larese Filon, F., Marquet, F., Midander, K., Reale, E., Bunge, A.L., 2020. Reflections on the OECD guidelines for in vitro skin absorption studies. *Regulatory Toxicology and Pharmacology*.
<https://doi.org/10.1016/j.yrtph.2020.104752>
- Jacobi, U., Kaiser, M., Toll, R., Mangelsdorf, S., Audring, H., Otberg, N., Sterry, W., Lademann, J., 2007. Porcine ear skin: An in vitro model for human skin. *Skin Research and Technology* 13, 19–24. <https://doi.org/10.1111/j.1600-0846.2006.00179.x>
- Janssens, M., Van Smeden, J., Gooris, G.S., Bras, W., Portale, G., Caspers, P.J., Vreeken, R.J., Hankemeier, T., Kezic, S., Wolterbeek, R., Lavrijsen, A.P., Bouwstra, J.A., 2012. Increase in short-chain ceramides correlates with an altered lipid organization and decreased barrier function in atopic eczema patients. *J Lipid Res* 53, 2755–2766. <https://doi.org/10.1194/jlr.P030338>
- Jiao, Q., Yue, L., Zhi, L., Qi, Y., Yang, J., Zhou, C., Jia, Y., 2022. Studies on stratum corneum metabolism: function, molecular mechanism and influencing factors. *J Cosmet Dermatol*. <https://doi.org/10.1111/jocd.15000>
- Jung, N., Namjoshi, S., Mohammed, Y., Grice, J.E., Benson, H.A.E., Raney, S.G., Roberts, M.S., Windbergs, M., 2022. Application of Confocal Raman Microscopy for the Characterization of Topical Semisolid Formulations and their Penetration into Human Skin Ex Vivo. *Pharm Res* 39, 935–948.
<https://doi.org/10.1007/s11095-022-03245-7>
- Kawana, M., Miyamoto, M., Ohno, Y., Kihara, A., 2020. Comparative profiling and comprehensive quantification of stratum corneum ceramides in humans and mice by LC/MS/MS. *J Lipid Res* 61, 884–895.
<https://doi.org/10.1194/jlr.ra120000671>
- Kottner, J., Lichterfeld, A., Blume-Peytavi, U., 2013. Transepidermal water loss in young and aged healthy humans: A systematic review and meta-analysis. *Arch Dermatol Res* 305, 315–323. <https://doi.org/10.1007/s00403-012-1313-6>
- Kourbaj, G., Gaiser, A., Bielfeldt, S., Lunter, D., 2023. Assessment of penetration and permeation of caffeine by confocal Raman spectroscopy in vivo and ex vivo by tape stripping. *Int J Cosmet Sci* 45, 14–28. <https://doi.org/10.1111/ICS.12820>

- Krombholz, R., Fressle, S., Lunter, D., 2022a. Ex vivo-In vivo correlation of retinol stratum corneum penetration studies by confocal Raman microspectroscopy and tape stripping. *Int J Cosmet Sci* 44, 299–308. <https://doi.org/10.1111/ics.12775>
- Krombholz, R., Fressle, S., Nikolić, I., Pantelić, I., Savić, S., Sakač, M.C., Lunter, D., 2022b. ex vivo–in vivo comparison of drug penetration analysis by confocal Raman microspectroscopy and tape stripping. *Exp Dermatol* 31, 1908–1919. <https://doi.org/10.1111/EXD.14672>
- Lambers, H., Piessens, S., Bloem, A., Pronk, H., Finkel, P., Household, S.L., 2006. Natural skin surface pH is on average below 5, which is beneficial for its resident flora. *Int J Cosmet Sci* 28, 359–370. <https://doi.org/10.1111/j.1467-2494.2006.00344.x>
- Latifi, S., Tamayol, A., Habibey, R., Sabzevari, R., Kahn, C., Geny, D., Eftekharpour, E., Annabi, N., Blau, A., Linder, M., Arab-Tehrany, E., 2016. Natural lecithin promotes neural network complexity and activity. *Sci Rep* 6. <https://doi.org/10.1038/srep25777>
- Lee, M., Won, K., Kim, E.J., Hwang, J.S., Lee, H.K., 2018. Comparison of stratum corneum thickness between two proposed methods of calculation using Raman spectroscopic depth profiling of skin water content. *Skin Research and Technology* 24, 504–508. <https://doi.org/10.1111/srt.12461>
- Lemery, E., Briançon, S., Chevalier, Y., Oddos, T., Gohier, A., Boyron, O., Bolzinger, M.-A., 2015. Surfactants have multi-fold effects on skin barrier function. *European Journal of Dermatology* 25, 424–435. <https://doi.org/10.1684/ejd.2015.2587>
- Levang, A.K., Zhao, K., Singh, J., 1999. Effect of ethanol/propylene glycol on the in vitro percutaneous absorption of aspirin, biophysical changes and macroscopic barrier properties of the skin, *International Journal of Pharmaceutics*. [https://doi.org/10.1016/s0378-5173\(99\)00055-1](https://doi.org/10.1016/s0378-5173(99)00055-1)
- Liu, Y., Binks, B.P., 2022. Fabrication of Stable Oleofoams with Sorbitan Ester Surfactants. *Langmuir* 38, 14779–14788. <https://doi.org/10.1021/acs.langmuir.2c02413>
- Liu, Y., Lunter, D.J., 2022. Confocal Raman spectroscopy at different laser wavelengths in analyzing stratum corneum and skin penetration properties of mixed PEGylated emulsifier systems. *Int J Pharm* 616, 121561. <https://doi.org/10.1016/j.ijpharm.2022.121561>
- Liu, Y., Lunter, D.J., 2021. Optimal configuration of confocal Raman spectroscopy for precisely determining stratum corneum thickness: Evaluation of the effects of polyoxyethylene stearyl ethers on skin. *Int J Pharm* 597. <https://doi.org/10.1016/j.ijpharm.2021.120308>
- Liu, Y., Lunter, D.J., 2020. Systematic investigation of the effect of non-ionic emulsifiers on skin by confocal raman spectroscopy—a comprehensive lipid analysis. *Pharmaceutics* 12. <https://doi.org/10.3390/pharmaceutics12030223>

- Łuczaj, W., Jastrz, A., Ab, , Do, M., Domingues, R., Domingues, P., Zbieta Skrzydlewska, E., De Luca, M.A., 2021. Changes in Phospholipid/Ceramide Profiles and Eicosanoid Levels in the Plasma of Rats Irradiated with UV Rays and Treated Topically with Cannabidiol Academic Editors: Nicola Simola and. International Journal of Molecular Sciences Article Int. J. Mol. Sci 22, 8700. <https://doi.org/10.3390/ijms22168700>
- Łuczaj, W., Wró Nski, A., Domingues, P., Domingues, M.R., Zbieta Skrzydlewska, E., 2020. Lipidomic Analysis Reveals Specific Differences between Fibroblast and Keratinocyte Ceramide Profile of Patients with Psoriasis Vulgaris. *molecules* 25(3). <https://doi.org/10.3390/molecules25030630>
- Lunter, D.J., 2017. Determination of skin penetration profiles by confocal Raman microspectroscopy: statistical evaluation of optimal microscope configuration. *Journal of Raman Spectroscopy* 48, 152–160. <https://doi.org/10.1002/jrs.5001>
- Lunter, D.J., 2016. How Confocal is Confocal Raman Microspectroscopy on the Skin? Impact of Microscope Configuration and Sample Preparation on Penetration Depth Profiles. *Skin Pharmacol Physiol* 29, 92–101. <https://doi.org/10.1159/000444806>
- Machado, M., Salgado, T.M., Hadgraft, J., Lane, M.E., 2010. The relationship between transepidermal water loss and skin permeability. *Int J Pharm* 384, 73–77. <https://doi.org/10.1016/j.ijpharm.2009.09.044>
- Mao, G., Flach, C.R., Mendelsohn, R., Walters, R.M., 2012. Imaging the distribution of sodium dodecyl sulfate in skin by confocal raman and infrared microspectroscopy. *Pharm Res* 29, 2189–2201. <https://doi.org/10.1007/s11095-012-0748-y>
- Montero-Vilchez, T., Segura-Fernández-nogueras, M.V., Pérez-Rodríguez, I., Soler-Gongora, M., Martínez-Lopez, A., Fernández-González, A., Molina-Leyva, A., Arias-Santiago, S., 2021. Skin barrier function in psoriasis and atopic dermatitis: Transepidermal water loss and temperature as useful tools to assess disease severity. *J Clin Med* 10, 1–12. <https://doi.org/10.3390/jcm10020359>
- Morris, S.A.V., Kasting, G.B., Ananthapadmanabhan, K.P., 2022. Surfactant equilibria and its impact on penetration into stratum corneum. *Curr Opin Colloid Interface Sci* 59, 101579. <https://doi.org/10.1016/J.COCIS.2022.101579>
- Nangia, S., Paul, V.K., Deorari, A.K., Sreenivas, V., Agarwal, R., Chawla, D., 2015. Topical oil application and trans-epidermal water loss in preterm very low birth weight infants-a randomized trial. *J Trop Pediatr* 61, 414–420. <https://doi.org/10.1093/tropej/fmv049>
- Ohno, Y., Nakamura, T., Iwasaki, T., Katsuyama, A., Ichikawa, S., Kihara, A., 2023. Determining the structure of protein-bound ceramides, essential lipids for skin barrier function. *iScience* 26. <https://doi.org/10.1016/j.isci.2023.108248>
- Orlando, A., Franceschini, F., Muscas, C., Pidkova, S., Bartoli, M., Rovere, M., Tagliaferro, A., 2021. A comprehensive review on Raman spectroscopy applications. *Chemosensors*. <https://doi.org/10.3390/chemosensors9090262>

- Pany, A., Klang, V., Brunner, M., Ruthofer, J., Schwarz, E., Valenta, C., 2018. Effect of physical and chemical hair removal methods on skin barrier function in vitro: Consequences for a hydrophilic model permeant. *Skin Pharmacol Physiol* 32, 8–21. <https://doi.org/10.1159/000493168>
- Pasparakis, M., Haase, I., Nestle, F.O., 2014. Mechanisms regulating skin immunity and inflammation. *Nat Rev Immunol*. <https://doi.org/10.1038/nri3646>
- Pekny, M., Lane, E.B., 2007. Intermediate filaments and stress. *Exp Cell Res*. <https://doi.org/10.1016/j.yexcr.2007.04.023>
- Pereira-Leite, C., Bom, M., Ribeiro, A., Almeida, C., Rosado, C., 2023. Exploring Stearic-Acid-Based Nanoparticles for Skin Applications-Focusing on Stability and Cosmetic Benefits. *Cosmetics* 10. <https://doi.org/10.3390/cosmetics10040099>
- Pinnagoda, J., Tupker, R.A., Agner, T., Serup, J., 1990. Guidelines for transepidermal water loss (TEWL) measurement A Report from the Standardization Group of the European Society of Contact Dermatitis, Contact Dermatitis.
- Schmid-Wendtner, M.H., Korting, H.C., 2006. The pH of the skin surface and its impact on the barrier function. *Skin Pharmacol Physiol*. <https://doi.org/10.1159/000094670>
- Schoenfelder, H., Liu, Y., Lunter, D.J., 2023. Systematic investigation of factors, such as the impact of emulsifiers, which influence the measurement of skin barrier integrity by in-vitro trans-epidermal water loss (TEWL). *Int J Pharm* 638, 122930. <https://doi.org/10.1016/J.IJPHARM.2023.122930>
- Schwindt, D.A., Wilhelm, K.P., Maibach, H.I., 1998. Water Diffusion Characteristics of Human Stratum Corneum at Different Anatomical Sites In Vivo. The Society for Investigative Dermatology, Inc.
- Snyder, R.G., Hsut, S.L., Krimm, S., Randall, H.M., 1978. Vibrational spectp in the C-H stretching region and the structure of the polymethylene chain. *Spectrochimica Acta* 34, 395–406.
- Staubach, P., Lunter, D.J., 2014. Basistherapie in der Dermatologie: Geeignete Grundlagen, Möglichkeiten und Grenzen. *Hautarzt* 65, 63–74. <https://doi.org/10.1007/s00105-013-2726-7>
- Steiner, M., Aikman-Green, S., Prescott, G.J., Dick, F.D., 2011. Side-by-side comparison of an open-chamber (TM 300) and a closed-chamber (Vapometer™) transepidermal water loss meter. *Skin Research and Technology* 17, 366–372. <https://doi.org/10.1111/j.1600-0846.2011.00509.x>
- Suzuki, M., Ohno, Y., Kihara, A., 2022. Whole picture of human stratum corneum ceramides, including the chain-length diversity of long-chain bases. *J Lipid Res* 63. <https://doi.org/10.1016/j.jlr.2022.100235>
- ter Horst, B., Chouhan, G., Moiemmen, N.S., Grover, L.M., 2018. Advances in keratinocyte delivery in burn wound care. *Adv Drug Deliv Rev*. <https://doi.org/10.1016/j.addr.2017.06.012>

- Tfaily, S., Gobinet, C., Josse, G., Angiboust, J.F., Manfait, M., Piot, O., 2012. Confocal Raman microspectroscopy for skin characterization: A comparative study between human skin and pig skin. *Analyst* 137, 3673–3682. <https://doi.org/10.1039/c2an16292j>
- Thomas, S.N., French, D., Jannetto, P.J., Rappold, B.A., Clarke, W.A., 2022. Liquid chromatography–tandem mass spectrometry for clinical diagnostics. *Nature Reviews Methods Primers* 2. <https://doi.org/10.1038/s43586-022-00175-x>
- Törmä, H., Lindberg, M., Berne, B., 2008. Skin barrier disruption by sodium lauryl sulfate-exposure alters the expressions of involucrin, transglutaminase 1, profilaggrin, and kallikreins during the repair phase in human skin in vivo. *Journal of Investigative Dermatology* 128, 1212–1219. <https://doi.org/10.1038/sj.jid.5701170>
- Usui, M.L., Mansbridge, J.N., Carter, W.G., Fujita, M., Olerud, J.E., 2008. Keratinocyte migration, proliferation, and differentiation in chronic ulcers from patients with diabetes and normal wounds. *Journal of Histochemistry and Cytochemistry* 56, 687–696. <https://doi.org/10.1369/jhc.2008.951194>
- Van Smeden, J., Janssens, M., Gooris, G.S., Bouwstra, J.A., 2014. The important role of stratum corneum lipids for the cutaneous barrier function ☆. *BBA - Molecular and Cell Biology of Lipids* 1841, 295–313. <https://doi.org/10.1016/j.bbalip.2013.11.006>
- Vater, C., Bosch, L., Mitter, A., Göls, T., Seiser, S., Heiss, E., Elbe-Bürger, A., Wirth, M., Valenta, C., Klang, V., 2022. Lecithin-based nanoemulsions of traditional herbal wound healing agents and their effect on human skin cells. *European Journal of Pharmaceutics and Biopharmaceutics* 170, 1–9. <https://doi.org/10.1016/j.ejpb.2021.11.004>
- Vater, C., Hlawaty, V., Werdenits, P., Cichoń, M.A., Klang, V., Elbe-Bürger, A., Wirth, M., Valenta, C., 2020. Effects of lecithin-based nanoemulsions on skin: Short-time cytotoxicity MTT and BrdU studies, skin penetration of surfactants and additives and the delivery of curcumin. *Int J Pharm* 580, 119209. <https://doi.org/10.1016/j.ijpharm.2020.119209>
- Vavrova, K., Kovačik, A., Opalka, L., 2017. Ceramides in the skin barrier. *European Pharmaceutical Journal* 64, 28–35. <https://doi.org/10.1515/AFPUC-2017-0004>
- Vukosavljevic, B., Murgia, X., Schwarzkopf, K., Schaefer, U.F., Lehr, C.M., Windbergs, M., 2017. Tracing molecular and structural changes upon mucolysis with N-acetyl cysteine in human airway mucus. *Int J Pharm* 533, 373–376. <https://doi.org/10.1016/j.ijpharm.2017.07.022>
- Wang, Z., Fingas, M., 1994. Analysis of sorbitan ester surfactants. Part I: High performance liquid chromatography. *Journal of High Resolution Chromatography* 17, 15–19. <https://doi.org/10.1002/jhrc.1240170104>
- Wertz, P.W., Downing, D.T., 1983. Ceramides of pig epidermis: structure determination. *J Lipid Res* 24, 759–765. [https://doi.org/10.1016/S0022-2275\(20\)37950-5](https://doi.org/10.1016/S0022-2275(20)37950-5)

Williams, A.C., Edwards, H.G.M., Barry, B.W., 1994. Raman Spectra of Human Keratotic Biopolymers: Skin, Callus, Hair and Nail. *JOURNAL OF RAMAN SPECTROSCOPY* 25, 95–98. <https://doi.org/10.1002/jrs.1250250113>

Zhang, Z., Lunter, D.J., 2018. Confocal Raman microspectroscopy as an alternative to differential scanning calorimetry to detect the impact of emulsifiers and formulations on stratum corneum lipid conformation. *European Journal of Pharmaceutical Sciences* 121. <https://doi.org/10.1016/j.ejps.2018.05.013>

2. Objectives

The thesis aimed to evaluate a TEWL protocol for in-vitro measurements and test the method's limitations. The following aspects were examined:

- Find out the correct duration and number of measurements required
- Combination of measurement and Franz diffusion cell system
- Incubation time limits
- Impact of injuries on porcine SC
- Analysis of different emulsifiers

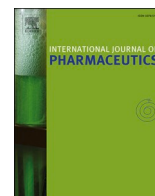
Further, a multimodal approach (TEWL, CRS, and LC-MS measurements) was implemented using the same in-vitro porcine skin sample for every method.

- Preparation concept for samples to analyze them beginning with TEWL following CRS and ending up with an extraction protocol for LC-MS without any spurious results
- Developing an LC-MS method for detecting ceramides in porcine SC, method duration, efficiency, the limit of detection (LOD), the limit of quantification (LOQ)
- Evaluating the most abundant ceramides by class and fatty acid moiety chain length
- Analysis of different sorbitan esters and other high interest emulsifiers

Lastly, a topical skin formulation was developed using sorbitan monostearate and PEG-100 stearyl ether.

- Investigating a formulation for topical skin treatment including one sorbitan ester
- Characterization by rheology and polarized light microscopy
- Testing in-vitro on porcine skin by measuring TEWL and analyzing lipid uptake by pyranine staining under a fluorescent microscope

3. Systematic investigation of factors, such as the impact of emulsifiers, which influence the measurement of skin barrier integrity by in-vitro trans-epidermal water loss (TEWL)



Systematic investigation of factors, such as the impact of emulsifiers, which influence the measurement of skin barrier integrity by in-vitro trans-epidermal water loss (TEWL)

Hans Schoenfelder, Yali Liu, Dominique Jasmin Lunter*

Department of Pharmaceutical Technology, Faculty of Science, Eberhard Karls University Tuebingen, Auf der Morgenstelle 8, 72076 Tuebingen, Germany

ARTICLE INFO

Keywords:

Cholesterol
Emulsifiers
In-vitro
Lecithin
Polyoxyethylene ethers
Sorbitan esters
Stratum corneum
Tewameter® VT 310
Trans-epidermal water loss

ABSTRACT

Trans-epidermal water loss (TEWL) has been the most widely used method to assess the integrity of the skin barrier and evaluate the irritation potential or the protective properties of topical products for many years. It detects the amount of water that diffuses across the stratum corneum (SC) to the external environment. As one of the most important functions of the skin is to keep water inside the body, an increase in TEWL is used to indicate the skin's impaired barrier function. So far, a variety of commercial instruments are available to measure the TEWL. Their applications mainly focus on the in-vivo TEWL measurements for dermatological examinations or formulation development. Recently, an in-vitro TEWL probe has also been commercially released enabling preliminary tests with excised skin samples. In our study, we first aimed to optimize the experimental procedures for detecting the in-vitro TEWL of porcine skin. Secondly, different kinds of emulsifiers were applied to the skin, including polyethylene glycol-containing emulsifiers (PEG-ylated emulsifiers), sorbitan esters, cholesterol, and lecithin. Sodium lauryl sulfate (SLS) was used as a positive control, and water as a negative control. Based on the findings, we established a protocol for accurately measuring the in-vitro TEWL values, emphasizing that the temperature of the skin sample should be constantly maintained at 32 °C. Subsequently, the influences of emulsifiers on the in-vitro TEWL were analyzed. They indicated a significant skin barrier impairment of PEG-20 cetyl ether, PEG-20 stearyl ether, and SLS on in-vitro skin. Furthermore, we interestingly found that there consistently was an alteration of the TEWL values, even after the application of water to the skin. Our findings are of special interest, as the European Medicines Agency (EMA) recommends the use of in-vitro TEWL to determine skin barrier intactness during Franz cell experiments. Thus, this study provides a validated protocol for measuring the in-vitro TEWL and elucidates the impact of emulsifiers on the skin barrier. It also improves the understanding of tolerable variations of in-vitro TEWL and offers recommendations for its use in research.

1. Introduction

Characterization of skin conditions evokes a wide variety of test methods. Trans-epidermal water loss (TEWL) is widely used and popular in research and diagnostics (Akdeniz et al., 2018; du Plessis et al., 2013; Hadgraft and Lane, 2009; Hopf et al., 2020; Levin and Maibach, 2005; Machado et al., 2010; Nangia et al., 2015). In the following examples, TEWL Data was used in several investigations: Some interesting studies were published regarding in-vivo TEWL measurement protocols (Alexander et al., 2018; du Plessis et al., 2013; Ilić et al., 2019), measurements of different anatomical sites and typical measured values (Akdeniz et al., 2018; du Plessis et al., 2013; Kottner et al., 2013; Pinnagoda et al.,

1990), consideration of ethnic backgrounds (Wilson et al., 1988), effects of active pharmaceutical ingredients (APIs) (Barba et al., 2019; Fokuhl and Müller-Goymann, 2013; Ilić et al., 2019), characterization of microneedle systems (Daugimont et al., 2010; Gomaa et al., 2010), skin penetration enhancing processes (Levang et al., 1999), tape-stripping quality (Pany et al., 2018; Simonsen and Fullerton, 2007; Vater et al., 2021), and sample treatment (Ilić et al., 2019; Pany et al., 2018). The guideline of the European Medicines Agency (EMA) requests that the skin barrier must not be changed over the incubation time by the applied formulations. To this end, it is proposed to use the TEWL as an integrity test during in-vitro permeation tests (Medicines Agency, 2018). For in-vitro TEWL measurement, the probe chamber is fixed directly to the

* Corresponding author.

E-mail address: dominique.lunter@uni-tuebingen.de (D.J. Lunter).

<https://doi.org/10.1016/j.ijpharm.2023.122930>

Received 16 February 2023; Received in revised form 31 March 2023; Accepted 1 April 2023

Available online 6 April 2023

0378-5173/© 2023 Elsevier B.V. All rights reserved.

skin on the Franz cell. Open or closed chambers are available and were investigated (du Plessis et al., 2013; Steiner et al., 2011) together with probes from different manufacturers. It was found that the open chamber systems are restricted in capacity in high values and the closed chambers are less sensitive to differences in lower ranges (Steiner et al., 2011). Most of the studies preferred an open chamber probe (Barba et al., 2019; Cristiano et al., 2020; Fokuhl and Müller-Goymann, 2013; Ilić et al., 2019; Levang et al., 1999; Simonsen and Fullerton, 2007), and only some used a closed chamber device (Gomaa et al., 2010; Pany et al., 2018).

Most formulations applied to skin contain emulsifiers that assure their physical stability. As our research group already showed, emulsifiers may influence the skin barrier function (Liu et al., 2022; Liu and Lunter, 2022, 2021, 2020; Zhang and Lunter, 2018). For the present study, we selected the following: oil in water (O/W) emulsifiers (PEG-20 cetyl ether (C20), PEG-20 stearyl ether (S20), PEG-40 stearyl ether (S40), PEG-100 stearyl ether (S100)), and water in oil (W/O) emulsifiers (sorbitan monostearate (Span 60), and sorbitan monooleate (Span 80)). These were utilized in marketed pharmaceutical semisolid formulations, as well as in vehicles used for compounding. Additionally, cholesterol and lecithin were selected. Cholesterol is used both as a weak emulsifier and a constituent of the stratum corneum (di Nardo et al., 1998; Groen et al., 2011). Lecithin is also used in topical formulations (Vater et al., 2022, 2020) and is a constituent of cell membranes (Latifi et al., 2016).

The primary aim of the current study was to optimize the experimental procedure for detecting the in-vitro TEWL. A secondary aim was to regard the effect of truly impaired skin simulated by incisions of different depths, treatment with sodium lauryl sulfate (SLS) (Khosrowpour et al., 2019), and longtime incubation to derive an understanding of the extent of TEWL increase. A further aim was to characterize the impact of pharmaceutical emulsifiers on the TEWL and to compare the achieved values to those of truly impaired skin. Altogether, this part of the study was expected to reveal a threshold below which the skin could still be regarded as intact after an in vitro permeation or penetration experiment. This study was performed with the background of several guidelines recommending the measurement of in vitro TEWL to describe skin intactness in vitro skin permeation and penetration experiments (Fda et al., 2019; Medicines Agency, 2018, 2014). In this study, the impact that emulsifiers exhibit on in-vitro skin was used to critically evaluate this recommendation. In conclusion, a recommendation for a protocol for future measurements is presented and a threshold is proposed up to which an integer skin barrier can be assumed.

2. Materials and methods

2.1. Materials

Sodium lauryl sulfate, cholesterol, sodium chloride, and potassium chloride were obtained from Caesar & Loretz GmbH (D-Hilden, Germany). Di-sodium-hydrogen phosphate, potassium-di-hydrogen phosphate, and Soy-lecithin were obtained from Carl Roth GmbH & Co. KG (D-Karlsruhe, Germany). PEG alkyl ethers including PEG-20 cetyl ether (C20), PEG-20 stearyl ether (S20), PEG-40 stearyl ether (S40), PEG-100 stearyl ether (S100), and sorbitan esters including sorbitan monostearate (Span 60) and sorbitan monooleate (Span 80) were purchased from Croda GmbH, (D-Nettetal, Germany). Parafilm® was obtained from Bemis Company Inc. (WI-Oshkosh, USA). All aqueous solutions were made with ultra-pure water from Elga Maxima (GB-High Wycombe, Great Britain). Phosphate-buffered saline (PBS) was prepared using sodium chloride, and potassium chloride obtained from Caesar & Loretz GmbH (D-Hilden, Germany), di-sodium-hydrogen phosphate, and potassium-di-hydrogen phosphate obtained from Carl Roth GmbH & Co. KG (D-Karlsruhe, Germany). Porcine ear skins (German landrace; age: 15 to 30 weeks; weight: 40 to 64 kg) were provided by the Department of Experimental Medicine at the University Clinics of Tuebingen. The Department of Pharmaceutical Technology at the University

of Tuebingen has been registered for the use of animal products (registration number: DE 08 416 1052 21).

2.2. Preparation of emulsifier solutions/dispersions

Testing solutions of C20, S20, S40, and S100 were prepared by dissolving the substances in water (Liu and Lunter, 2020), and Span 60, Span 80, cholesterol, lecithin, and SLS were prepared as 1 % solution/dispersion in water, sonicated (Bandelin Sonorex, Bandelin electronic GmbH & Co. KG, D-Berlin, Germany) for 15 min, and vortexed for 1 min (IKA Vortex 2, IKA-Werke GmbH & Co. KG, D-Staufen, Germany).

2.3. Porcine ear skin preparation

Because porcine ear skin is histologically and morphologically comparable to human skin, it was chosen as a replacement for human skin (Jacobi et al., 2007; Tfailli et al., 2012). Isotonic saline was used to clean the fresh pig ears. Full-thickness skin was removed from the cartilage, and blood was removed with cotton swabs and isotonic saline. The obtained postauricular skin sheets were dried with soft tissue. The skin was sliced into strips of about 3 cm in width. The skin sheet was stretched onto a Styrofoam plate to reduce the impact of wrinkles. With an electric hair trimmer (QC5115/15 Philips Electronics, NL-Eindhoven, Netherlands), bristles were cut to about 0.5 mm in length. After being dermatomed to a thickness of 1.0 mm (Dermatom GA 630 Acculan 3 TI Aesculap AG & Co. KG, D-Tuttlingen, Germany) the skin was punched out into circles with 25 mm diameter and placed in the freezer at minus 28 °C wrapped in aluminum foil. On the experiment day, the samples are thawed to room temperature (Lunter, 2016). The appropriateness use of thawed skin has already been shown in the literature (Hahn et al., 2010; Klang et al., 2012; Stracke et al., 2006).

2.4. Incubation of skin samples in Franz diffusion cells

Franz diffusion cells are a popular type of analytical setup for determining skin absorption in-vitro and are recommended by the European Medicines Agency (EMA), U.S. Food and Drug Administration (FDA), and Organisation of Economic Co-operation and Development (OECD) (du Plessis et al., 2013; Fda et al., 2019; Medicines Agency, 2018, 2014). Here, 12 mL Franz diffusion cells (Gauer Glas, D-Püttlingen, Germany) were filled with degassed, prewarmed (32 °C) phosphate-buffered saline (PBS) as the receptor fluid in a manual and vertical Franz diffusion cell system. The dermatomed skin circles were put on top of the acceptor compartment and the donor compartments were placed on top of the skin. The Franz diffusion cells were placed in a water bath that was 32 °C warm (Lauda type Alpha, Lauda Dr. R. Wobser GmbH & Co. KG, D-Lauda-Königshofen, Germany). The receptor fluid was stirred there at a 500-rpm rate (Variomag Poly 15, Thermo-Scientific, Thermo Electron LED GmbH, D-Langensfeld, Germany). After an expeditious equilibration period of 30 min, the initial TEWL values were generated with the protocol described in 2.5. After the initial TEWL measurements, 1 mL of each emulsifier solution/dispersion, water (negative control), or sodium lauryl sulfate (SLS) (positive control) was applied to the respective skin samples. Each donor compartment was then covered with a piece of parafilm to reduce evaporation. After a four-hour incubation, the second TEWL measurement was performed. A prior article from our group provides a thorough discussion of the strategy for the incubation of skin samples (Liu and Lunter, 2020). Experiments were performed in triplicate.

2.5. Measurement of trans-epidermal water loss (TEWL)

The TEWL was measured by basic device Multi Probe Adapter MPA 6 and probe In-vitro-Tewameter® VT 310 (Courage & Khazaka electronic GmbH, D-Köln, Germany), and calculated by the respective software. Room temperature was 22 °C and relative humidity (RH) was 25 %

(Klima logg pro TFA 30.3039 IT; Dostmann GmbH & Co. KG, D-Wertheim, Germany). Fig. 1 shows a short overview of the measurement protocol. The skin was equilibrated in the Franz cells for 30 min. Then, the Franz diffusion cell was taken out of the water bath and 2 mL PBS was taken out of the Franz diffusion cell acceptor compartment with a Sterican 21 G needle (B. Braun Melsungen AG, D-Melsungen, Germany) and 2 mL syringe Luer Lock (B. Braun Melsungen AG, D-Melsungen, Germany). This was done to facilitate subsequent handling. After taking off the skin from the donor compartment, the skin was dried with Kimtech® Science Precision Wipes white 4.4 × 8.4 in./po (11 × 21 cm) (Kimberly-Clark Professional, TX-Dallas, USA) and Gauze balls/cotton swabs (Fuhrmann GmbH, D-Much, Germany). After drying the skin, the probe was put on the acceptor compartment and the initial TEWL value was measured. After the measurement, the extracted 2 mL of PBS were put back into the Franz diffusion cell without air bubbles in the acceptor compartment and the Franz diffusion cell was put back into the water bath. Then, the measurement started with a measurement time of 90 s for each run. A minimum of five measurements were taken, which were regarded as the equilibration phase. More than five measurements were deemed necessary if the difference between three subsequent measurements exceeded $\pm 1.00 \text{ g}\cdot\text{m}^{-2}\cdot\text{h}^{-1}$. After the last measurement, the probe was taken off and the donor chamber was put back. The respective solution was applied to the skin and the incubation of four hours started. Afterward, the sample solution/dispersion was discarded, the skin was dried, and the TEWL was measured, as described above. The change of TEWL is the margin of the TEWL before and after the four hours of incubation in $\text{g}\cdot\text{m}^{-2}\cdot\text{h}^{-1}$.

2.6. Incision procedure

To simulate wounded skin, incisions were made with a scalpel by cutting the skin to a different depth: superficially, down to the viable epidermis, and almost fully through the skin.

2.7. Statistical analysis

Three replicates ($n = 3$) were used to originate the data. One-way analysis of variance (ANOVA) followed by the Dunnett test was used by GraphPad Prism 8.0 to detect statistical differences (GraphPad Software Inc., La Jolla, CA, USA). Different numbers of asterisks are used to indicate significant differences: * $p < 0.05$, ** $p < 0.01$, and *** $p < 0.001$.

3. Results

Different TEWL protocols emphasized the importance of the

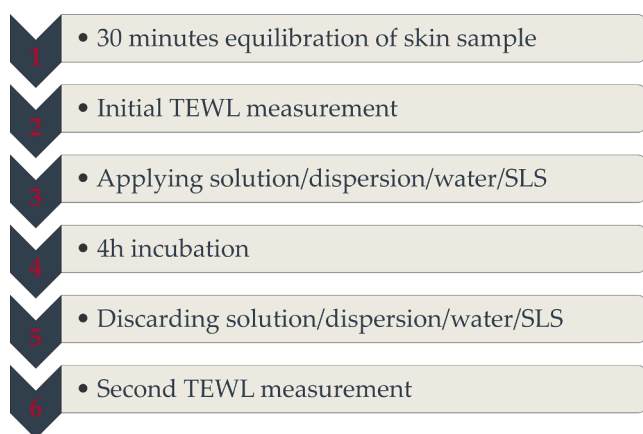


Fig. 1. Overview of *trans*-epidermal water loss (TEWL) measurement protocol. (SLS = sodium lauryl sulfate).

temperature of 32 °C, the human skin temperature, during incubation (Hopf et al., 2020). In our study, we also investigated the influence of temperature during TEWL measurement. Fig. 2a shows the result of a measurement utilizing a water-treated sample, that was performed after taking the Franz diffusion cell out of the water bath. The TEWL values decreased and sometimes increased without finding an equilibrium. Even after 15 measurements of 90 s each, no stable value was detected. To prove that the temperature is a pivotal parameter, the same water-treated sample was measured with the Franz diffusion cell remaining inside the water bath. As can be seen in Fig. 2b, the TEWL values plateaued and reached equilibrium after 14 min. The reliability of the detected values improved substantially. This shows that for *in-vitro* TEWL determination, the temperature during the measurement should not be underestimated.

After the incubation time, the removal of the emulsifier solutions/dispersions is another crucial factor. We achieved that with cotton swabs and Kimtech® tissues. In Fig. 3 the progression of TEWL values of one water-treated sample is shown measured after discarding the water but without drying, and after thorough drying with cotton swabs and Kimtech® tissues. The TEWL values of the undried measured sample stayed around $100 \text{ g}\cdot\text{m}^{-2}\cdot\text{h}^{-1}$, which is not the correct TEWL from the skin in this specific case; it just reflects the evaporation of the remaining water from the skin surface. The dried sample equilibrated during the measurement to around $30 \text{ g}\cdot\text{m}^{-2}\cdot\text{h}^{-1}$, which reflects actual *trans*-epidermal water loss. Our results reveal that no residual moisture must remain on the sample/skin surface, as this would bias the measurement. The probe is so sensitive, that every water drop will be detected, and data acquisition will be impaired. To counteract that, thorough drying of the sample surface is pivotal.

To obtain an impression of the effect of skin barrier impairment, we conducted two experiments: a) we injured the skin by cutting crosswise with a scalpel and b) we incubated the skin for several days without preservatives to initiate changes by microbial digestion. In Fig. 4, the results of the injured skin are shown. For this test, the porcine skin sample was slightly cut by a scalpel, just on the surface without cutting through the whole skin, at three different intensities. Injured sample 1 was cut only superficially, injured sample 2 was cut down to the viable epidermis, and injured sample 3 was cut down to the dermis. As expected, it is observed that injuries lead to higher TEWL values. Injured sample 1 represents a skin sample whose injury would not have been visible to the bare eye. This kind of injury might as well be present in skin samples selected for permeation testing. Here, a slightly higher TEWL (35 as opposed to $20 \text{ g}\cdot\text{m}^{-2}\cdot\text{h}^{-1}$) was obtained. With deeper cuts,

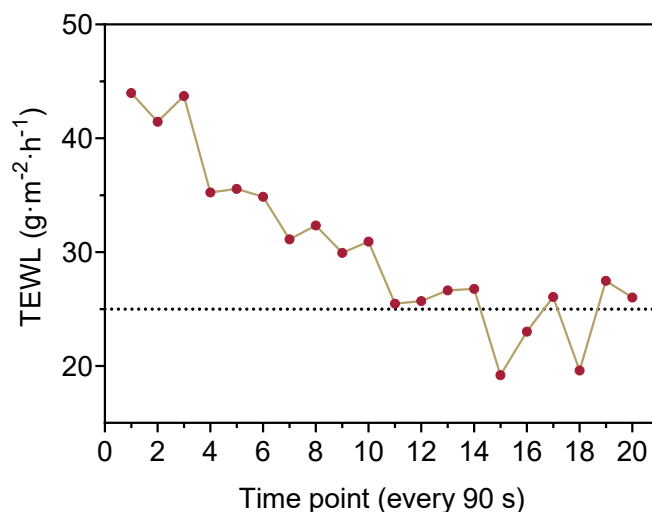


Fig. 2a. Water-treated porcine ear sample with Franz diffusion cell outside the water bath during the TEWL measurement with Tewameter® VT.

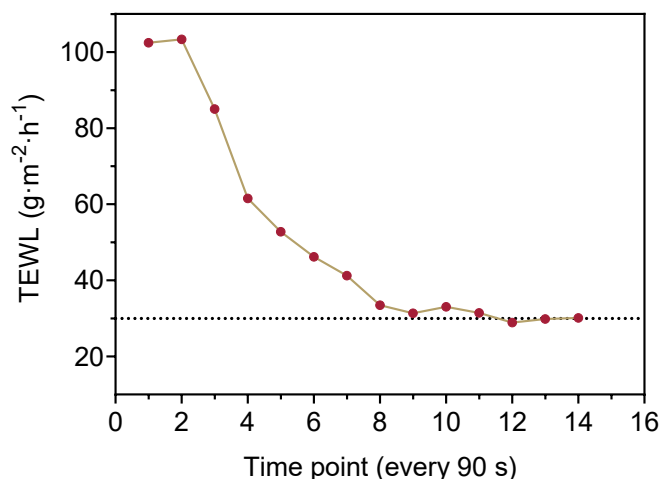


Fig. 2b. Water-treated porcine ear sample with Franz diffusion cell inside the water bath during the TEWL measurement with Tewameter® VT 310. Single values of one representative measurement.

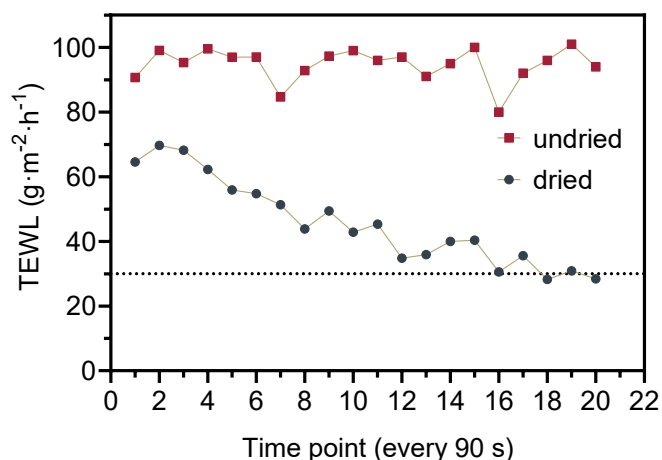


Fig. 3. TEWL measurement: an undried water-treated sample and a water-treated sample dried with a cotton swab and Kimtech® tissue. Single values of one representative measurement.

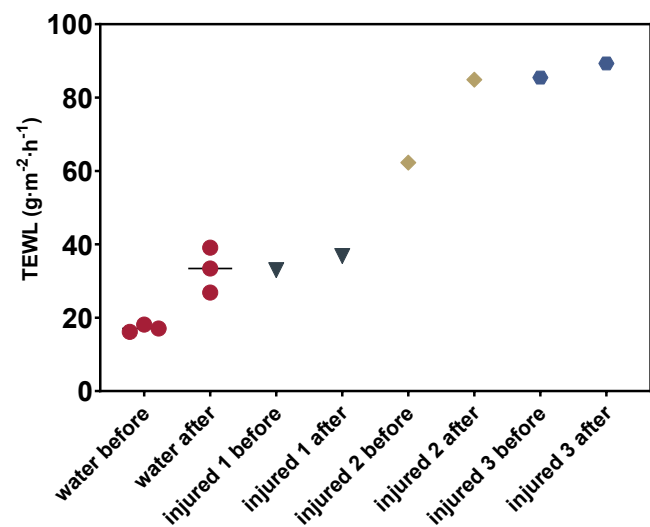


Fig. 4. TEWL-values of three water-treated samples are compared to three different water-treated injured skin samples. Symbols: single values; line: mean.

the TEWL first raised to $60 \text{ g}\cdot\text{m}^{-2}\cdot\text{h}^{-1}$ and then to around $90 \text{ g}\cdot\text{m}^{-2}\cdot\text{h}^{-1}$. Also, at the beginning, the TEWL measurement was much higher. Injuries like the one in injured skin sample 2 would be detectable by thorough visual inspection, and injuries similar to injuries in skin sample 3 would be very obvious. TEWL measurement is thus of pivotal importance to detect only slightly injured samples, not visible macroscopically. As even those slight/unseen/microscopic injuries may affect permeation, one must be sure, that the skin samples are in good condition without any injuries, and TEWL measurement is a good option to investigate this.

In a permeation experiment, the incubation time depends on the specific experimental protocol. One should be careful with long-time incubations, especially if no preservatives are added to the receptor medium, as changes due to microbial digestion may occur. Fig. 5 shows the results of a long-time experiment with three water-treated samples with measurements at $t = 0 \text{ h}$, $t = 24 \text{ h}$, $t = 48 \text{ h}$, and $t = 72 \text{ h}$. The 24- and 48-hours measurements already almost reached $50 \text{ g}\cdot\text{m}^{-2}\cdot\text{h}^{-1}$ and the maximum measurable value of around $90 \text{ g}\cdot\text{m}^{-2}\cdot\text{h}^{-1}$, which may be related to skin defects. After 72 h the TEWL decreased compared to the 48 h value. It was observed that the skin became coriaceous, which may be the reason for the evaporation of water out of the skin being restrained. The obtained TEWL values after 48 and 72 h are thus not utilizable. Overall, the incubation time should be as short as possible to avoid skin barrier impairment.

Next, we investigated the effect of emulsifiers on the TEWL value. Due to the limited number of skin samples that can be obtained per donor, we had to use two donors. To enable comparison of the results from the two donors, a water-treated sample and a sodium lauryl sulfate (SLS)-treated sample were used as negative and positive controls with each donor. As shown in Fig. 6a, the SLS-treated sample displayed a significant change in TEWL compared to the water-treated sample (9 vs 96 and 0 vs 76 $\text{g}\cdot\text{m}^{-2}\cdot\text{h}^{-1}$). SLS is well known to be stratum corneum disruptive (Törmä et al., 2008) and consequently results in ascending TEWL values. The results were thus expected. In Fig. 6b, C20 emerged as leading to the highest TEWL values among the PEG-ylated

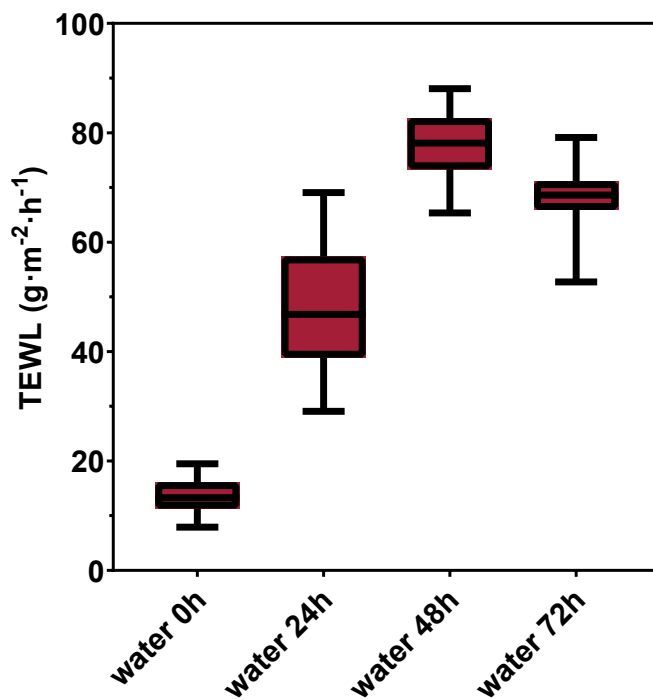


Fig. 5. Boxplots of TEWL-values of three water-treated samples measured over 72 h. The line in the middle indicates the median value, the extent of the whiskers the lowest and highest values. The lower and upper parts of the box depict the first and third quartile.

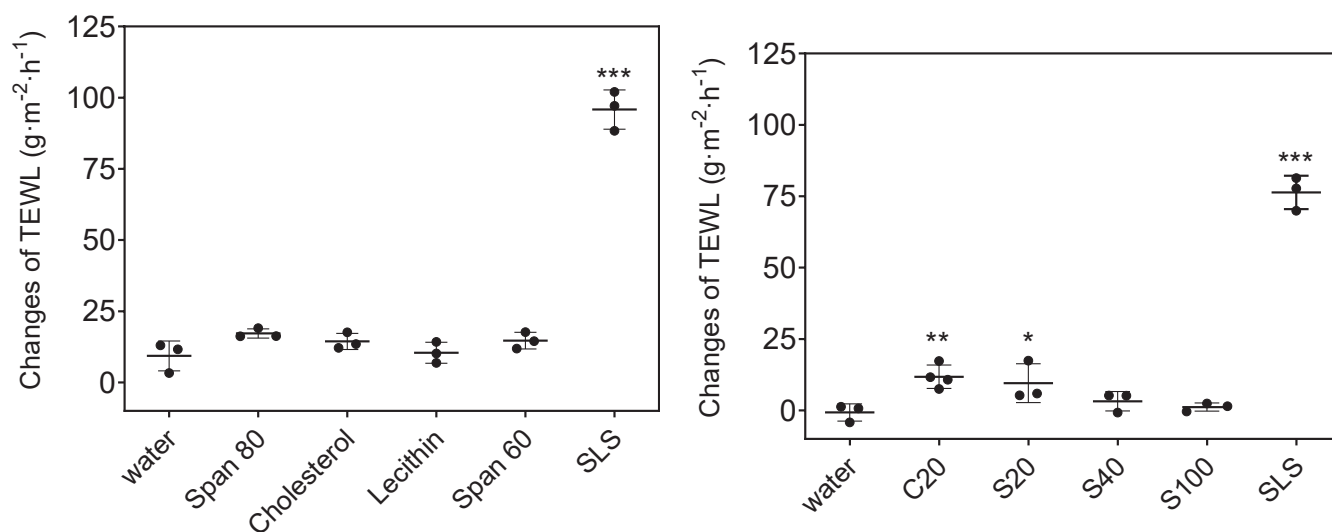


Fig. 6. A/b. TEWL-values of skin samples treated with emulsifiers or water as negative control or sodium lauryl sulfate (SLS) as positive control (a) skin from donor 1 treated with emulsifiers Span 60, Span 80, cholesterol, and lecithin (b) skin from donor 2 treated with emulsifiers C20, S20, S40, and S100; Mean \pm SD, $n \geq 3$. * $p < 0.05$, ** $p < 0.01$, *** $p < 0.001$.

emulsifiers, followed by S20, whereas S40 and S100 showed no significant distinction from the water-treated sample (Liu and Lunter, 2020). The four emulsifiers, Span 60, Span 80, cholesterol, and lecithin presented the same behavior as the water-treated sample, i.e., non-significant changes in TEWL. This behavior was expected as Span 60, Span 80, and cholesterol are w/o-emulsifiers, and our previous research also showed no significant influence of w/o-type PEG-ylated emulsifiers on stratum corneum lipids (Liu and Lunter, 2022, 2021, 2020). Lecithin has been shown in another research to be a mild emulsifier (Vater et al., 2022, 2020).

4. Discussion

SLS is a commonly used emulsifier, which is well known to be stratum corneum disruptive (Imokawa et al., 1989; Lemery et al., 2015; Mao et al., 2012; Morris et al., 2021; Törmä et al., 2008). In the current study, it was used as a positive control along with several other conventionally used emulsifiers to evaluate their effect on in-vitro TEWL. It was shown that C20 and S20 impair the skin barrier, whereas the other emulsifiers do not. The PEG-ylated emulsifiers C20, S20, S40, and S100 had already been used in our previous research. There, we found that C20 shows the most prominent effect on stratum corneum lipids, followed by S20, whereas S40 and S100 have shown no significant effects (Liu and Lunter, 2020). As the skin barrier is connected to the stratum corneum lipids to a great extent, we expected C20 and S20 to have an impact on TEWL as well. Comparing the effects of the PEGylated emulsifiers, the current results corresponded to our previous measurements by confocal Raman spectroscopy (CRS) (Liu and Lunter, 2020; Zhang and Lunter, 2018). In this previous study, we also found that C20 is as disruptive to the stratum corneum lipids content and conformation, as SLS (Liu et al., 2022; Liu and Lunter, 2022, 2021, 2020). The TEWL value of the skin sample treated with C20 is significantly elevated but not as much as that of the sample treated with SLS. When interpreting the results of the current study in conjunction with our previous studies on the impact of emulsifiers on the stratum corneum lipids (Zhang and Lunter 2018, Liu et al., 2022, Liu and Lunter, 2022, 2021, 2020), we can conclude that PEGylated emulsifiers with PEG- units below 10 and above 40 are well tolerated. Lecithin, as discussed in numerous literature exhibits beneficial effects on the skin. And, as our current results show, sorbitan esters also do not impair the skin barrier function as measured by TEWL. It can thus be concluded that stratum corneum lipids assessment does not give the full picture of skin barrier disruption even though stratum corneum

lipids are known to be of utmost importance to the skin barrier function. Further research will be conducted to evaluate the underlying mechanism.

The TEWL data indicated, that not only the skin was altered due to the emulsifier during the incubation process, but the skin itself also showed an alteration during the incubation. The EMA requests the integrity of the skin to be monitored during in-vitro testing, e.g. by TEWL measurement. One may assume that the background of this request is to show that the skin samples are not degraded e.g., due to microbiological digestion. Our results show that it would be misleading to expect zero change in TEWL during incubation. We, therefore, conclude that it has to be considered carefully, how the skin quality influences the TEWL value at the beginning of the experiment and which changes over the incubation period measurements are acceptable. We, therefore, recommend always including untreated samples in the TEWL measurement.

The integrity of skin samples should always be revised before the start of the experiment. Small injuries, which are not visible, can influence TEWL values and lead to false and higher values. These effects are also pivotal for shaving, electric epilation, and waxing (Pany et al., 2018) or damage by tape stripping (Simonsen and Fullerton, 2007) or organic solvents (Barba et al., 2019). In-vitro burn scars (Gardien et al., 2016) or other damage (du Plessis et al., 2013) can change TEWL values as well. The skin damage increased the TEWL values. Small skin damage led to values higher than water samples after incubation time, while intermediate and deep damages led to higher values than the positive control SLS. Like other authors (Barba et al., 2019; Ilić et al., 2019; Pany et al., 2018), we do not just recommend the starting TEWL value to be beyond $20 \text{ g}\cdot\text{m}^{-2}\cdot\text{h}^{-1}$, and we also recommend the change of TEWL to be below.

$20 \text{ g}\cdot\text{m}^{-2}\cdot\text{h}^{-1}$. Small injuries are already similar to the influence of the emulsifier C20. This emulsifier is a potent penetration enhancer (Liu et al., 2022; Liu and Lunter, 2022, 2021, 2020). Thus, we expect small injuries, not visible to the bare eye, to also lead to enhanced penetration. Table 1 summarizes the most important conditions for in vitro TEWL measurements.

5. Conclusion

Emulsifier solutions/dispersions were characterized by TEWL measurements. It was found that C20 and S20 showed significant negative effects on stratum corneum, which became evident in higher TEWL

Table 1
Most important conditions for in vitro TEWL measurements.

Aspect	Condition
Equilibration of skin	30 min
Dried skin for measurement	With Kimtech® and cotton swabs
Skin temperature	Maintain at 32 °C also during measurements
TEWL single measurement-time	90 s
Equilibration of TEWL measurements	Minimum 5 times 90 s each
Intact skin	TEWL change < 20 g·m ⁻² ·h ⁻¹
Incubation of skin	4 h
Removal of formulation	Kimtech® and cotton swabs
Second TEWL measurements	Dried skin

values. Furthermore, TEWL influencing aspects were analyzed and skin injuries and incubation time turned out to be crucial together, with thorough removal of the solutions from the skin samples prior to the measurement. The EMA guideline neither requests zero TEWL-changes nor does it recommend upper limits. Our results presented an overview of the main critical aspects and illustrated the importance of TEWL measurements in skin research and recommends an upper limit for acceptable TEWL-changes. TEWL measurement should always be used for skin experiments to control the intactness of the skin before any treatment. Furthermore, skin formulations should be tested regarding their impact on TEWL, to determine their influence on skin barrier function at an early stage of formulation development.

Statement of ethics.

Porcine ears were obtained from the University Hospital Tuebingen's Department of Experimental Medicine. The ethical committee at University Hospital Tuebingen allowed the use of live animals and their sacrifice in the Department of Experimental Medicine's experiments. These ears were acquired after the animal's death. Before the study, the Department of Pharmaceutical Technology was registered with the District Office of Tuebingen to utilize animal products (registration number: DE 08 416 1052 21).

CRediT authorship contribution statement

Hans Schoenfelder: Investigation, Data curation, Writing – original draft. **Yali Liu:** Investigation, Data curation, Writing – review & editing. **Dominique Jasmin Lunter:** Conceptualization, Methodology, Supervision, Resources, Writing – review & editing.

Declaration of Competing Interest

The authors declare that they have no known competing financial interests or personal relationships that could have appeared to influence the work reported in this paper.

Data availability

The data that has been used is confidential.

Acknowledgments

Martin Schenk at the Institute of Experimental Medicine of the University of Tuebingen is acknowledged for the donation of pig ears. Yali Liu was supported by the China Scholarship Council.

References

Akdeniz, M., Gabriel, S., Lichterfeld-Kottner, A., Blume-Peytavi, U., Kottner, J., 2018. Transepidermal water loss in healthy adults: a systematic review and meta-analysis update. *Br. J. Dermatol.* <https://doi.org/10.1111/bjd.17025>.
Alexander, H., Brown, S., Danby, S., Flohr, C., 2018. Research Techniques Made Simple: Transepidermal Water Loss Measurement as a Research Tool. *J. Invest. Dermatol.* <https://doi.org/10.1016/j.jid.2018.09.001>.

Barba, C., Alonso, C., Martí, M., Carrer, V., Yousef, I., Coderch, L., 2019. Selective modification of skin barrier lipids. *J Pharm Biomed Anal* 172, 94–102. <https://doi.org/10.1016/j.jpba.2019.04.040>.
Cristiano, M.C., Froio, F., Mancuso, A., Iannone, M., Fresta, M., Fiorito, S., Celia, C., Paolino, D., 2020. In vitro and in vivo trans-epidermal water loss evaluation following topical drug delivery systems application for pharmaceutical analysis. *J Pharm Biomed Anal* 186. <https://doi.org/10.1016/j.jpba.2020.113295>.
Daugimont, L., Baron, N., Vandermeulen, G., Pavselj, N., Miklavcic, D., Jullien, M.C., Cabodevila, G., Mir, L.M., Pr at, V., 2010. Hollow microneedle arrays for intradermal drug delivery and DNA electroporation. *J. Membr. Biol.* 236, 117–125. <https://doi.org/10.1007/s00232-010-9283-0>.
di Nardo, A., Wertz, P., Giannetti, A., Seidenari, S., 1998. Ceramide and Cholesterol Composition of the Skin of Patients with Atopic Dermatitis. *Acta Derm Venereol (Stockh)*.
du Plessis, J., Stefaniak, A., Eloff, F., John, S., Agner, T., Chou, T.C., Nixon, R., Steiner, M., Franken, A., Kudla, I., Holness, L., 2013. International guidelines for the in vivo assessment of skin properties in non-clinical settings: Part 2. transepidermal water loss and skin hydration. *Skin Res. Technol.* 19, 265–278. <https://doi.org/10.1111/srt.12037>.
Fda, Cder, hills, 2019. Transdermal and Topical Delivery Systems-Product Development and Quality Considerations Guidance for Industry DRAFT GUIDANCE.
Fokuhl, J., M uller-Goymann, C.C., 2013. Modified TEWL in vitro measurements on transdermal patches with different additives with regard to water vapour permeability kinetics. *Int J Pharm* 444, 89–95. <https://doi.org/10.1016/j.ijpharm.2013.01.035>.
Gardien, K.L.M., Baas, D.C., de Vet, H.C.W., Middelkoop, E., 2016. Transepidermal water loss measured with the Tewameter TM300 in burn scars. *Burns* 42, 1455–1462. <https://doi.org/10.1016/j.burns.2016.04.018>.
Gomaa, Y.A., Morrow, D.I.J., Garland, M.J., Donnelly, R.F., El-Khordagui, L.K., Meidan, V.M., 2010. Effects of microneedle length, density, insertion time and multiple applications on human skin barrier function: Assessments by transepidermal water loss. *Toxicol. In Vitro* 24, 1971–1978. <https://doi.org/10.1016/j.tiv.2010.08.012>.
Groen, D., Poole, D.S., Gooris, G.S., Bouwstra, J.A., 2011. Investigating the barrier function of skin lipid models with varying compositions. *Eur. J. Pharm. Biopharm.* 79, 334–342. <https://doi.org/10.1016/j.ejpb.2011.05.007>.
Hadgraft, J., Lane, M.E., 2009. Transepidermal water loss and skin site: A hypothesis. *Int J Pharm* 373, 1–3. <https://doi.org/10.1016/j.ijpharm.2009.02.007>.
Hahn, T., Hansen, S., Neumann, D., Kostka, K.H., Lehr, C.M., Muys, L., Schaefer, U.F., 2010. Infrared densitometry: A fast and non-destructive method for exact stratum corneum depth calculation for in vitro tape-stripping. *Skin Pharmacol Physiol* 23, 183–192. <https://doi.org/10.1159/000288165>.
Hopf, N.B., Champmartin, C., Schenk, L., Berthel, A., Chedik, L., du Plessis, J.L., Franken, A., Frasc, F., Gaskin, S., Johanson, G., Julander, A., Kasting, G., Kilo, S., Larese Filon, F., Marquet, F., Midander, K., Reale, E., Bunge, A.L., 2020. Reflections on the OECD guidelines for in vitro skin absorption studies. *Regul. Toxicol. Pharm.* <https://doi.org/10.1016/j.yrtph.2020.104752>.
Ilić, T., Savić, Sanela, Pantelić, I., Marković, B., Savić, Snežana, 2019. DEVELOPMENT OF SUITABLE WORKING PROTOCOL FOR IN VITRO TAPE STRIPPING: A CASE STUDY WITH BIOCOMPATIBLE ACECLOFENAC-LOADED TOPICAL NANOEMULSIONS. Symposium on Pharmaceutical Engineering Research SPHER 25–27. 10.24355/dbbs.084-202001221146-0.
Imokawa, G., Akasaki, S., Minematsu, Y., Kawai, M., 1989. Importance of intercellular lipids in water-retention properties of the stratum corneum: induction and recovery study of surfactant dry skin. *Arch Dermatol Res* 281, 45–51. <https://doi.org/10.1007/BF00424272>.
Jacobi, U., Kaiser, M., Toll, R., Mangelsdorf, S., Audring, H., Otberg, N., Sterry, W., Lademann, J., 2007. Porcine ear skin: An in vitro model for human skin. *Skin Res. Technol.* 13, 19–24. <https://doi.org/10.1111/j.1600-0846.2006.00179.x>.
Khosrowpour, Z., Ahmad Nasrollahi, S., Ayatollahi, A., Samadi, A., Firooz, A., 2019. Effects of four soaps on skin trans-epidermal water loss and erythema index. *J Cosmet Dermatol* 18, 857–861. <https://doi.org/10.1111/jocd.12758>.
Klang, V., Schwarz, J.C., Lenobel, B., Nadj, M., Auböck, J., Wolzt, M., Valenta, C., 2012. In vitro vs. in vivo tape stripping: Validation of the porcine ear model and penetration assessment of novel sucrose stearate emulsions. *Eur. J. Pharm. Biopharm.* 80, 604–614. <https://doi.org/10.1016/j.ejpb.2011.11.009>.
Kottner, J., Lichterfeld, A., Blume-Peytavi, U., 2013. Transepidermal water loss in young and aged healthy humans: A systematic review and meta-analysis. *Arch Dermatol Res* 305, 315–323. <https://doi.org/10.1007/s00403-012-1313-6>.
Latifi, S., Tamayol, A., Habibey, R., Sabzevari, R., Kahn, C., Geny, D., Eftekharpour, E., Annabi, N., Blau, A., Linder, M., Arab-Tehrany, E., 2016. Natural lecithin promotes neural network complexity and activity. *Sci Rep* 6. <https://doi.org/10.1038/srep25777>.
Lemery, E., Brianc on, S., Chevalier, Y., Oddos, T., Gohier, A., Boyron, O., Bolzinger, M.-A., 2015. Surfactants have multi-fold effects on skin barrier function. *Eur. J. Dermatol.* 25, 424–435. <https://doi.org/10.1684/ejd.2015.2587>.
Levang, A.K., Zhao, K., Singh, J., 1999. Effect of ethanol/propylene glycol on the in vitro percutaneous absorption of aspirin, biophysical changes and macroscopic barrier properties of the skin. *International Journal of Pharmaceutics*.
Levin, J., Maibach, H., 2005. The correlation between transepidermal water loss and percutaneous absorption: An overview. *J. Control. Release.* <https://doi.org/10.1016/j.jconrel.2004.11.035>.
Liu, Y., Ilić, T., Pantelić, I., Savić, S., Lunter, D.J., 2022. Topically applied lipid-containing emulsions based on PEGylated emulsifiers: Formulation, characterization, and evaluation of their impact on skin properties ex vivo and in vivo. *Int J Pharm* 626, 122202. <https://doi.org/10.1016/j.ijpharm.2022.122202>.

- Liu, Y., Lunter, D.J., 2020. Systematic investigation of the effect of non-ionic emulsifiers on skin by confocal raman spectroscopy—a comprehensive lipid analysis. *Pharmaceutics* 12. <https://doi.org/10.3390/pharmaceutics12030223>.
- Liu, Y., Lunter, D.J., 2021. Profiling skin penetration using PEGylated emulsifiers as penetration enhancers via confocal Raman spectroscopy and fluorescence spectroscopy. *Eur. J. Pharm. Biopharm.* 166, 1–9. <https://doi.org/10.1016/j.ejpb.2021.04.027>.
- Liu, Y., Lunter, D.J., 2022. Confocal Raman spectroscopy at different laser wavelengths in analyzing stratum corneum and skin penetration properties of mixed PEGylated emulsifier systems. *Int J Pharm* 616, 121561. <https://doi.org/10.1016/j.ijpharm.2022.121561>.
- Lunter, D.J., 2016. How confocal is confocal raman microspectroscopy on the skin? Impact of microscope configuration and sample preparation on penetration depth profiles. *Skin Pharmacol Physiol* 29, 92–101. <https://doi.org/10.1159/000444806>.
- Machado, M., Salgado, T.M., Hadgraft, J., Lane, M.E., 2010. The relationship between transepidermal water loss and skin permeability. *Int J Pharm* 384, 73–77. <https://doi.org/10.1016/j.ijpharm.2009.09.044>.
- Mao, G., Flach, C.R., Mendelsohn, R., Walters, R.M., 2012. Imaging the distribution of sodium dodecyl sulfate in skin by confocal raman and infrared microspectroscopy. *Pharm Res* 29, 2189–2201. <https://doi.org/10.1007/s11095-012-0748-y>.
- Medicines Agency, E., 2014. Committee for Medicinal Products for Human Use (CHMP) Guideline on quality of transdermal patches.
- Medicines Agency, E., 2018. Draft guideline on quality and equivalence of topical products.
- Morris, S.A.V., Xu, L., Ananthapadmanabhan, K.P., Kasting, G.B., 2021. Surfactant Penetration into Human Skin from Sodium Dodecyl Sulfate and Lauramidopropyl Betaine Mixtures. *Langmuir* 37, 14006–14014. <https://doi.org/10.1021/acs.langmuir.1c01867>.
- Nangia, S., Paul, V.K., Deorari, A.K., Sreenivas, V., Agarwal, R., Chawla, D., 2015. Topical oil application and trans-epidermal water loss in preterm very low birth weight infants—a randomized trial. *J Trop Pediatr* 61, 414–420. <https://doi.org/10.1093/tropej/fmv049>.
- Pany, A., Klang, V., Brunner, M., Ruthofer, J., Schwarz, E., Valenta, C., 2018. Effect of physical and chemical hair removal methods on skin barrier function in vitro: Consequences for a hydrophilic model permeant. *Skin Pharmacol Physiol* 32, 8–21. <https://doi.org/10.1159/000493168>.
- Pinnagoda, J., Tupker, R.A., Agner, T., Serup, J., 1990. Guidelines for transepidermal water loss (TEWL) measurement A Report from the Standardization Group of the European Society of Contact Dermatitis. *Contact Dermatitis*.
- Simonsen, L., Fullerton, A., 2007. Development of an in vitro skin permeation model simulating atopic dermatitis skin for the evaluation of dermatological products. *Skin Pharmacol. Physiol.* 230–236. <https://doi.org/10.1159/000104421>.
- Steiner, M., Aikman-Green, S., Prescott, G.J., Dick, F.D., 2011. Side-by-side comparison of an open-chamber (TM 300) and a closed-chamber (Vapometer™) transepidermal water loss meter. *Skin Res. Technol.* 17, 366–372. <https://doi.org/10.1111/j.1600-0846.2011.00509.x>.
- Stracke, F., Weiss, B., Lehr, C.M., König, K., Schaefer, U.F., Schneider, M., 2006. Multiphoton microscopy for the investigation of dermal penetration of nanoparticle-borne drugs. *J. Invest. Dermatol.* 126, 2224–2233. <https://doi.org/10.1038/SJ.JID.5700374>.
- Tfaily, S., Gobinet, C., Josse, G., Angiboust, J.F., Manfait, M., Piot, O., 2012. Confocal Raman microspectroscopy for skin characterization: A comparative study between human skin and pig skin. *Analyst* 137, 3673–3682. <https://doi.org/10.1039/c2an16292j>.
- Törmä, H., Lindberg, M., Berne, B., 2008. Skin barrier disruption by sodium lauryl sulfate-exposure alters the expressions of involucrin, transglutaminase 1, profilaggrin, and kallikreins during the repair phase in human skin in vivo. *J. Invest. Dermatol.* 128, 1212–1219. <https://doi.org/10.1038/sj.jid.5701170>.
- Vater, C., Hlawaty, V., Werdenits, P., Cichoń, M.A., Klang, V., Elbe-Bürger, A., Wirth, M., Valenta, C., 2020. Effects of lecithin-based nanoemulsions on skin: Short-time cytotoxicity MTT and BrdU studies, skin penetration of surfactants and additives and the delivery of curcumin. *Int J Pharm* 580, 119209. <https://doi.org/10.1016/j.ijpharm.2020.119209>.
- Vater, C., Apanovic, A., Riethmüller, C., Litschauer, B., Wolzt, M., Valenta, C., Klang, V., 2021. Changes in skin barrier function after repeated exposition to phospholipid-based surfactants and sodium dodecyl sulfate in vivo and corneocyte surface analysis by atomic force microscopy. *Pharmaceutics* 13. <https://doi.org/10.3390/pharmaceutics13040436>.
- Vater, C., Bosch, L., Mitter, A., Göls, T., Seiser, S., Heiss, E., Elbe-Bürger, A., Wirth, M., Valenta, C., Klang, V., 2022. Lecithin-based nanoemulsions of traditional herbal wound healing agents and their effect on human skin cells. *Eur. J. Pharm. Biopharm.* 170, 1–9. <https://doi.org/10.1016/j.ejpb.2021.11.004>.
- Wilson, D., Berardesca, E., Maibach, H.I., Berardesca, E., 1988. In vitro transepidermal water loss: differences between black and white human skin. *Br. J. Dermatol.*
- Zhang, Z., Lunter, D.J., 2018. Confocal Raman microspectroscopy as an alternative method to investigate the extraction of lipids from stratum corneum by emulsifiers and formulations. *Eur. J. Pharm. Biopharm.* 127, 61–71. <https://doi.org/10.1016/j.ejpb.2018.02.006>.

4. Development and characterization of topical formulation for maintenance therapy containing sorbitan monostearate with and without PEG-100-stearate

Development and characterization of topical formulation for maintenance therapy containing sorbitan monostearate with and without PEG-100-stearate

Hans Schoenfelder  | Yvonne Wiedemann | Dominique Jasmin Lunter

Department of Pharmaceutical Technology, Faculty of Science, Eberhard Karls Universität Tübingen, Tuebingen, Germany

Correspondence

Dominique Jasmin Lunter, Department of Pharmaceutical Technology, Faculty of Science, Eberhard Karls Universität Tübingen, Auf der Morgenstelle 8, Tuebingen 72076, Germany.
Email: dominique.lunter@uni-tuebingen.de

Abstract

Objective: Basic therapy is an integral part of the treatment of chronic skin diseases. However, the formulation of skin products should be analysed with respect to the physical stability and tolerance by the patients before applying them to diseased skin. In particular, the suitability of the formulation for use on damaged skin should be taken into consideration so that no exacerbation of the condition is caused.

Methods: The following approach investigated two formulations with the emulsifier sorbitan monostearate and one with the addition of polyethylene glycol 100 stearyl ether. The characterization included rheology, macroscopic and microscopic cream analysis compared to marketed products for basic therapy. Pyranine staining of stratum corneum (SC) and trans-epidermal water loss (TEWL) measurements were performed with ex vivo porcine SC to assess skin barrier function.

Results: The rheological characterization showed a gel-like, viscoelastic behaviour of the formulations and a viscosity in the same order of magnitude as the marketed products. Staining with pyranine revealed that skin damage caused by sodium lauryl sulfate was compensated by treatment with the developed formulations. Following the same trend, TEWL results clearly showed decreasing values, which evidence improved skin barrier function.

Conclusion: In conclusion, the developed sorbitan monostearate formulations can potentially improve deficient skin barrier function as a part of basic therapy of skin diseases and act as a superior alternative to market products comprising a minimum of well-chosen ingredients.

KEYWORDS

basic therapy, formulation/stability, skin barrier, skin physiology/structure, sorbitan ester, trans-epidermal water loss

This is an open access article under the terms of the [Creative Commons Attribution](https://creativecommons.org/licenses/by/4.0/) License, which permits use, distribution and reproduction in any medium, provided the original work is properly cited.

© 2024 The Author(s). *International Journal of Cosmetic Science* published by John Wiley & Sons Ltd on behalf of Society of Cosmetic Scientists and Societe Francaise de Cosmetologie.

Résumé

Objectif: la thérapie de base fait partie intégrante du traitement des maladies chroniques de la peau. Cependant, la formulation des produits pour la peau doit être analysée en termes de stabilité physique et de tolérance par les patients avant de les appliquer sur la peau malade. En particulier, il convient de prendre en compte l'adéquation de la formulation à être utilisée sur une peau lésée afin d'éviter toute exacerbation de l'affection.

Méthodes: l'approche suivante a étudié deux formulations avec l'émulsifiant monostéarate de sorbitane et une autre avec l'ajout d'éther de stéaryle de polyéthylène glycol 100. La caractérisation comprenait la rhéologie, l'analyse macroscopique et microscopique de la crème par rapport aux produits commercialisés pour la thérapie de base. Une coloration à la pyranine de la couche cornée et des mesures de la perte d'eau transépidermique ont été effectuées avec des couches cornées ex vivo de porc pour évaluer la fonction de barrière cutanée.

Résultats: la caractérisation rhéologique a montré un comportement viscoélastique de type gel des formulations et une viscosité du même ordre de grandeur que les produits commercialisés. La coloration à la pyranine a révélé que les lésions cutanées causées par le laurylsulfate de sodium étaient compensées par le traitement avec les formulations développées. Suivant la même tendance, les résultats de la perte d'eau transépidermique ont clairement montré des valeurs en baisse, ce qui témoigne de l'amélioration de la fonction de barrière cutanée.

Conclusion: en conclusion, les formulations de monostéarate de sorbitane développées peuvent potentiellement améliorer la fonction de barrière cutanée déficiente dans le cadre d'une thérapie de base des maladies de la peau et constituer une alternative supérieure.

INTRODUCTION

The treatment of various chronic skin diseases is a significant challenge. The most common therapies combine basic therapy with API- (active pharmaceutical ingredient) containing formulations [1–3]. Basic therapy involves applying nourishing topical products with or without special additives to improve or assist the therapy of skin diseases [2]. Cosmetic products are commonly applied in various galenic forms, mostly creams or ointments. The composition of a formulation offers various possibilities but also poses grand challenges. Specifically, the used ingredients should be examined for their effects on skin. Emulsifiers like sodium lauryl sulfate (SLS) turned out to be skin-disruptive [4–8]. Zhang, Liu, and Lunter characterized alternative emulsifiers for dermal application with respect to their potential to extract lipids from the skin and thus impair skin barrier function. Most of the investigated emulsifiers turned out to be non-skin-irritative. However, some emulsifiers, like C20 (Polyethylene glycol-20 cetyl ether), did impair the skin barrier function [9–13]. The objective of the following study was to develop formulations for

basic therapy that contain a minimum of selected ingredients, including non-skin-irritative emulsifiers to support the treatment as much as possible. Psoriasis and dermatitis could be a potential field of use. The hydrophilic formulations contain rather large amounts of the oil phase, which in turn contains a relevant amount of white soft paraffin, which may exert a semi-occlusive effect on the skin; thus, the formulation will be suitable for rather dry skin. Two formulations were developed with the emulsifier sorbitan monostearate (HLB 5 due to Croda). One formulation contained only sorbitan monostearate as emulsifier while the second formulation, additionally, contained polyethylene glycol 100 stearyl ether (S100) (HLB 19 due to Croda). S100 was also analysed in the past and found to be skin-friendly [14]. The skin thickness and lipid content, measured by confocal Raman microscopy, were not reduced in comparison to other PEGs. So it was concluded not to extract lipids from the skin. Linoleic acid and cholesterol were added in an equimolar ratio similar to their natural occurrence in skin to substitute for the decreased lipids content of diseased skin [9, 13]. Medium-chain triglycerides (MCT) were used as oil phase and are also proven to improve skin

TABLE 1 Overview of formulations (*F*) regarding composition. *R* stands for recipe and final version used for rheology, TEWL measurement, and staining.

	F1-1	F1-2/R1	F2-1	F2-2	F2-3/R2
White soft paraffin	65%	40%	50%	50%	35%
Cholesterol	0.13%	0.13%	0.13%	0.13%	0.13%
Linoleic acid	0.085%	0.085%	0.085%	0.085%	0.085%
Span 60	5%	5%	1%	5%	5%
S100	–	–	1%	5%	5%
MCT 312	10%	10%	10%	10%	10%
Water	Ad 100%	Ad 100%	Ad 100%	Ad 100%	Ad 100%
Time	2 min	2 min	2 min	2 min	2 min
rpm	1000 rpm	1000 rpm	1000 rpm	1000 rpm	1000 rpm
Phasing	O/W	O/W	O/W	O/W	O/W

health [15]. The combination of linoleic acid, cholesterol, and MCT can be seen as the components that improve skin barrier function. White soft paraffin was used to obtain a cream of medium viscosity. The formulations were then characterized by their rheological behaviour, macroscopic and microscopic appearance, physical stability and the ability to improve the skin barrier function. TEWL measurements were used to this end in combination with pyranine staining to visualize the lipids in the SC [9, 16].

MATERIALS AND METHODS

Materials

SLS, sodium chloride and potassium chloride were obtained from Caesar & Loretz GmbH (D-Hilden, Germany). Disodium-hydrogen phosphate and potassium-di-hydrogen phosphate were obtained from Carl Roth GmbH & Co. KG (D-Karlsruhe, Germany). MCT (medium-chain triglycerides, Myritol® 312) were obtained from BASF (D-Ludwigshafen, Germany). Sorbitan ester sorbitan monostearate (Span 60) and Brij S100 (Polyethylene glycol 100 stearyl ether) were purchased from Croda GmbH (D-Nettetal, Germany). Methyl orange was obtained from Merck KGaA (D-Darmstadt, Germany). Blue-violet (Dragocolor® KSMFST) was obtained from Symrise AG (D-Holzminden, Germany). Trypsin (from porcine pancreas, lyophilized powder, type II-S) and trypsin inhibitor (from glycine max [soybean], lyophilized powder) were obtained from Sigma (Sigma-Aldrich Chemie GmbH, D-Steinheim, Germany). Linoleic acid was obtained from Thermo Scientific (Thermo Fisher Scientific GmbH, GB-Heysham, Great Britain). Pyranine was obtained from Alfa Aesar (GB-Heysham, Great Britain). White soft paraffin (Vaseline album) was obtained from Hansen & Rosenthal GmbH & Co. KG (D-Hamburg, Germany). Lipo Lotio Cordes® was obtained from Ichthyol-Gesellschaft (Cordes, Hermann & Co., GmbH & Co. KG, D-Hamburg, Germany). CeraVe moisturizing creme was obtained from

L'Oréal Deutschland GmbH (D-Düsseldorf, Germany). Alfason® Repair was obtained from Karo Pharma AB (S-Stockholm, Sweden). Parafilm® was obtained from Bemis Company Inc. (WI-Oshkosh, USA). Ultra-pure water was generated by Elga Maxima (GB-High Wycombe, Great Britain). Phosphate-buffered saline (PBS) was prepared using sodium chloride and potassium chloride obtained from Caesar & Loretz GmbH (D-Hilden, Germany), disodium-hydrogen phosphate, and potassium-di-hydrogen phosphate obtained from Carl Roth GmbH & Co. KG (D-Karlsruhe, Germany). Porcine ear skins (German landrace; age: 15–30 weeks; weight: 40–64 kg) were provided by a local butcher. The Department of Pharmaceutical Technology at the University of Tuebingen has been registered for the use of animal products (registration number: DE 08416105221).

Preparation of formulations and solutions

The two different formulations were manufactured by a mixing system (Topitec Automatic, Wepa Apothekenbedarf GmbH & Co KG, D-Hillscheid, Germany). The compositions are listed in Table 1. The oil phase was heated to 80°C and then cooled to room temperature under stirring. After combining the water and oil phases, both after cooling down to room temperature, they were mixed. As mixing parameters 2, 4 and 6 min at 1000, 1500 and 2000 rpm mixing speed were evaluated. The optimal configuration was set to 4 min and 1500 rpm.

An SLS solution was used to impair the skin barrier. It consisted of 1% SLS (w/w) in an aqueous solution.

Formulation characterization

Rheological measurements were carried out using a Physica MCR 501 rheometer (Anton Paar GmbH, AT-Graz, Austria) with a plate/plate geometry (PP 25; diameter: 25 mm; gap size: 0.2 mm). The temperature was

maintained at 32°C for all measurements to simulate skin temperature. After the samples were applied to the plate, the recovery and equilibrating time of 2 min was set. To determine the dynamic viscosity η , the shear stress was measured as a function of the shear rate in the 1–1000 s⁻¹ range. An oscillatory amplitude sweep test was performed in the strain range of 1–1000% deformation and a frequency of 6.28 rad s⁻¹ to analyse the viscoelastic behaviour. The linear viscoelastic (LVE) range was determined. Subsequently, the frequency sweep tests were conducted in the angular frequency (ω) range of 100–1 rad s⁻¹ and a strain amplitude of 1% deformation. The viscoelastic characteristics were revealed by the storage modulus (G') and loss modulus (G''). All measurements were performed in triplicate [13].

The phasing of the creams was investigated using the water-soluble dye methyl orange and the oil-soluble dye blue-violet to stain the water or oil phase, respectively.

Optical microscopy

The formulations were characterized by a polarization microscope (Microscope Axio Imager Z1, Carl Zeiss AG, D-Oberkochen, Germany) with a 20× objective (numerical aperture 0.8, Plan-Apochromat, Carl Zeiss AG, D-Oberkochen, Germany) and respective software Zeiss Zen Blue (Carl Zeiss AG, D-Oberkochen, Germany). The formulations were examined for homogeneity and the presence of cholesterol needles [13].

Porcine ear skin preparation

Porcine skin was chosen as a surrogate for human skin [17, 18] because the skin is histologically and morphologically comparable to human skin [19]. The skin was prepared as described in earlier publications of our group [20, 21]. Fresh pig ears were cleaned with isotonic saline. Full-thickness skin was removed from the cartilage, and blood was removed with isotonic saline and cotton swabs. The obtained postauricular skin was dried with soft tissue and sliced into strips of about 3 cm in width. The skin was stretched onto a Styrofoam plate to reduce the impact of wrinkles. With an electric hair trimmer (QC5115/15 Philips Electronics, NL-Eindhoven, The Netherlands), bristles were cut to about 0.5 mm in length. After being dermatomed to a thickness of 1.0 mm (Dermatom GA 630 Acculan 3 TI Aesculap AG & Co. KG, D-Tuttlingen, Germany), the skin was punched out into circles of 25 mm diameter and placed in the freezer at minus 28°C wrapped in aluminium foil. On the day of the experiment, the

samples were thawed to room temperature on paper tissue soaked with PBS [21].

Incubation of skin samples in Franz diffusion cells

Franz diffusion cells are a typical type of analytical setup for determining skin absorption *ex vivo*, and the method described herein has been used extensively by our group in the past, as described in previous publications [9, 10, 20, 21]. Prior articles from our group thoroughly discuss the strategy for incubating skin samples with emulsifiers [10, 22]. Franz diffusion cells (Gauer Glas, D-Püttlingen, Germany) were filled with 12 mL degassed, prewarmed (32°C) PBS as the receptor fluid. The skin samples were put on top of the acceptor compartments, and the donor compartments were placed on top of the skin. The Franz diffusion cells were placed in a water bath at 32°C (Lauda type Alpha, Lauda Dr. R. Wobser GmbH & Co. KG, D-Lauda-Königshofen, Germany). The receptor fluid was continuously stirred at a 500-rpm rate (Variomag Poly 15, Thermo-Scientific, Thermo Electron LED GmbH, D-Langensfeld, Germany). After an expeditious equilibration period of 30 min, the initial TEWL values were generated using the protocol described in 2.7. After the initial TEWL measurements, 1 mL of SLS solution was applied to the respective skin samples to induce skin barrier impairment. Each donor compartment was then covered with a piece of parafilm to reduce evaporation. After a 4-h incubation, the residual SLS solution was wiped off the skin, and the second TEWL measurement was performed [10, 22]. After that, the formulations or water were applied to the skin samples for another 4 h. Formulations were applied as previously validated using a rod made of acrylic glass with around 4 mg for each sample to mimic in-use conditions as described in Liu et al. [13]. Afterwards, another final TEWL measurement was performed. Experiments were performed in triplicate.

Measurement of trans-epidermal water loss (TEWL)

The TEWL was measured by basic device Multi Probe Adapter MPA 6 and probe In-vitro-Tewameter® VT 310 (Courage & Khazaka electronic GmbH, D-Köln, Germany) and calculated by the respective software. Room temperature was 22°C, and relative humidity (RH) was 25% (Klima logg pro TFA 30.3039 IT; Dostmann GmbH & Co. KG, D-Wertheim, Germany) skin temperature was 32°C. After 30 min, each Franz diffusion cell was taken

out of the water bath, and 2 mL PBS was taken out of the Franz diffusion cell acceptor compartment with a needle attached to a 2 mL syringe to facilitate TEWL measurements. After taking off the solution of SLS or the formulation from the donor compartment, the skin was dried with tissues and cotton swabs. The TEWL probe was placed on the acceptor compartment and the extracted 2 mL of PBS were returned back to the Franz diffusion cell. The Franz diffusion cell was placed back into the water bath, and the initial TEWL value was measured. The measurement started with a measurement time of 90 s for each run. A minimum of five measurements were taken and regarded as the equilibration phase. More than five measurements were necessary if the difference between the three subsequent measurements exceeded $\pm 1.00 \text{ g}\cdot\text{m}^{-2}\cdot\text{h}^{-1}$. After the last measurement, the probe was removed, and the donor chamber was put back on top of the Franz diffusion cell. At first, 1 mL of SLS was pipetted on the samples, incubated for 4 h to impair skin. Afterwards, SLS solution was discarded, the skin was dried, and the TEWL was measured, as described above. For the second incubation, the respective formulation or water (1 mL) was applied to the skin, and the incubation of 4 h started again. Afterwards, the formulations or water were discarded, the skin was dried, and the TEWL was measured again, as described above. The TEWL change is expressed as the TEWL margin before and after the 4 h of incubation in $\text{g}\cdot\text{m}^{-2}\cdot\text{h}^{-1}$. This procedure was validated and is already described in detail in a prior article by our group [23].

SC isolation and drying

The trypsin digestion process isolated the SC as described by Kligman et al. [9, 24]. This isolation procedure has been proven not to influence the lipid content or the lipid lamellar organization [25]. The obtained skin samples were placed dermal side down on filter paper soaked with 0.2% trypsin diluted in PBS solution. After incubating the skin samples overnight, the SC was peeled off gently and immersed in 0.05% trypsin inhibitor diluted in PBS solution for 1 min. Afterward, the isolated SC was washed with fresh, purified water five times. Before the measurements, samples were stored in a desiccator for drying for 3 days [14].

Pyranine staining

After trypsin digestion, as described in 2.8., the SC samples were stained with an aqueous pyranine (3 mg/mL) solution to visualize the lipid matrix between the corneocytes. After 60 s of staining, the samples were washed thrice with

deionized water for 20 s in a different beaker. The dried samples, stored for a minimum of 3 days in a desiccator, were examined for fluorescence under illumination with blue light (450–490 nm) of a microscope (Microscope Axio Imager Z1, Carl Zeiss AG, D-Oberkochen, Germany) with a 20× objective (numerical aperture 0.8, Plan-Apochromat, Carl Zeiss AG, D-Oberkochen, Germany) and respective software Zeiss Zen Blue (Carl Zeiss AG, D-Oberkochen, Germany). This procedure was previously described by Zhang et al. [9] and Pagnoni et al. [16].

Statistical analysis

Three replicates ($n=3$) were used to originate the data. Kruskal–Wallis test was used with GraphPad Prism 8.0 to detect statistical differences (GraphPad Software Inc., La Jolla, CA, USA). Different numbers of asterisks are used to indicate significant differences: * $p < 0.05$, ** $p < 0.01$, and *** $p < 0.001$.

RESULTS

Formulation and process development

During the formulation development, the impact of the parameters of the mixing system on the formulations microstructure were checked by polarization microscopy [13]. The homogenous distribution of white soft paraffin and the absence of cholesterol crystals were aimed for. The homogenous distribution of white soft paraffin was improved by increasing the mixing time from 2 to 4 min and the shear rate from 1000 to 1500 rpm. A higher mixing time of 6 min or a shear rate of 2000 rpm did not improve the formulation further. At the highest shear rate, foaming effects appeared (air was trapped in the formulation) and decreased physical stability, which was macroscopically visible. Thus, 4 min at 1500 rpm were chosen as optimal settings. After 1, 2 and 3 months, the formulations R1 and R2 were checked for cholesterol crystals or any other modifications. Images after storage are slightly darker than after manufacture which may be a result of a slightly thicker sample between slide and cover slip. Altogether, the structure and texture did not change. No cholesterol crystal growth was found as shown in Figure 1a–f. The distribution of white soft paraffin was not influenced either. So we conclude that no relevant changes in microstructure took place during storage.

The different formulations were checked with respect to their macroscopic appearance. The formulation should be a cream with medium viscosity and a white homogeneous colour. White soft paraffin was reduced from 65% to 40% for R1 and 50% to 35% for R2 because, under the

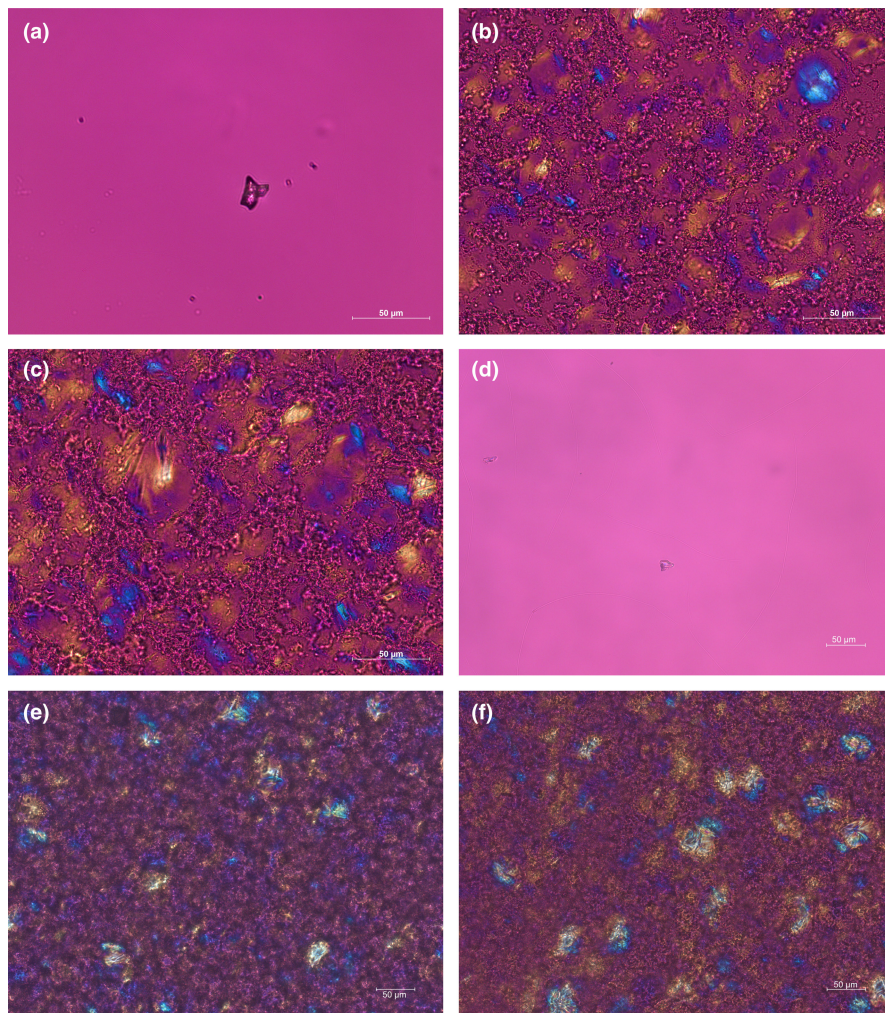


FIGURE 1 Microscopic images of stability assessment of formulations R1 and R2 with cholesterol in MCT as positive control after 3 months of storage. (a) Shows cholesterol in MCT on the first day. The sample was heated up like the formulations were produced. (b) Shows the formulation R1 immediately after manufacturing. (c) Shows the formulation R2 immediately after manufacturing. (d) Shows cholesterol in MCT after 3 months of storage at room temperature. (e) Shows the formulation R1 after 3 months of storage at room temperature. (f) Shows the formulation R2 after 3 months of storage at room temperature.

polarizing microscope, many areas of white soft paraffin were found not to have been homogenized. This was additionally improved by increasing mixing speed and time, as described above. Accordingly, the amount of water was increased. After colouring the phases R1 and R2 with methyl orange and blue-violet, both were determined to be oil in water (o/w) creams. As sorbitan monostearate is a weak emulsifier with low HLB-value (hydrophilic-lipophilic balance), Polyethylene glycol 100 stearyl ether is a high HLB emulsifier, and the amount of water in the formulation was high, this behaviour was expected.

For the following test on ex vivo porcine skin, the formulations R1 and R2 were selected because they showed the best results in comparison to the self-determined requirements.

Formulation characterization by rheology

The aim was to create a medium viscosity formulation that is easy to apply even on damaged skin. Since the spreadability of semisolid formulations is a consequence

of the viscoelastic behaviour, rheology is a suitable and valid method for characterization [26]. The formulations R1 and R2 and three market products with different viscosities were analysed. The results in Figure 2b show that the dynamic viscosities of the formulations R1 and R2 are between one marketed product with low viscosity and two with higher viscosity. The formulations thus appear to show appropriate viscosities. R1 and R2 showed shear thinning behaviour and a small hysteresis area under shear stress. This pseudo-plasticity is desirable as it improves application through a sliding effect and creates a pleasant feeling [27].

The amplitude and frequency sweeps are shown in Figure 2c–f. Both formulations R1 and R2 show gel-like behaviour with the storage modulus ($G' > G''$) being higher than the loss modulus. The formulation R1 shows higher values than R2 due to a stiffer gel network built by the single emulsifier sorbitan monostearate, which is solid at room temperature and forms crystalline networks in the cream. The emulsifier mixture with S100 in R2 reduces the stiffness of the network, as the emulsifier is liquid at room temperature. Thus, the crystalline network is

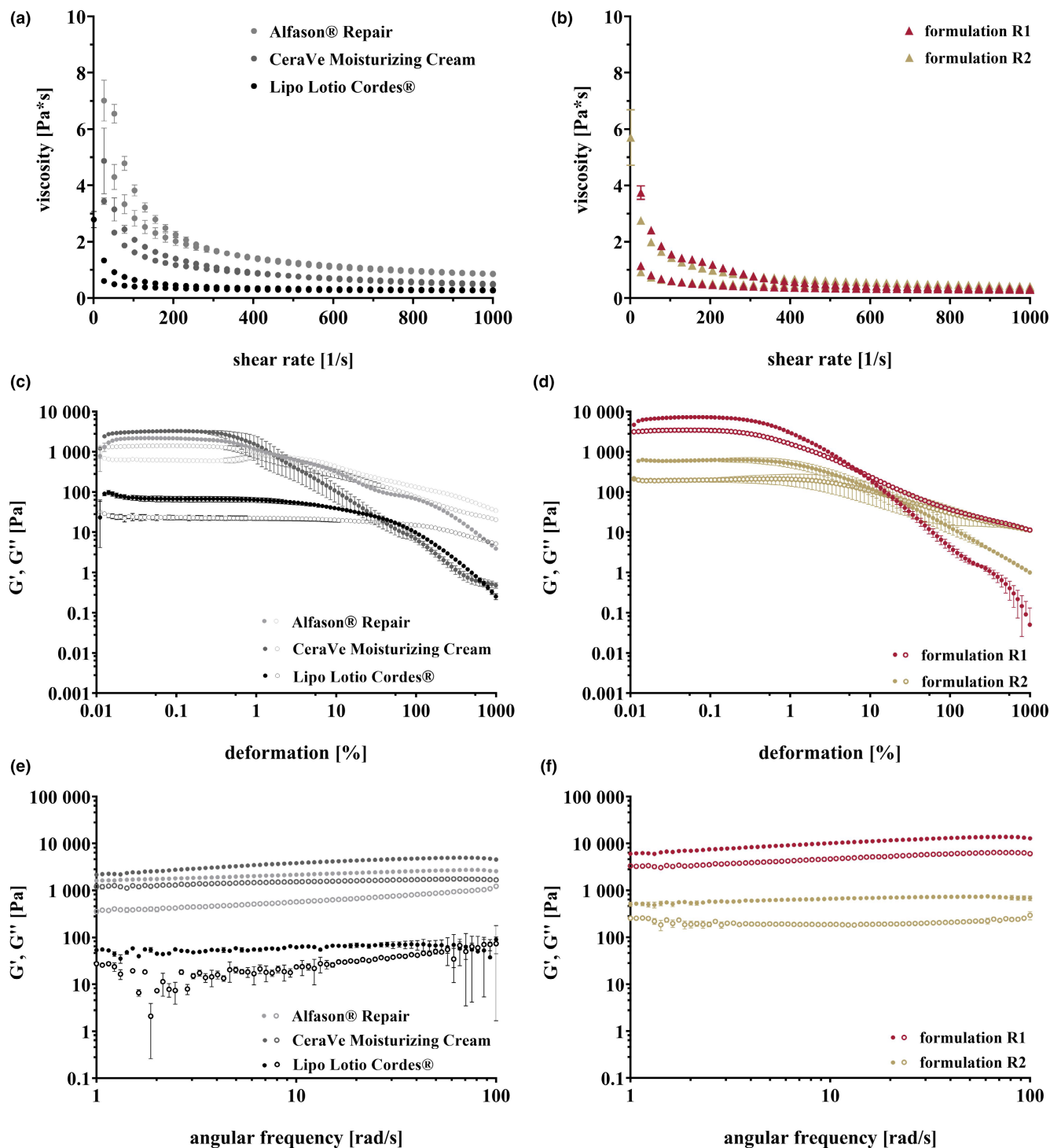


FIGURE 2 Viscosity curves of formulations (a) and market products (b). Amplitude sweep for formulations (c) and market products (d). Frequency sweep for formulations (e) and market products (f). Mean \pm SD, $n = 3$.

loosened. The crossover indicates the point at which both moduli are equal ($G' = G''$). Here, the character shifts from an elastic-dominated behaviour to a viscous-dominated behaviour and the sample begins to flow. For both developed formulations, the crossover point is between those of the marketed products indicating a structural strength in the same order of magnitude. At high shear rates during

application, both formulations will show viscous flow, regardless of the composition. The gel strength (G' in the LVE range) of the developed formulations is similar to or higher than the gel strength of the marketed products. The consistently high values during the frequency sweep (Figure 2e) show a high short- and long-term stability of the inner structure of the formulations [28]. The different

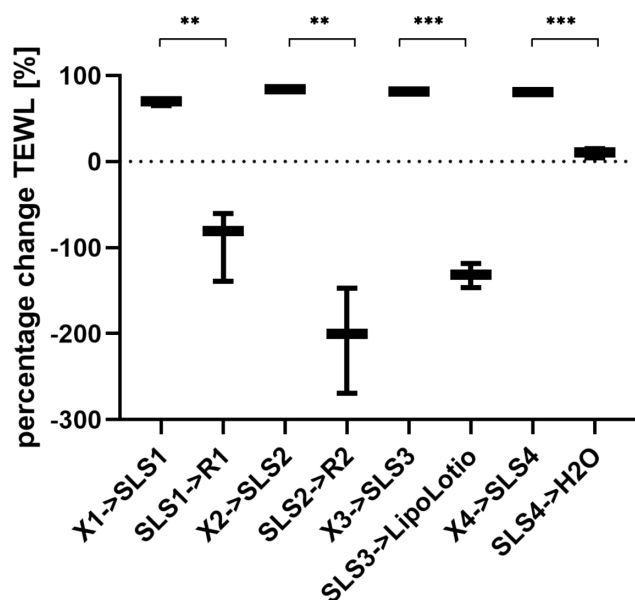


FIGURE 3 TEWL measurements of skin samples treated with formulations or water as the negative control. X1–4 stands for the samples ($n = 3$) at the initial measurement of four TEWL experiments. X1–4 → SLS1–4 indicates the difference between the first and the second measurements of the samples exposed to SLS. SLS1–4 → R1/R2/Lipo Lotio Cordes®/H₂O represents the difference of the second measurements with the third measurements. Results are shown as the change in TEWL percentage. Formulations R1, R2, market product showed significant improving TEWL effects (values in minus scale). Whereas every SLS-treated sample showed significant adverse effects (values in positive scale). The water control sample showed no change, shown as zero value, after SLS treatment. Mean ± SD, $n \geq 3$. * $p < 0.05$, ** $p < 0.01$, *** $p < 0.001$.

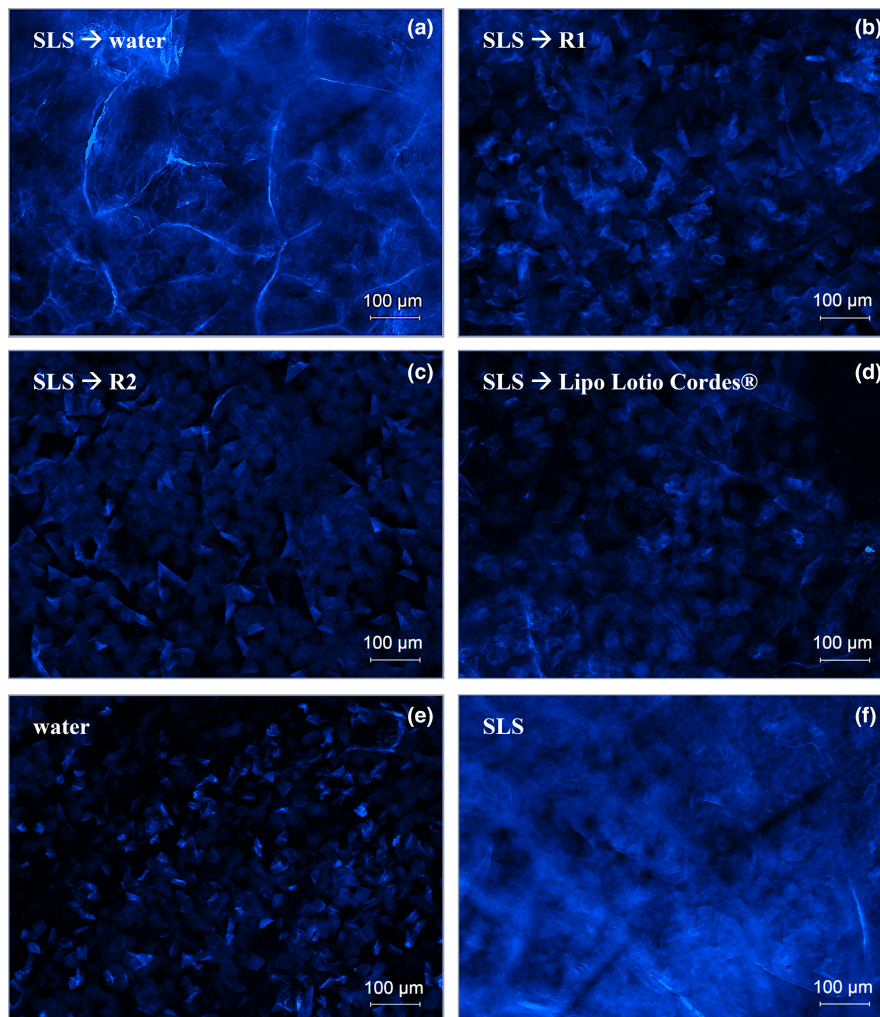
emulsifier composition has no influence on the rheological stability. The market products show similar behaviour, although the recognizable fluctuations suggest a lower short-term stability of the product at higher frequencies. It can be assumed that user acceptance of the developed formulations is high because of the similar rheological properties compared to marketed products.

Ex vivo characterization: TEWL and pyranine staining

The TEWL values were detected thrice in this study. The first measurement was used to check the skin integrity prior to the experiment. This is also recommended by the EMA draft guideline on the quality and equivalence of topical products [29]. The second measurement was to check if SLS impaired the skin barrier function. The damage, was expected as SLS had been found in our prior research to extract lipids from the skin [4–10]. To thus impaired skin, the formulations were applied and skin barrier function improvement, which means a reduction of

TEWL values, was checked for in the third TEWL measurement. Finally, the TEWL margin was calculated. The results of the TEWL measurements are shown in Figure 3. As expected, SLS, as the positive control, showed significantly increased TEWL values for all samples (on average $80 \text{ g} \cdot \text{m}^{-2} \cdot \text{h}^{-1}$). SLS is skin-disruptive [7] and has shown highly increased TEWL values in previous experiments [23] which can be explained by lipids extraction from the SC [9, 10, 13]. After applying the formulations, the TEWL decreased for the formulations R1, R2, and the marketed product Lipo Lotio Cordes®. The negative control, 1 mL of deionized water, showed no reduction. The formulations and the marketed product improved the skin barrier function. In comparison, R2 showed the strongest improvement, evidenced by the highest extent of TEWL change. We assume that the delivery of lipids to the skin is the main reason for improvement of the skin barrier. Consequently, the skin can hold back water, and the TEWL values decrease. In contrast, water did not stabilize the skin barrier function, and increased TEWL values persisted. This is in accordance with our previous research, where formulations showed positive effects on the skin barrier function [9]. Pyranine staining was used to visualize the lipids in the SC and to test our assumption of the formulations replacing previously extracted lipids as a reason for skin barrier improvement. The method is based on the binding capacity of keratin [9, 16]. The more keratin filaments are exposed in the SC due to an impairment of the skin barrier as a result of lipid extraction, the more intense the binding of pyranine to keratin and, thus, the more intense the colour. Lipid extraction was performed by incubating the skin with SLS. The damaged but subsequently untreated skin served as a positive control, while undamaged skin incubated only with water served as a negative control. The developed formulations, the marketed products or water were applied to the impaired skin. All samples were subsequently stained with pyranine to draw conclusions regarding the intensity of the lipid extraction. The references are important for interpreting the skin barrier impairment of formulations or ingredients. Because the results are a visual analysis of brightness or darkness, water, as a negative control, has no influence on the SC lipids and shows dark colour, while SLS, as a positive control, extracts lipids and thus give a bright colour. As expected, there was a clear difference between these two control samples visible in Figure 4: the water-treated sample (Figure 4e) had fewer bright areas in a dark blue background, whereas the SLS-treated sample (Figure 4f) showed high brightness and a little dark background. This shows that, as expected, the SLS-treated sample exhibits much more skin barrier damage than the water-treated one. An intense coloration, comparable to the positive control, can also be seen when the skin was treated with

FIGURE 4 Microscopic images of pyranine stained stratum corneum after treatment of SLS-impaired skin with water (a), R1 (b), R2 (c) and market product Lipo Lotio Cordes® (d). Skin treatment with water (e) as negative control and SLS as positive control (f) as positive control.



water (Figure 4a) after exposure to SLS. The treatment with the formulations R1 (Figure 4b), R2 (Figure 4c), and the marketed product Lipo Lotio Cordes® (Figure 4d) shows only a slight coloration which is comparable to the negative control (water-treated sample). The formulation R2 lead to increased recovery compared to the marketed product and R1 which is shown by the different colour intensity. Therefore, lipid replenishment is possible by treatment with the formulations. A difference in the degree of skin barrier restoration was observed after treatment with different formulations. Therefore, not every formulation is equally suitable for the treatment of damaged skin and in our case, R2 outperformed the other formulations.

DISCUSSION

Treating chronically diseased skin is challenging and depends to a large extent on the patient's compliance. Lifelong basic therapy is necessary [1]. The design of creams or ointments, therefore, has to follow the customers' wishes, like white colour and smooth touch on their skin or quick

absorption without stickiness. During formulation development, objective measures like microscopy and rheology are preferred over subjective perception and were thus also used in the current study. The results showed that the creams had a well-distributed water and oil phase, with no particles like cholesterol crystals or other agglomerates. The rheological properties showed a cream of medium viscosity with good short- and long-term stability. To test the effect of the formulation on impaired skin, porcine skin samples were first partially extracted with SLS and afterwards treated with the developed creams and the marketed reference product. The well-established method of TEWL measurements was used to detect the different effects on the skin barrier function. The creams showed positive effects by decreasing TEWL values after barrier impairment. The precision of the TEWL measurement has already been shown, and TEWL is a suitable tool to characterize the impact of formulations on the skin barrier function [23, 30, 31]. As the samples were thoroughly cleaned from the cream, no occlusion effects or residual amounts of the formulations could have influenced the TEWL measurement. The decrease in TEWL values after 4 h of incubation with

the formulations showed the ability to improve the skin barrier function as an important part of basic therapy. In addition to the TEWL values, pyranine staining followed by fluorescent microscopic analysis is another well-established method to detect skin barrier impairment visually after exposure to creams or other semisolid or liquid skin care products [9]. The samples treated with creams showed repaired skin with fewer bright areas, similar to the negative control. The difference to the positive control with much more brightness was visible. Therefore, lower accessibility to keratin filaments and, thus, an increased skin barrier function as a result of higher lipids content can be deduced. Combining the results of these two methods, it is obvious that the developed creams, especially R2, positively affected the SC as compensation for the initial damage caused by SLS was achieved after the formulations were applied. The use of sorbitan esters, the most common w/o-emulsifiers in pharmaceutical formulations [32–34], can thus be recommended for formulations for basic therapeutics.

CONCLUSION

Basic therapy is an essential pillar of therapy for chronically diseased skin. Patients mostly use different cosmetic or pharmaceutical products for the prevention or treatment of chronic disease manifestations of the skin. Products are usually selected without sufficient basic knowledge of the ingredients contained in the preparations and their suitability for damaged skin. This is cost-intensive, and most cosmetic products are not well-analysed with respect to the adverse effects of ingredients. Even products with SLS are still commonly used although the negative effect of this substance has already been extensively studied. The testing of new and old formulations for suitability on diseased skin should be focused on in the future to ensure that no damage occurs to patients. Formulations have been developed that can be produced cost-effectively on site using standard manufacturing methods e.g., in hospital pharmacies with the function of increasing the integrity of damaged skin acutely or preventively. They are therefore attractive alternatives to market products and can be of great benefit in the basic therapy of chronic skin diseases.

In the next steps, the formulations R1 and R2 should be tested in human patients with chronic skin diseases to gain access to a product for basic therapy that can be produced in local and clinical pharmacies.

ACKNOWLEDGMENTS

Open Access funding enabled and organized by Projekt DEAL.

CONFLICT OF INTEREST STATEMENT

The authors declare no conflicts of interest.

ETHICS STATEMENT

Porcine ears were obtained from a local butcher after the animal's death. Before the study, the Department of Pharmaceutical Technology was registered with the District Office of Tuebingen to utilize animal products (registration number: DE 08416105221).

ORCID

Hans Schoenfelder  <https://orcid.org/0009-0004-1547-2665>

REFERENCES

1. Staubach P, Lunter DJ. Basistherapie in der Dermatologie: Geeignete Grundlagen, Möglichkeiten Und Grenzen Hautarzt. *Hautarzt*. 2014;65(1):63–74. <https://doi.org/10.1007/s00105-013-2726-7>
2. Daniels R. Basistherapeutika: Was zeichnet moderne Pflegeprodukte zum Schutz und zur Wiederherstellung der Hautbarriere aus? *Hautarzt*. 2017;68:912–5. <https://doi.org/10.1007/s00105-017-4044-y>
3. Daniels R, Knie U. Galenik der Dermatika - Grundlagen, Eigenschaften, Freisetzung. *JDDG*. 2007;5:367–83. <https://doi.org/10.1111/j.1610-0387.2007.06321.x>
4. Lemery E, Briançon S, Chevalier Y, Oddos T, Gohier A, Boyron O, et al. Surfactants have multi-fold effects on skin barrier function. *Eur J Dermatol*. 2015;25(5):424–35. <https://doi.org/10.1684/ejd.2015.2587>
5. Mao G, Flach CR, Mendelsohn R, Walters RM. Imaging the distribution of sodium dodecyl sulfate in skin by confocal raman and infrared microspectroscopy. *Pharm Res*. 2012;29(8):2189–201. <https://doi.org/10.1007/s11095-012-0748-y>
6. Imokawa G, Akasaki S, Minematsu Y, Kawai M. Importance of intercellular lipids in water-retention properties of the stratum corneum: induction and recovery study of surfactant dry skin. *Arch Dermatol Res*. 1989;281(1):45–51. <https://doi.org/10.1007/BF00424272>
7. Törmä H, Lindberg M, Berne B. Skin barrier disruption by sodium lauryl sulfate-exposure alters the expressions of involucrin, transglutaminase 1, profilaggrin, and kallikreins during the repair phase in human skin in vivo. *J Invest Dermatol*. 2008;128(5):1212–9. <https://doi.org/10.1038/sj.jid.5701170>
8. Morris SAV, Xu L, Ananthapadmanabhan KP, Kasting GB. Surfactant penetration into human skin from sodium dodecyl sulfate and Lauramidopropyl betaine mixtures. *Langmuir*. 2021;37(48):14006–14. <https://doi.org/10.1021/acs.langmuir.1c01867>
9. Zhang Z, Lunter DJ. Confocal Raman microspectroscopy as an alternative method to investigate the extraction of lipids from stratum corneum by emulsifiers and formulations. *Eur J Pharm Biopharm*. 2018;1(127):61–71. <https://doi.org/10.1016/j.ejpb.2018.02.006>
10. Liu Y, Lunter DJ. Systematic investigation of the effect of non-ionic emulsifiers on skin by confocal Raman spectroscopy—a

- comprehensive lipid analysis. *Pharmaceutics*. 2020;12(3):223. <https://doi.org/10.3390/pharmaceutics12030223>
11. Liu Y, Lunter DJ. Profiling skin penetration using PEGylated emulsifiers as penetration enhancers via confocal Raman spectroscopy and fluorescence spectroscopy. *Eur J Pharm Biopharm*. 2021;166:1–9. <https://doi.org/10.1016/j.ejpb.2021.04.027>
 12. Liu Y, Lunter DJ. Confocal Raman spectroscopy at different laser wavelengths in analyzing stratum corneum and skin penetration properties of mixed PEGylated emulsifier systems. *Int J Pharm*. 2022;616:121561. <https://doi.org/10.1016/j.ijpharm.2022.121561>
 13. Liu Y, Ilić T, Pantelic I, Savić S, Lunter DJ. Topically applied lipid-containing emulsions based on PEGylated emulsifiers: formulation, characterization, and evaluation of their impact on skin properties ex vivo and in vivo. *Int J Pharm*. 2022;626:122202. <https://doi.org/10.1016/j.ijpharm.2022.122202>
 14. Liu Y, Lunter DJ. Optimal configuration of confocal Raman spectroscopy for precisely determining stratum corneum thickness: evaluation of the effects of polyoxyethylene stearyl ethers on skin. *Int J Pharm*. 2021;15:597. <https://doi.org/10.1016/j.ijpharm.2021.120308>
 15. Steinbrenner I, Houdek P, Pollok S, Brandner JM, Daniels R. Influence of the oil phase and topical formulation on the wound healing ability of a birch bark dry extract. *PLoS One*. 2016;11(5):e0155582. <https://doi.org/10.1371/journal.pone.0155582>
 16. Pagnoni A, Kligman AM, Stoudemayer T. Pyranine, a fluorescent dye, detects subclinical injury to sodium lauryl sulfate. *J Cosmet Sci*. 1998;49:33–8.
 17. Tfaili S, Gobinet C, Josse G, Angiboust JF, Manfait M, Piot O. Confocal Raman microspectroscopy for skin characterization: a comparative study between human skin and pig skin. *Analyst*. 2012;137(16):3673–82. <https://doi.org/10.1039/c2an16292j>
 18. Jacobi U, Kaiser M, Toll R, Mangelsdorf S, Audring H, Otberg N, et al. Porcine ear skin: an in vitro model for human skin. *Skin Res Technol*. 2007;13(1):19–24. <https://doi.org/10.1111/j.1600-0846.2006.00179.x>
 19. Pasparakis M, Haase I, Nestle FO. Mechanisms regulating skin immunity and inflammation. *Nat Rev Immunol*. 2014;14(5):289–301. <https://doi.org/10.1038/nri3646>
 20. Lunter DJ. Determination of skin penetration profiles by confocal Raman microspectroscopy: statistical evaluation of optimal microscope configuration. *J Raman Spectrosc*. 2017;48(2):152–60. <https://doi.org/10.1002/jrs.5001>
 21. Lunter DJ. How confocal is confocal Raman microspectroscopy on the skin? Impact of microscope configuration and sample preparation on penetration depth profiles. *Skin Pharmacol Physiol*. 2016;29(2):92–101. <https://doi.org/10.1159/000444806>
 22. Liu Y, Lunter DJ. Selective and sensitive spectral signals on confocal Raman spectroscopy for detection of ex vivo skin lipid properties. *Transl Biophotonics*. 2020;2(3):1–9. <https://doi.org/10.1002/tbio.202000003>
 23. Schoenfelder H, Liu Y, Lunter DJ. Systematic investigation of factors, such as the impact of emulsifiers, which influence the measurement of skin barrier integrity by in-vitro trans-epidermal water loss (TEWL). *Int J Pharm*. 2023;10(638):122930. <https://doi.org/10.1016/J.IJPHARM.2023.122930>
 24. Kligman AM. Preparation of isolated sheets of human stratum Corneum. *Arch Dermatol*. 1963;88(6):702. <https://doi.org/10.1001/ARCHDERM.1963.01590240026005>
 25. Van Smeden J, Janssens M, Gooris GS, Bouwstra JA. The important role of stratum corneum lipids for the cutaneous barrier function. *Biochim Biophys Acta*. 2014;1841:295–313. <https://doi.org/10.1016/j.bbali.2013.11.006>
 26. Adejokun DA, Dodou K. Quantitative sensory interpretation of rheological parameters of a cream formulation. *Cosmetics*. 2020;7(1):141–50. <https://doi.org/10.3390/cosmetics7010002>
 27. Gianeti MD, Gaspar LR, De Camargo FB, Campos PMBGM. Benefits of combinations of vitamin A, C and E derivatives in the stability of cosmetic formulations. *Molecules*. 2012;17(2):2219–30. <https://doi.org/10.3390/molecules17022219>
 28. Nunes A, Gonçalves L, Marto J, Martins AM, Silva AN, Pinto P, et al. Investigations of olive oil industry by-products extracts with potential skin benefits in topical formulations. *Pharmaceutics*. 2021;13(4):465. <https://doi.org/10.3390/pharmaceutics13040465>
 29. European Medicines Agency. Draft guideline on quality and equivalence of topical products. The Netherlands: European Medicines Agency; 2018. Available from: www.ema.europa.eu/contact
 30. Simonsen L, Fullerton A. Development of an in vitro skin permeation model simulating atopic dermatitis skin for the evaluation of dermatological products. *Skin Pharmacol Physiol*. 2007;20:230–6. <https://doi.org/10.1159/000104421>
 31. Cristiano MC, Froiio F, Mancuso A, Iannone M, Fresta M, Fiorito S, et al. In vitro and in vivo trans-epidermal water loss evaluation following topical drug delivery systems application for pharmaceutical analysis. *J Pharm Biomed Anal*. 2020;15:186. <https://doi.org/10.1016/j.jpba.2020.113295>
 32. Liu Y, Binks BP. Fabrication of stable oleofoams with sorbitan ester surfactants. *Langmuir*. 2022;38(48):14779–88. <https://doi.org/10.1021/acs.langmuir.2c02413>
 33. Fiume MM, Bergfeld WF, Belsito DV, Hill RA, Klaassen CD, Liebler DC, et al. Safety assessment of sorbitan esters as used in cosmetics. *Int J Toxicol*. 2019;38(2_suppl):60S–80S. <https://doi.org/10.1177/1091581819871877>
 34. Upadhyay KK, Tiwari C, Khopade AJ, Bohidar HB, Jain SK. Sorbitan ester organogels for transdermal delivery of sumatriptan. *Drug Dev Ind Pharm*. 2008;33(6):617–25. <https://doi.org/10.1080/03639040701199266>

How to cite this article: Schoenfelder H, Wiedemann Y, Lunter DJ. Development and characterization of topical formulation for maintenance therapy containing sorbitan monostearate with and without PEG-100-stearate. *Int J Cosmet Sci*. 2024;00:1–11. <https://doi.org/10.1111/ics.13023>

5. Ceramides profiling of porcine skin and systematic investigation of the impact of sorbitan esters (SEs) on the barrier function of the skin

This document is confidential and is proprietary to the American Chemical Society and its authors. Do not copy or disclose without written permission. If you have received this item in error, notify the sender and delete all copies.

Ceramides profiling of porcine skin and systematic investigation of the impact of sorbitan esters (SEs) on the barrier function of the skin

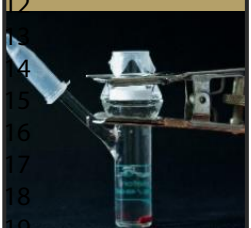
Journal:	<i>Molecular Pharmaceutics</i>
Manuscript ID	Draft
Manuscript Type:	Article
Date Submitted by the Author:	n/a
Complete List of Authors:	Schoenfelder, Hans; University of Tübingen, Pharmaceutical Technology Reuter, Moritz; University of Tübingen Faculty of Science, Pharmacy Evers, Dirk-Heinrich; RaDes GmbH Herbig, Miachel; RaDes GmbH Lunter, Dominique; University of Tübingen Faculty of Science, Pharmacy

SCHOLARONE™
Manuscripts

1
2
3
4
5
6
7
8
9

In-vitro test design

10
11 **Franz cells**
12
13
14
15
16
17
18
19
20 **Incubation**
21

A photograph showing a Franz cell, a device used for measuring the permeability of skin, placed on a laboratory bench. A beaker containing a liquid is positioned next to it, and a pipette is shown dispensing liquid into the cell.

22
23
24
25
26
27
28
29
30

TEWL

A photograph of a TEWL (Transepidermal Water Loss) measurement device, which is used to assess the skin's barrier function. It consists of a probe and a sensor that measure the evaporation of water from the skin.

Skin barrier function



Trypsination

A photograph of a petri dish containing a tryptic digestion medium, used for isolating skin cells (SC isolation). The dish contains several small, light-colored spots of the medium.

SC isolation



CRM

A photograph of a CRM (Cosy-Q) instrument, used for measuring lipid content and conformation. It is a specialized NMR spectrometer.

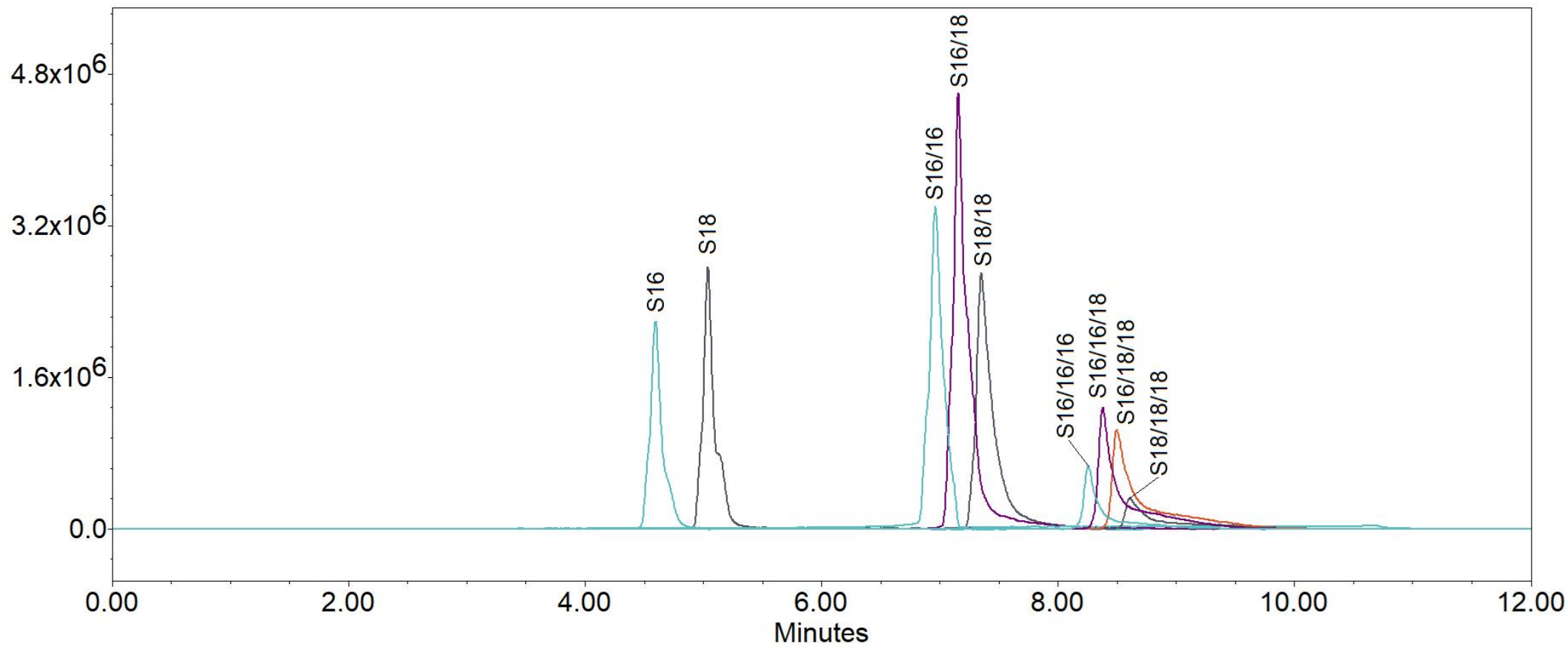
Lipid content, conformation

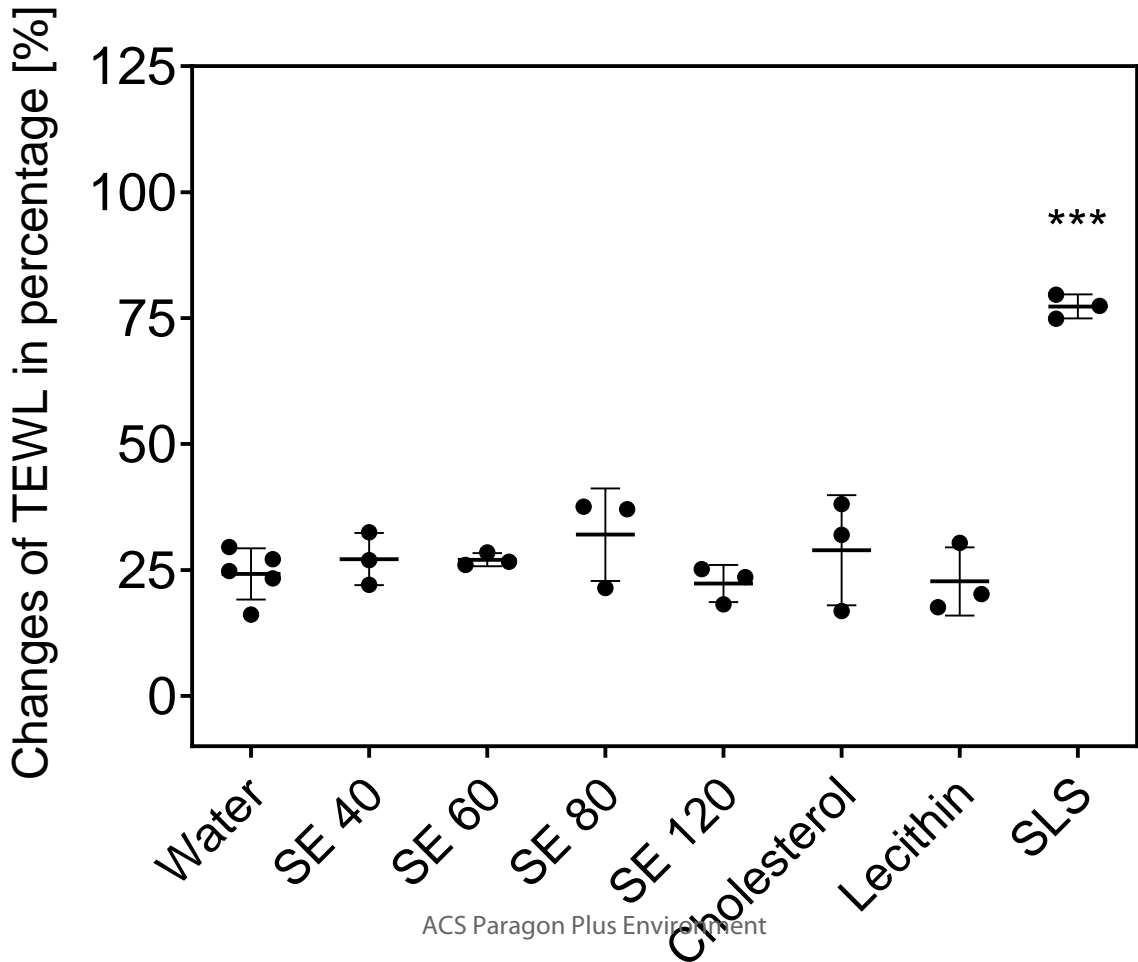


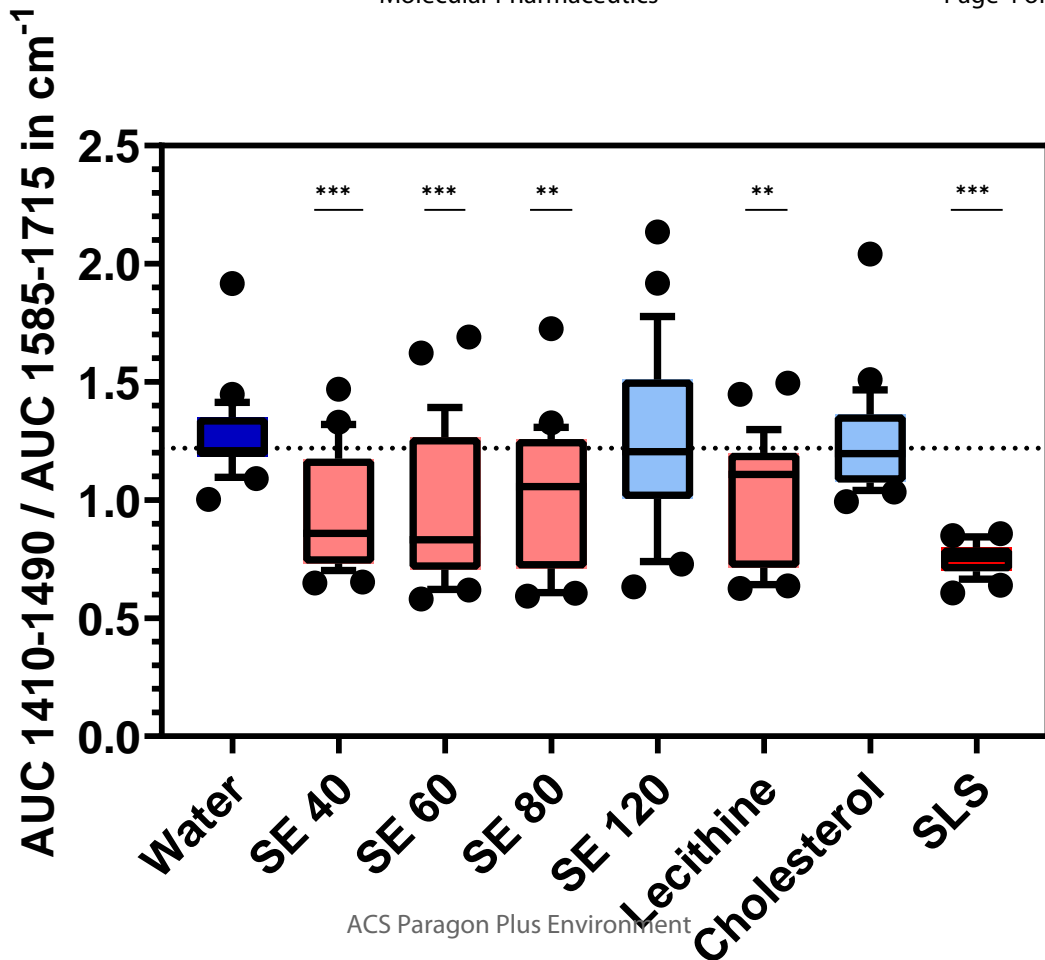
LC-MS

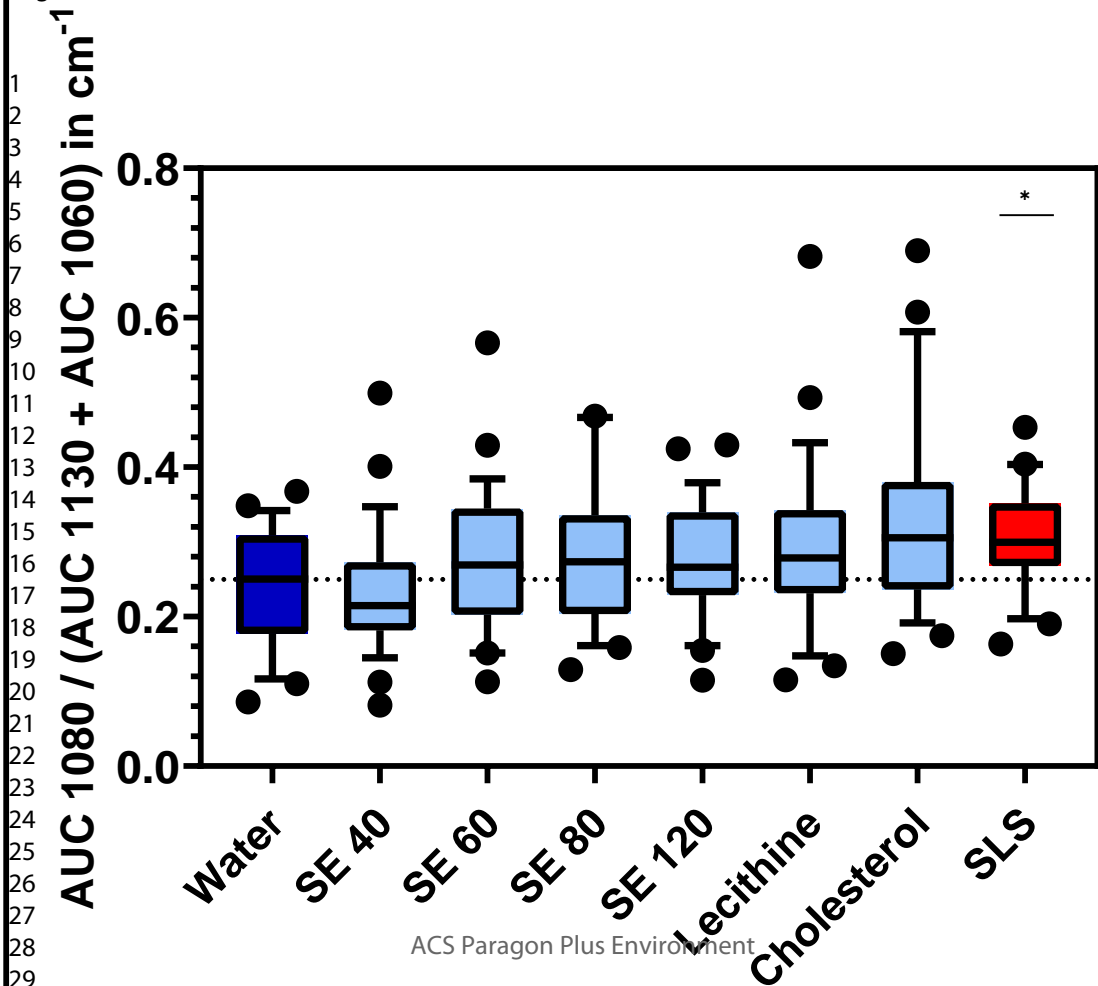
A photograph of an LC-MS (Liquid Chromatography-Mass Spectrometry) instrument, used for measuring ceramide content. It is a complex piece of laboratory equipment.

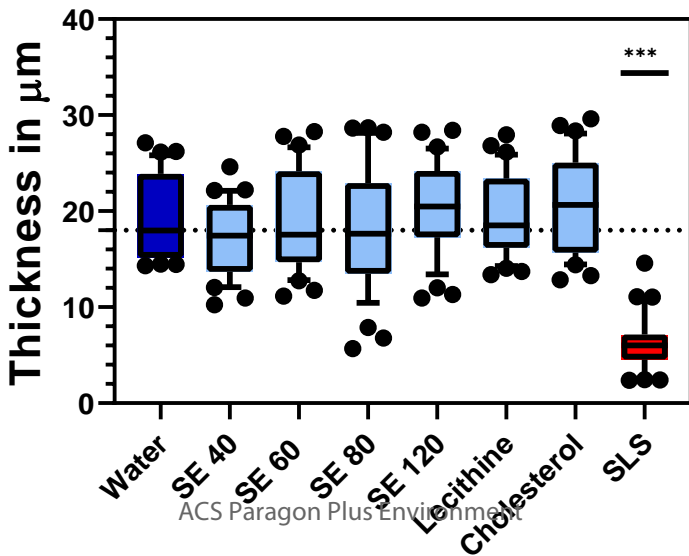
Ceramides content





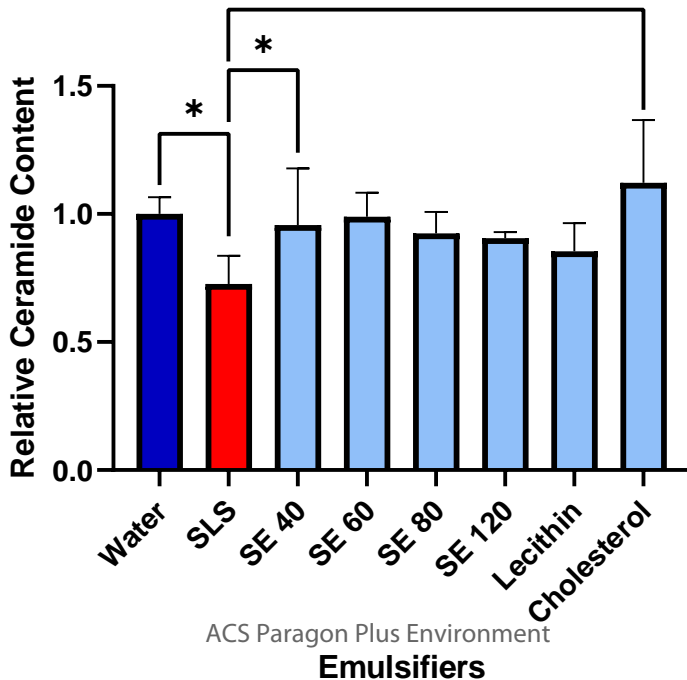






Molecular Pharmaceutics

**



Ceramides profiling of porcine skin and systematic investigation of the impact of sorbitan esters (SEs) on the barrier function of the skin

Sorbitan esters are skin-friendly and usable for topical formulations



Emulsifiers

- Sorbitan esters SE40, SE60, SE80, SE120
 - Cholesterol
 - Lecithin



Testing

- Porcine skin as in-vitro model skin
- TEWL measurements
- CRS for lipid content
- LC-MS analysis for ceramides



Results

- TEWL results showed no negative effects
- CRS showed a reduction in lipid content
- Ceramides were not affected negatively



Molecular Pharmaceutics
Journal



ACS Paragon Plus Environment
Schoenfelder, Reuter,
Evers, Herbig, Lunter

<https://pubs.acs.org/journal/mpohbp>

1
2
3
4
5
6
7 Ceramides profiling of porcine skin and systematic
8
9
10
11 investigation of the impact of sorbitan esters (SEs)
12
13
14
15 on the barrier function of the skin
16
17
18
19
20
21

22 *Hans Schoenfelder*¹, *Moritz Reuter*¹, *Dirk-Heinrich Evers*², *Michael E. Herbig*², *Dominique*
23
24 *Jasmin Lunter*^{1*}
25
26
27
28
29

30 ¹Department of Pharmaceutical Technology, Faculty of Science, Eberhard Karls Universität
31
32 Tübingen, Auf der Morgenstelle 8, 72076 Tuebingen, Germany
33
34
35
36
37

38
39 ²RaDes GmbH, Schnackenburgallee 114, 22525, Hamburg, Germany
40
41
42
43
44
45
46
47
48
49
50
51
52
53
54
55
56
57
58
59
60

1
2
3 Keywords
4
5

6 Ceramides; CRS; emulsifiers; in-vitro; LC-MS; lipids; porcine skin; sorbitan ester; SC; trans-
7
8 epidermal water loss
9
10

11
12
13
14
15 Abstract
16
17

18 The SC (Stratum corneum) lipids provide the main barrier of the skin against the environment.
19 Ceramides make up about half of the lipids by weight and are thus of particular interest.
20 Emulsifiers are used in a multitude of topical formulations, e.g. to stabilize emulsions against
21 coalescence. Investigations showed that some emulsifiers have the potential to impair the skin
22 barrier function. SEs (Sorbitan ester) were frequently used emulsifiers in pharmaceutical and
23 cosmetic dermal formulations. Further, cholesterol and lecithin were used as natural alternatives.
24 However, information of their impact on ceramides is very scarce. Thus, we first analyzed the SEs
25 by LC-MS regarding their composition. Then developed an LC-MS method to identify and
26 quantify the ceramides in porcine skin and subsequently investigated the impact of emulsifiers on
27 the ceramides profile. Besides the LC-MS measurements, the effect of emulsifiers on the skin
28 barrier function was investigated by trans-epidermal water loss (TEWL) measurements and
29 confocal Raman spectroscopy (CRS). Throughout the experiments, water was used as a negative
30 control, and sodium lauryl sulfate (SLS) as a positive control. It was found that SEs are mixtures
31 of mono-, di-, and triesters, partially with complex fatty acid distribution. LC-MS measurements
32 of the total ceramide content of the SC samples revealed the SE 60 as well as the cholesterol-
33 treated samples to be those showing the least ceramide depletion, implying a high skin tolerability
34 in general. The TEWL measurements showed that the SEs 40, 60, 80, and 120 showed no
35
36
37
38
39
40
41
42
43
44
45
46
47
48
49
50
51
52
53
54
55
56
57
58
59
60

1
2
3 significant changes in skin barrier function. The lipid content, measured by CRS, was mostly
4 decreased except for SE 120. Conformation, lateral packing order, and SC thickness, also
5 measured by CRS, showed no significant differences. These detailed investigations lead to the
6 view that SEs, are skin-friendly substances and can be used for topical applications, e.g. those
7 commonly used to treat skin diseases.
8
9
10
11
12
13
14
15
16
17

18 **1. Introduction**

19
20 Porcine skin is one of the most frequently used surrogates of human skin ^{1,2}. It compares to
21 human skin in terms of thickness, number of hair follicles, and immune cells ³. Regarding
22 penetration of exogenous substances, like pharmaceutical as well as cosmetical actives or
23 excipients, porcine skin, of all animal skins, yields results closest to human skin ^{4,5}. Porcine skin
24 is also used to investigate the impact of exogenously applied substances on the skin barrier function
25 ⁶⁻⁹. Here, for example, the impact of emulsifiers like Polyethylene glycol (PEG)-ethers and
26 polysorbates has been studied recently ^{10,11}. The skin barrier function is provided mainly by the
27 SC lipids. These consist of 50 % (m/m) ceramides, 25 % (m/m) free fatty acids, and 25 % (m/m)
28 cholesterol and its derivatives ¹². The ceramide portion, comprising a wide range of ceramide classes
29 as well as chain lengths, their conformation and packing order have been shown to play a pivotal
30 role in maintaining skin barrier integrity ^{11,13-18}. Although it is known that the ratio of ceramides,
31 free fatty acids, and cholesterol are similar in human and porcine skin, only few studies exist
32 investigating the exact composition of the SC lipids of porcine skin with high-accuracy analytic
33 methods like LC-MS ^{19,20}. Yet, this information is crucial in detecting and accurately quantifying
34 changes in the ceramide content of the skin.
35
36
37
38
39
40
41
42
43
44
45
46
47
48
49
50
51
52
53
54
55
56
57
58
59
60

Therefore, the aim of the study was to determine the ceramide profile of porcine skin by LC-MS and subsequently use this sophisticated method to investigate the impact of emulsifiers on skin barrier integrity. To obtain a full picture, the methods of trans-epidermal water loss (TEWL) and confocal Raman spectroscopy (CRS) were also applied as seen in Figure 1. TEWL is a parameter conventionally used in *in-vivo* studies as a measure of skin barrier function and to identify the impact of cosmetic or pharmaceutical treatments on the skin barrier^{21,22}. CRS allows to investigate the total amount of lipids in a skin sample as well as the lateral packing order of the lipids^{11,17,18,23–25}. The results of our multimodal approach were expected to give a comprehensive picture of the impact of emulsifiers on the skin barrier function. SEs, cholesterol, and lecithin were chosen to be used as examples of classical chemical emulsifiers and natural alternatives.

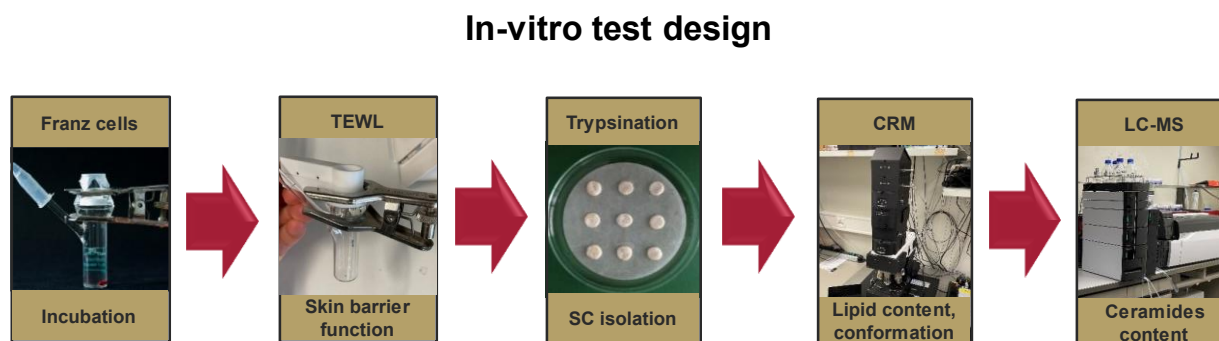


Fig. 1. Overview of the analysis of the SC with Franz cells, TEWL measurements, trypsinization step, CRS, and LC-MS measurements.

2. Materials and methods

2.1. Materials

SLS, sodium chloride, and potassium chloride were obtained from Caesar & Loretz GmbH (D-Hilden, Germany). LC-MS-Grade 2-propanol, methanol, acetonitrile, formic acid, acetic acid ethyl ester, and in normal quality di-sodium-hydrogen phosphate and potassium-di-hydrogen phosphate were obtained from Carl Roth GmbH & Co. KG (D-Karlsruhe, Germany). MS-grade Ammonium acetate was obtained by VWR International GmbH (D-Darmstadt, Germany). Tert-butylmethylether was obtained by Supelco (Sigma-Aldrich Chemie GmbH, D-Taufkirchen, Germany). HPLC-Grade dichloromethane was obtained from Fisher Scientific U.K. Limited (UK-Loughborough/Leicestershire). SEs including sorbitan monopalmitate (SE 40), sorbitan monostearate (SE 60), sorbitan monooleate (SE 80), and sorbitan monoisostearate (SE 120) were purchased from Croda GmbH, (D-Nettetal, Germany). LC-MS-Grade ammonium formate and in normal quality trypsin (from porcine pancreas, lyophilized powder, type II-S) and trypsin inhibitor (from glycine max (soybean), lyophilized powder) were obtained by Sigma-Aldrich Co. (MO-St. Louis, USA). LC-MS standards CER1 (d18:1/26:0/18:1(d9)) (N-[26-oleoyloxy(d9)hexacosanoyl]-D-erythro-sphingosine), Deuterated Ceramide Lipidomix® (N-palmitoyl(d7)-D-erythro-sphingosine, N-stearoyl(d7)-D-erythro-sphingosine, N-lignoceroyl(d7)-D-erythro-sphingosine, N-nervonyl(d7)-D-erythro-sphingosine), CER3(d9) (N-palmitoyl(d9) D-ribo-phytosphingosine), CER5-2'R(d9) (N-(2'-(R)-hydroxypalmitoyl(d9)) D-erythro-sphingosine), CER6-2'R(d9) (N-(2'-(R)-hydroxypalmitoyl(d9)) D-ribo-phytosphingosine), CER7-2'R, 6R (d9) (N(2'-(R)-hydroxypalmitoyl(d9)) 6R-hydroxysphingosine), CER8(d9) (N-palmitoyl(d9) 6R-hydroxysphingosine), CER9(d9) (t18:0/26:0/18:1(d9)) (N-[26-oleoyloxy(d9)

1
2
3 hexacosanoyl]-D-ribo-phytosphingosine), CER10(d9) (N-palmitoyl(d9) dihydrosphingosine) and
4
5 CER11-2'R(d9) (N-(2'-(R)-hydroxypalmitoyl(d9)) D-erythro-sphingosine) were obtained from
6
7 Avanti Polar Lipids Incorporation (AL-Birmingham; USA). Parafilm® was obtained from Bemis
8
9 Company Inc. (WI-Oshkosh, USA). All aqueous solutions were made with ultra-pure water from
10
11 Elga Maxima (GB-High Wycombe, Great Britain). Phosphate buffered saline (PBS) was prepared
12
13 using sodium chloride, and potassium chloride obtained from Caesar & Loretz GmbH (D-Hilden,
14
15 Germany), di-sodium-hydrogen phosphate, and potassium-di-hydrogen phosphate obtained from
16
17 Carl Roth GmbH & Co. KG (D-Karlsruhe, Germany). Nitrogen was obtained from an in-house
18
19 tank and argon 5.0 was delivered by Westfalen AG (D-Muenster, Germany). Porcine ear skins
20
21 (German landrace; age: 15 to 30 weeks; weight: 40 to 64 kg) were provided by a local butcher.
22
23
24
25
26 The Department of Pharmaceutical Technology at the University of Tuebingen has been registered
27
28 for the use of animal products (registration number: DE 08 416 1052 21).
29
30
31
32

33 2.2. LC-MS analysis of the composition of SEs

34
35 SEs were analyzed by a ultra-high-performance liquid chromatography (UPLC) system
36
37 (ACQUITY UPLC H-Class PLUS, Waters) connected to a single quadrupole mass spectrometer
38
39 (QDa, Waters, mass range 30 to 1250 m/z) as a detector. An Acquity UPLC HSS Cyano, 100 Å,
40
41 1.8 µm, 2.1 x 50 mm UPLC column from Waters GmbH (D-Eschborn, Germany) was used. Prior
42
43 to analysis, SEs were dissolved at 0.5 mg/mL in methanol. The column temperature was set to
44
45 45 °C and the autosampler temperature to 25 °C. The injection volume was set to 1 µL, and the
46
47 flow rate of the eluent was 0.5 mL/min. In total three mobile phases were used. **A:** 10 mM
48
49 ammonium acetate and 5 mM acetic acid. **B:** acetonitrile + 10 % tert-butylmethylether. **C:**
50
51
52
53
54
55
56
57
58
59
60

1
2
3 methanol. Each run was conducted using individual linear gradients. The detection was carried out
4
5 as the respective 1-fold charged ammonium ions at a cone voltage of 15 V.
6
7
8
9

10 2.3. Preparation of emulsifier solutions/dispersions

11
12 Testing solutions/dispersion of SE 40, SE 60, SE 80, SE 120, lecithin, cholesterol, and SLS were
13
14 prepared as 1 % solution/dispersion (w/w) in water, sonicated (Bandelin Sonorex, Bandelin
15
16 electronic GmbH & Co. KG, D-Berlin, Germany) for 15 min, and vortexed for 1 min (IKA Vortex
17
18 2, IKA-Werke GmbH & Co. KG, D-Staufen, Germany) as described previously ²².
19
20
21
22
23

24 2.4. Porcine ear skin preparation

25
26 Porcine skin is histologically and morphologically comparable to human skin, therefore it was
27
28 chosen as a surrogate for human skin ^{1,2}. The skin was prepared as described in earlier publications
29
30 of our group ^{26,27}. Fresh pig ears were cleaned with isotonic saline. Full-thickness skin was
31
32 removed from the cartilage, and blood was removed with isotonic saline and cotton swabs. The
33
34 obtained postauricular skin was dried with soft tissue. The skin was sliced into strips of about 3 cm
35
36 in width. The skin was stretched onto a Styrofoam plate to reduce the impact of wrinkles. With an
37
38 electric hair trimmer (QC5115/15 Philips Electronics, NL-Eindhoven, Netherlands), bristles were
39
40 cut to about 0.5 mm in length. After being dermatomed to a thickness of 1.0 mm (Dermatom GA
41
42 630 Acculan 3 TI Aesculap AG & Co. KG, D-Tuttlingen, Germany) the skin was punched out into
43
44 circles of 25 mm diameter and placed in the freezer at minus 28 °C wrapped in aluminum foil. On
45
46 the day of the experiment, the samples were thawed to room temperature on a piece of paper tissue
47
48 soaked with phosphate buffered saline pH 7.4 (PBS) ²⁷.
49
50
51
52
53
54
55
56
57
58
59
60

2.5. Incubation of skin samples in Franz diffusion cells

Franz diffusion cells are a typical type of analytical setup for determining skin absorption *ex vivo* and the method described herein has been used extensively by our group in the past as described in previous publications^{11,17,26,27}. Prior articles from our group provide a thorough discussion of the strategy for the incubation of skin samples with emulsifiers^{11,28}. Franz diffusion cells (Gauer Glas, D-Püttlingen, Germany) were filled with 12 mL degassed, prewarmed (32 °C) PBS as the receptor fluid. The skin samples were put on top of the acceptor compartments and the donor compartments were placed on top of the skin. The Franz diffusion cells were placed in a water bath at 32 °C temperature (Lauda type Alpha, Lauda Dr. R. Wobser GmbH & Co. KG, D-Lauda-Königshofen, Germany). The receptor fluid was continuously stirred at a 500-rpm rate (Variomag Poly 15, Thermo-Scientific, Thermo Electron LED GmbH, D-Langensfeld, Germany). After an expeditious equilibration period of 30 minutes, the initial TEWL values were generated with the protocol described in 2.6. After the initial TEWL measurements, 1 mL of each emulsifier solution/dispersion, water (negative control), or SLS (positive control) was applied to the respective skin samples. Each donor compartment was then covered with a piece of parafilm to reduce evaporation. After a four-hour incubation, the residual formulation was wiped off the skin and the second TEWL measurement was performed^{11,28}. Experiments were performed in triplicate.

2.6. Measurement of trans-epidermal water loss (TEWL)

The TEWL was measured by basic device Multi Probe Adapter MPA 6 and probe In-vitro-Tewameter® VT 310 (Courage & Khazaka electronic GmbH, D-Köln, Germany), and calculated by the respective software. Room temperature was 22 °C and relative humidity (RH) was 25 %

1
2
3 (Klima logg pro TFA 30.3039 IT; Dostmann GmbH & Co. KG, D-Wertheim, Germany). After 30
4 minutes, each Franz diffusion cell was taken out of the water bath and 2 mL PBS was taken out of
5 the Franz diffusion cell acceptor compartment with a needle attached to a 2 mL syringe. After
6 taking off the donor compartment, the skin was dried with tissues and cotton swabs. The probe
7 was put on the acceptor compartment and the initial TEWL value was measured. Then, the
8 measurement started with a measurement time of 90 seconds for each run. A minimum of five
9 measurements were taken, which were regarded as the equilibration phase. More than five
10 measurements were deemed necessary if the difference between three subsequent measurements
11 exceeded $\pm 1.00 \text{ g}\cdot\text{m}^{-2}\cdot\text{h}^{-1}$. After the last measurement, the probe was taken off and the donor
12 chamber was put back on top of the Franz diffusion cell. The withdrawn 2 mL PBS were filled
13 back, and the respective emulsifier solution/dispersion was applied to the skin and the incubation
14 of four hours started. Afterwards, the emulsifier solution/dispersion was discarded, the skin was
15 dried, and the TEWL was measured, as described above. The change of TEWL is the margin of
16 the TEWL before and after the four hours of incubation in $\text{g}\cdot\text{m}^{-2}\cdot\text{h}^{-1}$. This procedure was validated
17 and is already described in detail in a prior article by our group ²².

2.7. SC isolation and drying

20
21
22
23
24
25
26
27
28
29
30
31
32
33
34
35
36
37
38
39
40
41
42 The SC was isolated by trypsin digestion process as described by Kligman et al. ^{17,29}. This
43 isolation procedure has been proven not to influence the lipid content or the lipid lamellar
44 organization. The obtained skin samples were placed dermal side down on filter paper soaked with
45 0.2 % trypsin diluted in PBS solution. After the incubation of skin samples overnight, digested SC
46 was peeled off gently and immersed into 0.05 % trypsin inhibitor diluted in PBS solution for 1 min.

1
2
3 Afterwards, the isolated SC was washed with fresh purified water for five times. Before the
4
5 measurements, samples were stored in a desiccator for drying for three days³⁰.
6
7

10 2.8. SC thickness measured by micrometer gauge

11
12 After treatment with different emulsifiers, the SC thicknesses were measured with the eddy
13
14 current method, using a Fischer DUALSCOPE® FMP20 portable instrument equipped with an
15
16 FTA3.3-5.6H probe (Helmut Fisher, D-Sindelfingen, Germany). To reduce the effects of hair
17
18 which can accidentally cause errors when measuring the distance between the SC surface and
19
20 sample substrate, hair was very gently removed when washing the isolated SC in water. SC
21
22 samples were then put on round glass plates for DUALSCOPE® and the following CRS
23
24 measurements. Each skin sample was measured over 12 times at different places. The averages
25
26 and standard deviations were then calculated for comparison³⁰.
27
28
29
30
31
32

33 2.9. CRS measurements

34 2.9.1. CRS set-up

35
36
37 After drying, the SC sheets were fixed onto the scan table of the alpha300 R confocal Raman
38
39 microscope (WITec GmbH, D-Ulm, Germany). This CRS device was equipped with a 532 nm
40
41 excitation laser, UHTS 300 spectrometer, and DV401A-BV CCD camera. To avoid skin samples'
42
43 damage due to high laser intensity, the laser power was set to 10 mW, adjusted by the optimal
44
45 power meter (PM100D, Thorlabs GmbH, D-Dachau, Germany). The objective 100 x 0.9 NA (EC
46
47 Epiplan-neofluor, Carl Zeiss, D-Jena, Germany) was used. During the measurement, the light was
48
49 focused through the objective onto the SC surface. The backscattered light from the SC was then
50
51 dispersed by an optical grating (600 g/mm to obtain the spectral range from 0 – 4000 cm⁻¹ or
52
53
54
55
56
57
58
59
60

1
2
3 1800 g/mm to achieve higher spectral resolution for analysis of trans-gauche-ratio). The scattered
4
5 light was collected and analyzed on a charge-coupled device (DV401A-BV CCD detector) which
6
7 had been cooled down to -60 °C in advance. The CRS measurements were performed based on a
8
9 method developed by Zhang et al.²⁵
10

11
12 The spectra were collected with an integration time of 5 seconds and 5 accumulations. To
13
14 achieve spectral signals of lipids from the skin surface and measure SC thickness at the same time,
15
16 the spectra were detected with the focus point moving from -15 μm beneath the skin to 15 μm
17
18 above the skin. The spectra were recorded with the step size of 1 μm. The skin surface was
19
20 determined as the half maximum of the keratin signal intensity (ν (CH₃), 2920 - 2960 cm⁻¹) as
21
22 described before^{25,28,30,31}.
23
24
25
26
27

28 2.9.2. Pre-processing of CRS spectra

29
30 The obtained Raman spectra were edited with spectral cosmic ray removal (CRR), following a
31
32 principal component analysis (PCA), and background subtraction (SubBG) which was performed
33
34 by the WITec Project 6.0 Software (WITec GmbH, D-Ulm, Germany). The background
35
36 subtraction in the HWN region was applied with the mode shape 300 and the fingerprint region
37
38 and trans-gauche-ratio with the mode polynomial third order and zero smoothing points. After that,
39
40 the AUC extracted in this study was the integrated area under a specified peak of the spectrum and
41
42 could be calculated using the trapezoidal method on WITec Project 6.0 Software^{11,28}.
43
44
45
46
47
48

49 2.9.3. Skin lipid content analysis by CRS

50
51 Based on previous research, the spectral signal in the fingerprint region is more sensitive to
52
53 analyze the skin lipid content than that in the high wavenumbers region³². In detail, the δ (CH₂,
54
55
56
57
58
59
60

1
2
3 CH₃)-mode at 1425 – 1490 cm⁻¹ is derived to a large extent from lipids in the SC. The ν (C=O)-
4 mode at 1630 – 1710 cm⁻¹ (amide I mode) is derived from proteins. In general, the spectral
5 intensity varies to some extent between different skin samples and different donors. The amide-I
6 mode displays the least variation within one donor or among different donors^{23,33}. To account for
7 the described variation of spectral intensity, the lipid-related signals were normalized to the amide-I
8 I signal for calculating the total lipid content^{28,30}.

19 2.9.4. Analysis of lipid conformation by CRS

20
21 The lipid conformation was determined by the trans-gauche-ratio in the fingerprint region. At
22 the positions of 1060 cm⁻¹ and 1130 cm⁻¹ the trans conformation is displayed. The peak at 1080 cm⁻¹
23 represents the gauche conformation. Gauche conformation represents a more disordered state of
24 lipids, whereas lipids in trans conformation are more ordered^{24,33}. The AUCs under the respective
25 peaks are used to calculate the trans-gauche-trans ratio as $AUC_{1080} / (AUC_{1060} + AUC_{1130})$ and was
26 described in detail by Snyder³⁴. Accordingly, a higher value represents a more disordered
27 conformation of lipids. This procedure was also described in detail by our group^{11,25}.

40 2.10. LC-MS analysis of ceramides

42 2.10.1. Sample preparation for LC-MS ceramide analysis

43
44 The glass slides carrying the SC sheets were crushed and transferred into 2 mL reaction vessels
45 (Eppendorf SE, D-Hamburg, Germany). The vessels were then filled with 2 mL of the extraction
46 medium, containing by volume eight parts methanol to two parts of ethyl acetate as well as the
47 internal standards of ceramides NS16d7, NS24d7 as well as Ceramide EOS26d9. The mixture was
48 then shaken for three hours (IKA Vibrax VXR basic, IKA-Werke GmbH & Co. KG, D-Staufen,
49
50
51
52
53
54
55
56
57
58
59
60

Germany), sonicated for 15 minutes (Bandelin Sonorex, Bandelin electronic GmbH & Co. KG, D-Berlin, Germany) and vortexed for 1 minute (IKA Vortex 2, IKA-Werke GmbH & Co. KG, D-Staufen, Germany). The sample tubes were then centrifuged at 13,400 rpm for 10 minutes (MiniSpin®, Eppendorf SE, D-Hamburg, Germany) and the supernatant taken off and filtered into HPLC vials using a 0.2 µm PTFE filter (Chromafil, Macherey-Nagel GmbH & Co. KG, D-Düren, Germany).

2.10.2. LC-MS measurements of ceramides

Samples were analyzed using reverse-phase UPLC (UPLC, Nexera LC-40, Shimadzu Corporation, Kyoto, Japan) coupled with mass spectrometry (LCMS-8045, Shimadzu Corporation, Kyoto, Japan). The UPLC separation step was performed using a binary gradient, with the total method duration being 20 minutes. The UPLC used a flow rate of 0.4 ml/min and the following gradient: Eluent A: 10 µM ammonium formate in water; Eluent B: 0.1 % (v/v) formic acid in isopropanol/acetonitrile 50/50. Concentration of eluent B over time: 0 min: 10 %; 0.5 min: 20 %; 1 min: 40 %; 12.5 min: 92.5 % (Nonlinear curve); 12.6 min: 100 %; 17 min: 100 %; 18 min: 20 %; 20 min: 20 % (Flushing step). Ceramide content was determined in the mass spectrometer using the following settings: ESI positive ionization mode; interface voltage: 3 kV; interface temperature: 220 °C; desolvation temperature: 355 °C. Ceramides were quantified using multiple reaction monitoring (MRM) to obtain higher specificity in the extraction matrix: Precursor ions in the Q1 were either the $[M+H]^+$ ion for the ceramide groups NP, AP, NDS, ADS, EOS, EOP, and EODS, or $[M-H_2O+H]^+$ for ceramide groups NS and AS. After fragmentation, the LCB-specific fragments³⁵ were used for product ion quantification of the ceramides. A full table of the precursor ions, collision energies, as well as the corresponding product ions, can be found in the supplementary material in Table S2. The measured ceramide species comprise a chain length

1
2
3 range of C16 to C28 for non-EO ceramides as well as C28 to C35 for EO ceramides. To account
4
5 for variability in ionization, the obtained intensities were then normalized by the internal standards
6
7 of Ceramide NS16d7, NS24d7 as well as Ceramide EOS26d9, depending on the retention time as
8
9 well as the ceramide species, see supplementary material for details. Concentrations were then
10
11 calculated from the normalized intensities using calibration curves of ADS16d9, AP16d9,
12
13 NP16d9, AS16d9, NS16d9, NDS16d9 as well as EOS26d9 and EOP26d9. For the EODS
14
15 ceramides, the ADS16d9 calibration curve was used for calculation of the concentrations. The
16
17 water-treated sample (negative control) was used for the ceramide profiling. The calculated
18
19 concentrations were then normalized using the mass of the extracted SC to obtain the final
20
21 ceramide content. Raw data processing was performed using Shimadzu LabSolutions™, while
22
23 subsequent and standard calculations were performed using Microsoft Excel as well as R.
24
25
26
27
28
29

30 31 2.11. Statistical Analysis

32
33 Three replicates (n = 3) were used to originate the data. Kruskal-Wallis test was used with
34
35 GraphPad Prism 8.0 to detect statistical differences (GraphPad Software Inc., La Jolla, CA, USA).
36
37 Different numbers of asterisks are used to indicate significant differences: * p < 0.05, ** p < 0.01,
38
39 and *** p < 0.001.
40
41
42
43

44 45 3. Results

46 47 3.1. Results on composition of SEs

48
49 LC-MS analysis revealed that all SE variants investigated are a mixture of mono-, di-, and
50
51 triesters of sorbitan with fatty acids. The ratio of the peak areas of mono- to di- to triesters is around
52
53 1.2 : 3.0 : 1.6 in all cases, with 19.1 % to 25.9 % monoesters, 49.8 % to 54.4 % diesters, and
54
55
56
57
58
59

1
2
3 24.3 % to 29.6 % triesters (Table 1). When the theoretical saponification values for the distribution
4
5 pattern obtained from peak area distribution are calculated, the values are 3 % to 17 % higher than
6
7 the measured saponification values according to the certificates of analysis.
8
9

10 The theoretical saponification values were calculated for all batches of the different SE variants
11
12 (based on the fatty acid composition assuming that these are exclusively sorbitan mono variants).
13
14 The calculated values are all below the real values found and also below the lower specification
15
16 limit (Table S1).
17
18

19 This confirms that a relevant fraction of di- and triesters must be present, but the values for these
20
21 species calculated from the peak areas may be too high. Potential explanations for this discrepancy
22
23 could be the presence of certain amounts of unesterified compounds (free sorbitan and anhydrides
24
25 of sorbitan and/or free fatty acids) or different ionization behavior of the mono-, di-, and triesters
26
27 in the mass spectrometric analysis. In future studies, further refinement of the analytical methods
28
29 is needed to obtain a precise understanding of the excipient's composition with regard to the ratio
30
31 of mono-, di-, and triesters. With the exception of SE 40, for which only palmitic acid could be
32
33 determined in relevant concentration, all other SE emulsifiers contain more than one fatty acid
34
35 species in relevant concentrations. In Figure 2 the composition of SE 60 (designation: sorbitan
36
37 monostearate) is shown. It shows the amount of similar contents of palmitic (C16) and stearic
38
39 (C18) acid. The absolute content of sorbitan monopalmitate (S16) and sorbitan monostearate (S18)
40
41 is around ten percent (Area %) for both. With regards to their peak area distribution, the S16_16
42
43 and the S18_18 diesters are both contained at around 15 %, and the mixed diester S16_18 at around
44
45 23 %. The uniformly composed triesters S16_16_16 and S18_18_18 are present at around 3 %,
46
47 whereas the two mixed triesters S16_16_18 and S16_18_18 are present at around 9 %. The
48
49 composition is in agreement with the Pharm. Eur. monograph “sorbitan stearate” which requires
50
51
52
53
54
55
56
57
58
59
60

40.0 % to 60.0 % of stearic acid and a sum of the contents of palmitic and stearic acids: minimum 90.0 % for sorbitan stearate (type I) ³⁶. Whereas Pharm. Eur. provides specifications of the fatty acid distribution for sorbitan stearate, sorbitan palmitate and sorbitan oleate, no specification of the ratios of mono-, di-, and triesters are given.

These findings provide important evidence for a better understanding of SE emulsifiers. They can all be considered of a mixture of species of different polarity and HLB values. SE 60 contains species with an HLB of 2.1 (sorbitan tristearate) to 6.7 (sorbitan monopalmitate) ³⁷ and can, therefore, be considered as a lipophilic complex emulsifier.

Table 1. Distribution for mono-, di-, and triesters of different Span variants (Peak area %)

Emulsifier name	Nominal composition	Sum of monoesters	Sum of diesters	Sum of triesters
SE 40	sorbitan monopalmitate	19.1	51.3	29.6
SE 60	sorbitan monostearate	19.7	54.4	25.9
SE 80	sorbitan monooleate	20.0	52.0	28.0
SE 120	sorbitan monoisostearate	25.9	49.8	24.3

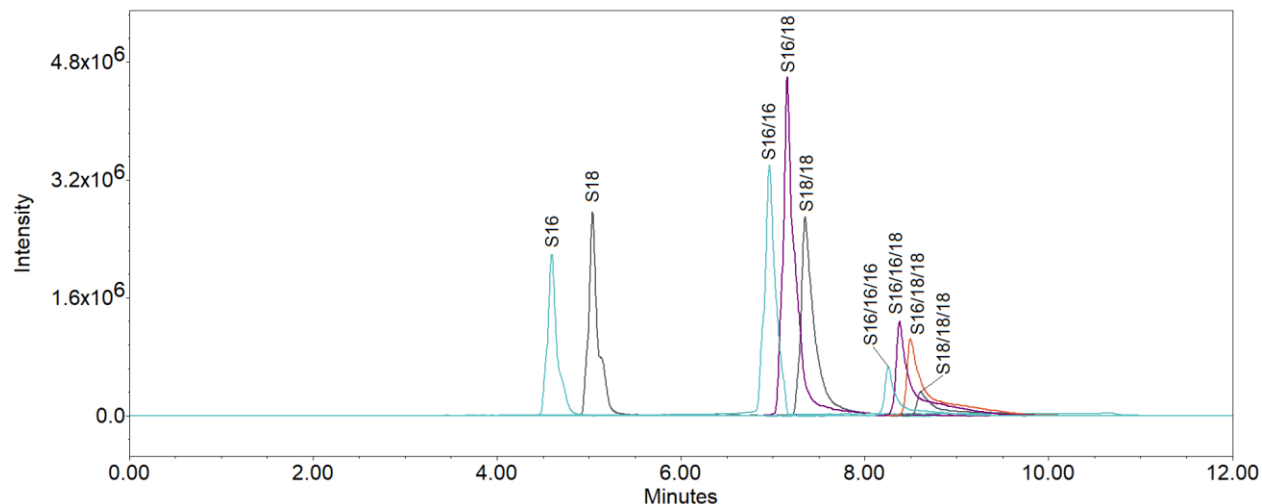
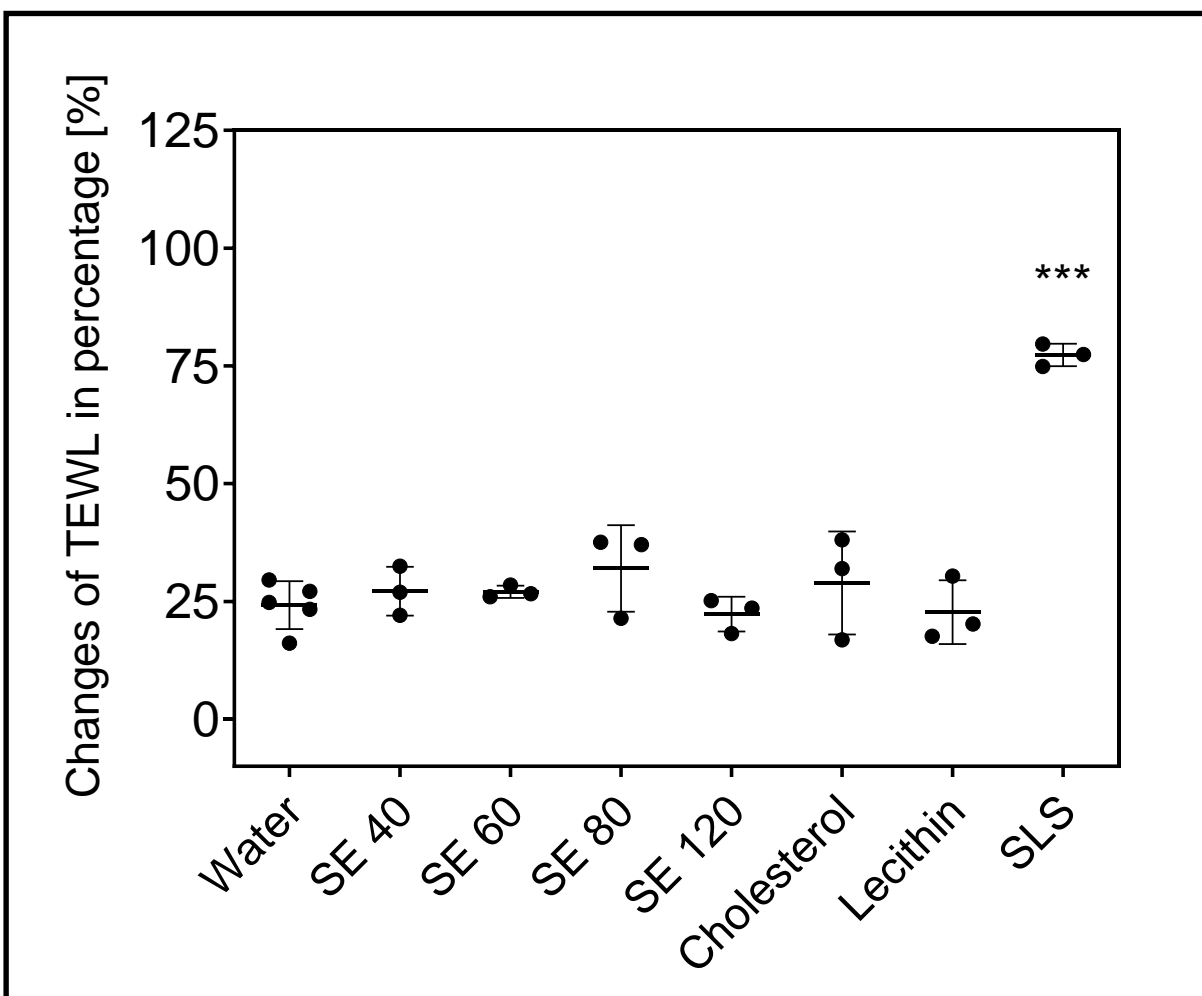


Fig. 2. Spectrum of SE 60 with intensity over time: first S16 and S18 as monoesters, second S16/16, S16/18, and S18/18 as diesters, and third S16/16/16, S16/16/18, S16/18/18, and S18/18/18 as triesters.

3.2. TEWL results

The TEWL is not just a value to describe the skin barrier function. It is also a kind of quality control for the utilized skin samples in ex vivo experiments. According to the EMA draft guideline on quality and equivalence of topical products³⁸ before any experiment, one should check for skin damage or other parameters that might influence the results. We investigated the TEWL change after incubation of skin samples with emulsifier solutions/dispersions to elucidate their impact on the skin barrier function and possible damage thereof. Figure 3 shows the results of the TEWL measurements. As expected, SLS as the positive control, showed significantly increased TEWL values compared to the water-treated sample used as negative control (23 vs. 77 g m⁻²·h⁻¹). SLS is well-known as skin disruptive³⁹ and already showed strongly increased TEWL values in previous experiments²². The TEWL change as a result of treatment with SEs, cholesterol, and lecithin was

1
2
3 not significant compared to the water treated sample. Our previous research had shown that many
4 o/w-emulsifiers impair the skin barrier *ex-vivo*. Also, some w/o-emulsifiers (e.g., glycerol
5 monostearate), were found to impair the skin barrier function while most did not (e.g., PEG-2-fatty
6 alcohol ethers, cetostearyl alcohol). The current results confirm the expectation that w/o-
7 alcohol ethers, cetostearyl alcohol). The current results confirm the expectation that w/o-
8 emulsifiers are not as prone to affect the skin barrier function as o/w-emulsifiers are ^{11,17,18,22,40,41}.
9
10 Lecithin was also shown by other research ^{42,43} to be a mild emulsifier, which was again confirmed
11 herein.
12
13
14
15
16
17
18
19
20
21
22



1
2
3 **Fig. 3.** TEWL measurements of emulsifiers with water as negative control and SLS as positive
4 control. Results are shown as the change of TEWL in percentage. Emulsifiers SE 40, SE 60, SE
5 80, SE 120, cholesterol, and lecithin are in between, in which only SLS showed significant
6 negative effects. Mean \pm SD, $n \geq 3$. * $p < 0.05$, ** $p < 0.01$, *** $p < 0.001$.
7
8
9
10
11
12
13
14

15 3.3. CRS results

16
17 The lipid content was determined in the fingerprint region by lipid signals normalized to the
18 amide-I-mode. Our antecedent research described this method in detail ^{11,17,28}. In Figure 4a the
19 results are shown. SLS was, as the positive control, the most different from the negative control
20 (water) (***) $p < 0.001$) followed by SE 40 and SE 60. Also significantly decreased were the lipids
21 contents of skin samples treated with SE 80 and lecithin. SE 120 and cholesterol did not
22 significantly decrease the lipids contents and behaved like the negative control ¹¹. It should also
23 be noted that results from emulsifier-treated samples gave higher variability than samples treated
24 with the positive or negative control. This is an effect that has already shown up in previous
25 research and seems to be linked to partial extraction of the lipids ^{11,17,18,41}.
26
27
28
29
30
31
32
33
34
35
36
37

38 With respect to the lipids, increased values of the trans-gauche-ratio show a conformation
39 change, which leads to lower resistance of the SC against xenobiotics ^{24,33}. The results of the lipid
40 conformation, analysis are shown in Figure 4b. Here, SLS significantly increased the trans-gauche-
41 ratio and thus the disorder of lipids. All tested emulsifiers did not yield significantly different
42 results compared to the negative control. Interestingly, SE 80 and cholesterol-treated skin samples
43 gave higher variability than other emulsifier-treated samples. This is an interesting finding, as
44 previous research had shown that emulsifiers that extracted lipids from the SC also induced a
45 higher degree of disorder, as reflected by an increased trans-gauche-ratio. A possible explanation
46
47
48
49
50
51
52
53
54
55
56
57
58
59
60

1
2
3 may be the low degree of lipid extraction by the currently investigated emulsifiers compared to
4 those previously investigated. Lipid extraction may be too low to result in significantly impaired
5 lipid conformation^{11,17}.
6
7
8
9

10 The thickness of the SC is another indicator of the effect of an emulsifier on the SC integrity.
11 After treatment with emulsifiers, the SC can get thinner, which leads to impaired skin barrier
12 function. Figure 4c shows that the thickness of SLS-treated SC was significantly decreased by 13
13 micrometers. The other emulsifiers did not affect SC thickness significantly. This complies with
14 the previous measurements which also showed no significant impact of the investigated
15 emulsifiers on SC lipids content and conformation.
16
17
18
19
20
21
22
23
24
25
26
27
28
29
30
31
32
33
34
35
36
37
38
39
40
41
42
43
44
45
46
47
48
49
50
51
52
53
54
55
56
57
58
59
60

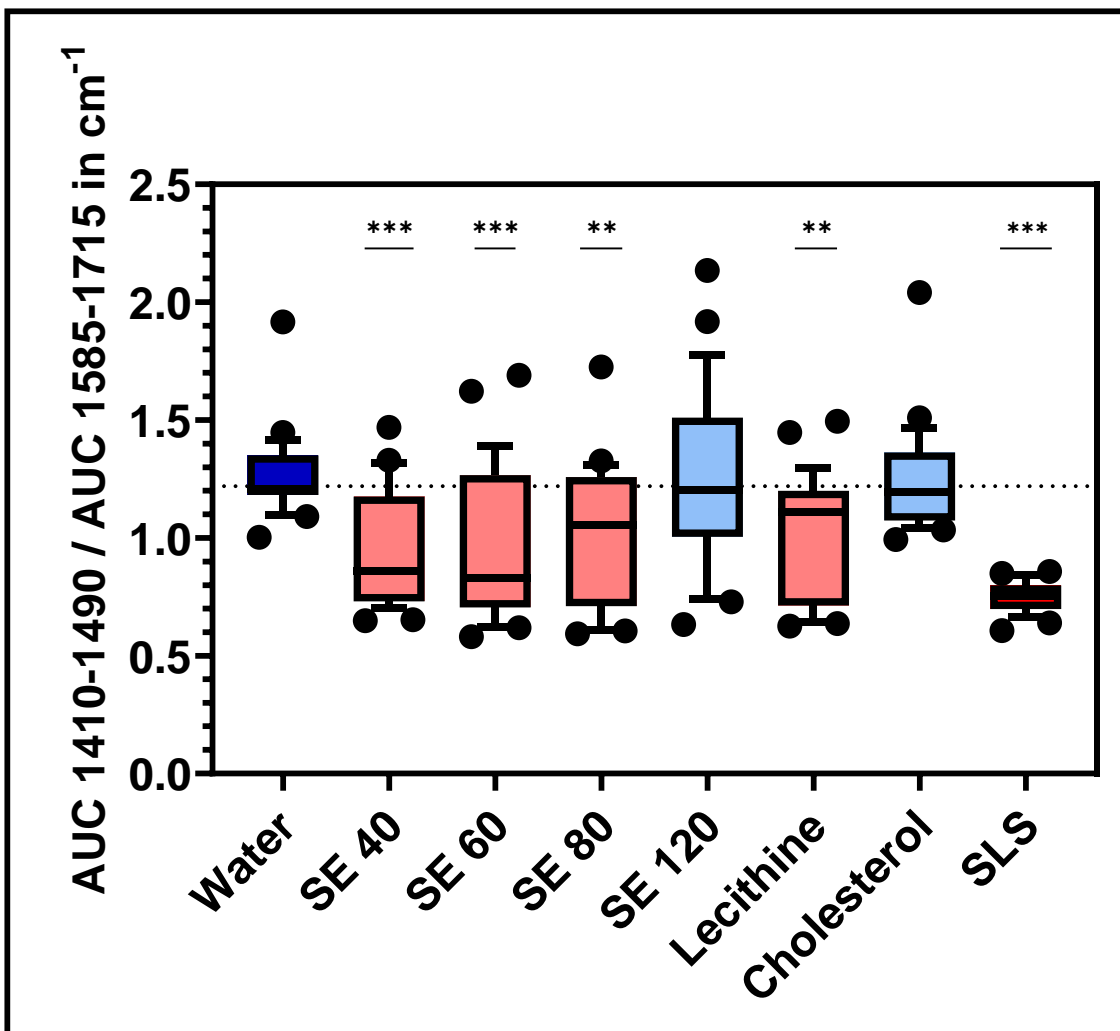


Fig. 4a. CRS fingerprint lipid content measurements of emulsifiers with water as negative control and SLS as positive control. Emulsifiers SE 40, SE 60, SE 80, SE 120, cholesterol, and lecithin are in between, in which all emulsifiers except SE 120 and cholesterol showed significant negative effects. Mean \pm SD, $n \geq 3$. * $p < 0.05$, ** $p < 0.01$, *** $p < 0.001$.

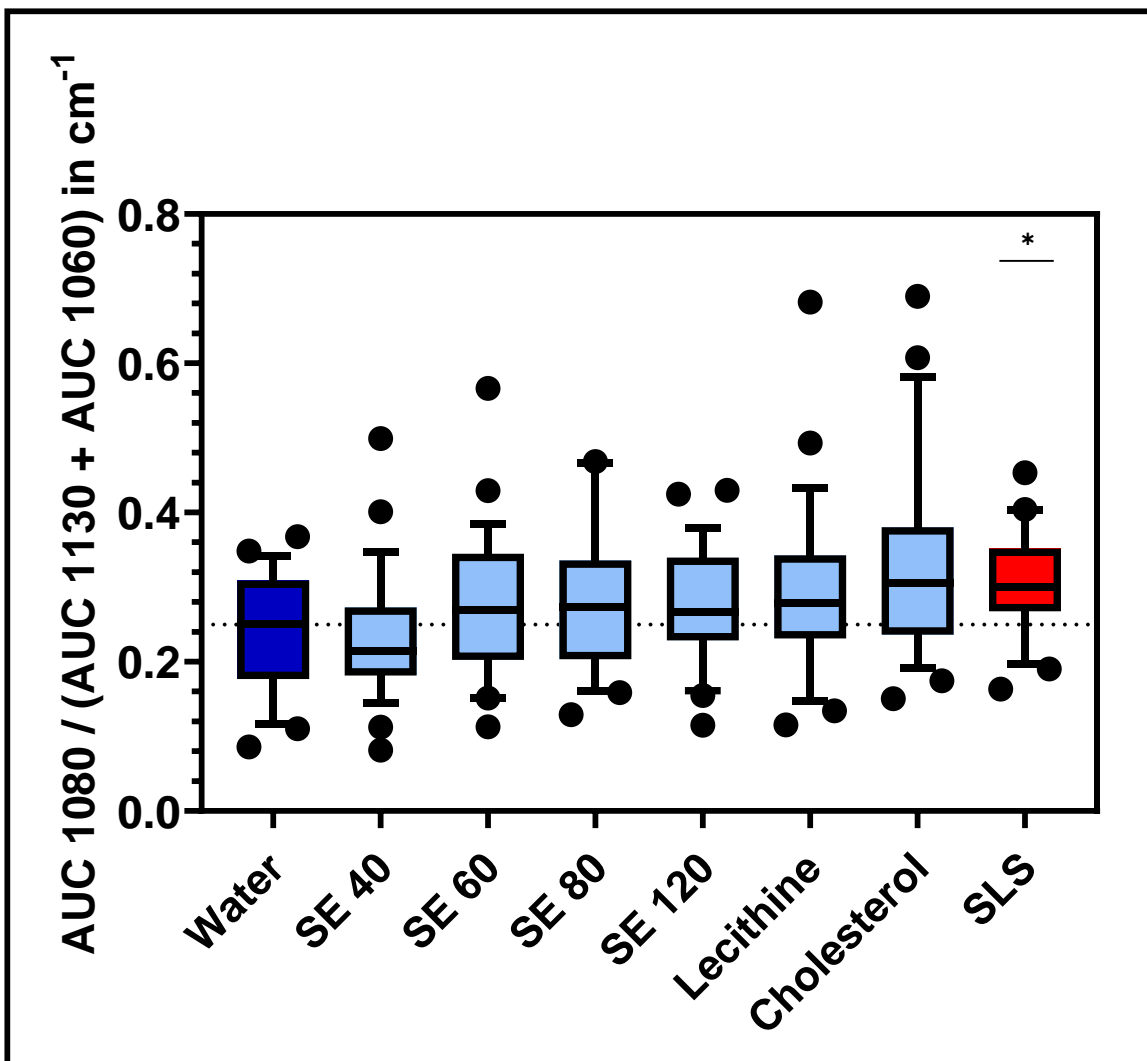


Fig. 4b. CRS trans-gauche-ratio lipid conformation measurements of emulsifiers with water as negative control and SLS as positive control. Emulsifiers SE 40, SE 60, SE 80, SE 120, cholesterol, and lecithin are in between, in which only SLS showed a significant negative effect by a higher ratio value. Mean \pm SD, $n \geq 3$. * $p < 0.05$, ** $p < 0.01$, *** $p < 0.001$.

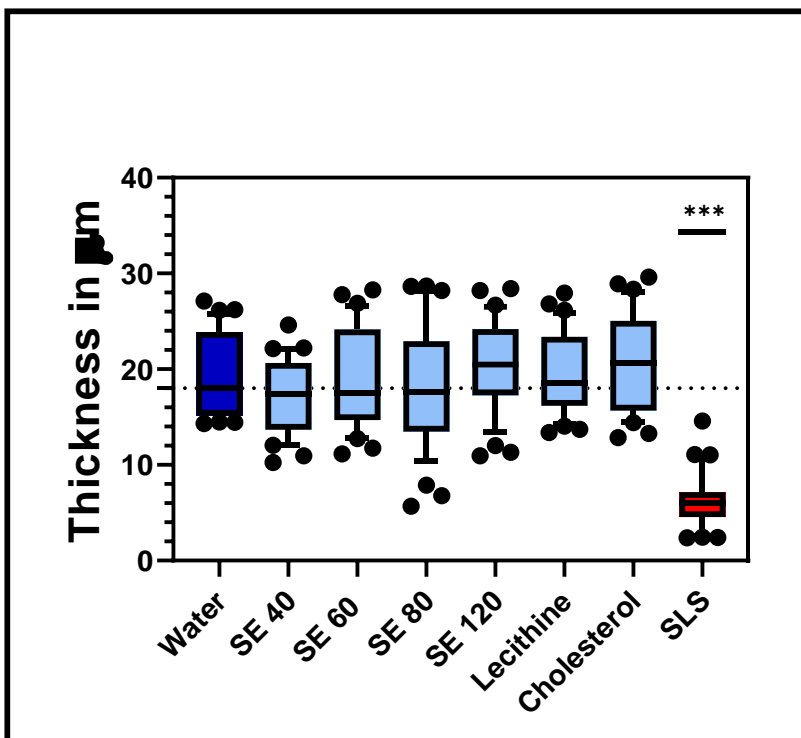


Fig. 4c. DUALSCOPE® FMP20 SC thickness measurements of emulsifiers with water as negative control and SLS as a positive control. Emulsifiers SE 40, SE 60, SE 80, SE 120, cholesterol, and lecithin are in between, in which only SLS showed significant negative effects. Mean \pm SD, $n \geq 3$. * $p < 0.05$, ** $p < 0.01$, *** $p < 0.001$.

3.4. LC-MS results

The analysis of the skin's ceramide content yielded a clear relative lipid class and chain length distribution as seen in Table 2. The lipophilic ceramide classes NS as well as NDS were found to be the most abundant ceramide classes present in porcine skin, while the more hydrophilic ceramide classes NP and AP were only present in low quantities, contrasting sharply to human skin ceramide composition, where the hydrophilic ceramide classes containing phytosphingosine

1
2
3 (Overwhelmingly represented as ceramide class NP and AP) as well as hydroxysphingosine
4
5 (Overwhelmingly represented as ceramide class NH and AH) represent the most abundant
6
7 ceramide classes ^{20,35,44}. Of the ω -esterified ultra-long chain ceramide classes, the sphingosine-
8
9 containing EOS was the most abundant, although the detected quantity of EO-type ceramides in
10
11 general was very low. Regarding the chain length distribution, the most common chain length of
12
13 the regular ceramide classes is 16 carbon atoms, followed by 24 and 26 carbon atoms, respectively.
14
15 Again, this contrasts with the composition generally given for human skin, where C24 and C26
16
17 can be found as the most common chain lengths. For EO-type ceramides, the by far most abundant
18
19 ceramide chain length, comprising more than half of the measured ω -esterified ceramides, contains
20
21 30 carbon atoms, which mirrors the composition of human skin in this regard ^{20,35,44}. Consequently,
22
23 the composition of the ultra-long chain ceramides of the porcine skin, in ceramide class as well as
24
25 chain length distribution, shows much less difference to the human ultra-long chain ceramide
26
27 composition than the shorter chain length, non-esterified ceramides present in the skin.
28
29
30
31
32

33 The total ceramide content of the treated skin samples obtained from the LC-MS measurements
34
35 is pictured in Figure 5. The ceramide content is given as the relative proportion of ceramides
36
37 detected per mass of the SC of the water-treated sample. The only treatment showing a significant
38
39 reduction in total ceramide content compared to the water-treated control is the positive control
40
41 SLS. All other investigated emulsifiers showed no significant difference, confirming that no
42
43 ceramides were extracted from the SC.
44
45
46
47
48
49
50
51
52
53
54
55
56
57
58
59
60

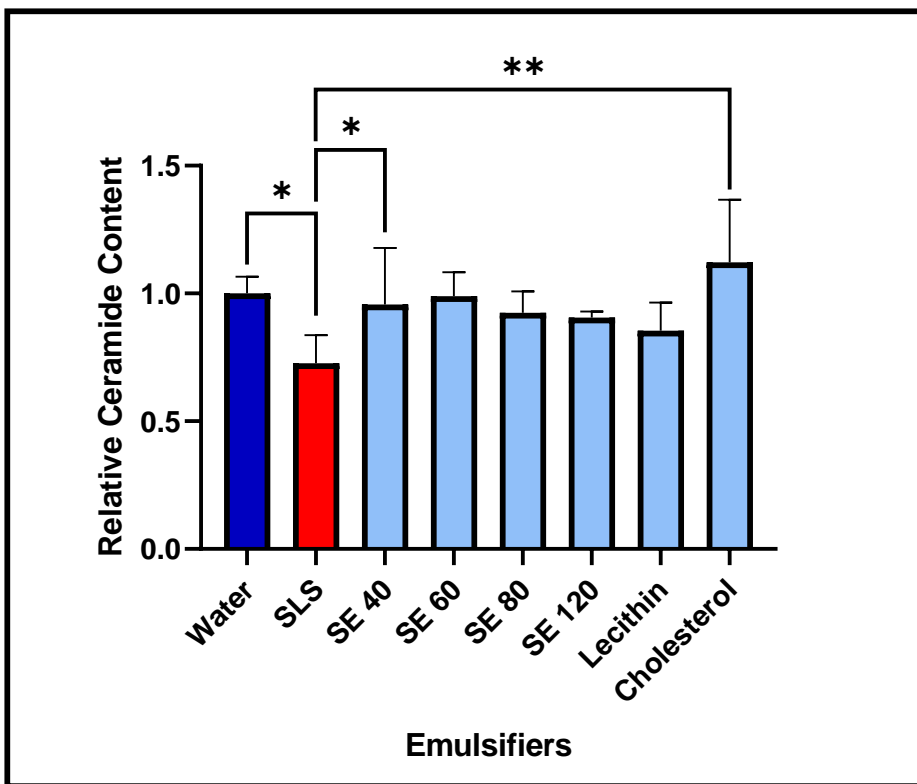


Fig. 5. LC-MS measurements of emulsifiers with water as negative control and SLS as a positive control showing the relative ceramide content. Emulsifiers SE 40, SE 60, SE 80, SE 120, cholesterol, and lecithin are in between, in which SLS showed significant negative effects. SE 60 and cholesterol showed significantly the lowest loss of ceramides referring to SLS. Mean \pm SD, $n = 3$. * $p < 0.05$, ** $p < 0.01$, *** $p < 0.001$.

Table 2. Relative abundances of ceramide species of the porcine SC. Relative abundance in the case of the ceramide chain lengths is calculated for ω -esterified ceramides and regular ceramides separately, as the measured range of ceramide chain length of the two groups differ. Asterisks denote chain lengths belonging to ω -esterified ceramides. Sphingosine- and dihydrosphingosine-based ceramide classes as well as chain lengths of 16, 24 and 26 carbon atoms dominate the picture for the regular ceramide classes. For ω -esterified ceramides, the most abundant ceramides are of the ceramide class EOS and contain 30 carbon atoms in their fatty acid chain.

Ceramide Class:	NS	N DS	A S	A D S	NP	A P	EO DS	E O S	EO P												
Relative Abundance in Percent by Weight:	37. 92	38. 08	8. 54	4. 2	5.9 9	4. 09	0.0 6	1. 11	0.0 1												
Ceramide Chain Length (Number of Carbon Atoms):	16	17	18	19	20	21	22	23	24	25	26	27	28	28 *	29 *	30 *	3 1 *	32 *	33 *	34 *	35 *
	32. 61	1.1 5	3. 82	0. 95	12. 18	1. 35	8.9 1	2. 62	18. 46	2. 45	8. 91	1. 07	5. 52	13. 42	6. 07	52. 99	6. 2	16. 96	1. 25	2. 94	0. 17

4. Discussion

SEs are among the most common w/o-emulsifiers in the field of pharmaceutically-used emulsifiers⁴⁵⁻⁴⁷. In our current research it was found, that the investigated SEs were all mixtures of mono-, di-, and triesters with an approximate ratio of 1.2 : 3.0 : 1.6 with regards to their peak area in the chromatogram. This is in contrast to their common designation as “sorbitan monoesters” and to the HLB values assigned to them which refer to the monoester³⁷ and demonstrates that all tested SEs consist of species of varying solubility properties and polarity, including the unpolar triesters for with HLB values around 2⁴⁸.

While in the USP the denomination “monoesters” is still used⁴⁹, the current English version 11 of Pharm. Eur. states only “sorbitan esters”³⁶. Monographs are available for sorbitan stearate, sorbitan palmitate which give no information and specification on the ratio between mono-, di-, and triesters. Therefore, it cannot be excluded, that the distribution patterns of the different esters varies between suppliers. Whereas the monoesters function primarily as w/o emulsifiers, the triesters may mix with oil phases of emulsion-type formulations. The less polar di- and triesters may also contribute to a favorable skin tolerability of this class of emulsifiers.

In the main part of this study, the SEs, together with the physiological emulsifiers of lecithin and cholesterol, were analyzed by a multimodal approach to achieve a thorough characterization of the impact of these emulsifiers on the porcine skin. This multimodal approach (TEWL, lipid order and ceramide content) further enabled for the first time a comparison of results derived from different methods without bias due to the use of different samples for each method. Looking at the TEWL results, the SEs proved to be skin-friendly, causing no skin barrier impairment. In this respect, they behaved similarly to lecithin and cholesterol, which also showed a high skin tolerability in the

1
2
3 TEWL measurements. Yet, CRS measurements showed emulsifier-treated skin sites having
4 significantly decreased lipid contents (except for SE 120 and cholesterol due to high variability),
5 while the lipid conformation was not affected. This conformation is an indicator of the lateral
6 packaging of lipids: lipids in orthorhombic order are more resistant to intrusion of xenobiotics and
7 thus provide a higher skin barrier function^{50,51}. The results from the TEWL measurements as well
8 as the CRS imply a mixed effect on the skin: While most of the tested emulsifiers decreased the
9 lipid content, they did not cause lipid conformation disordering, which correlates well with the
10 TEWL results implying an unimpaired skin barrier function of the treated sites. The information
11 about the lipid conformation state obtained from CRS may therefore be of higher significance for
12 investigating possible skin barrier impairment than the total lipid content measured: As stated
13 before, disordering of the skin lipid conformation is associated with a steep increase in skin barrier
14 permeability. Interestingly, the penetration-enhancing effect of the disordering of skin lipids is
15 even pronounced in certain nonionic emulsifiers such as Polysorbate 80, which show no lipid
16 depletion in CRS studies^{41,52}. The absence of lipid disordering effects of the investigated nonionic
17 emulsifiers in this study demonstrates the skin tolerability of these substances, which is further
18 substantiated by the thickness of the SC remaining constant after incubation with them. Adding to
19 these results, total ceramide content measured by LC-MS analysis showed that the total ceramide
20 content to not be significantly decreased after treatment with any of the investigated emulsifiers.
21 Only SLS as positive control lead to a statistically significant depletion of ceramides, as is typical
22 for this surfactant and seen in previous studies^{53,54}. For the investigated emulsifiers, these results
23 hint towards a disconnection between the lipid content determined by CRS and the ceramide
24 content determined by LC-MS. This could possibly be explained by depletion in fatty acids and
25 cholesterol rather than ceramides⁵⁵, which will be the subject of further studies. Nonetheless, the
26
27
28
29
30
31
32
33
34
35
36
37
38
39
40
41
42
43
44
45
46
47
48
49
50
51
52
53
54
55
56
57
58
59
60

1
2
3 neutral effect of the investigated emulsifiers on the ceramide content compared to the aggressive
4
5 positive control further qualifies the investigated emulsifiers as skin-friendly and suitable for use
6
7 in dermal products.
8
9

10 11 12 **5. Conclusion** 13

14 Emulsifiers that are used in topical formulations have to be examined for their safe use.
15
16 We found that all SEs investigated in this study, contrary to what their designations suggest, are
17
18 mixtures of mono-, di-, and triglycerides. Therefore, these compounds are mixtures of species of
19
20 different polarity which may have different functions in formulations. With the combination of
21
22 TEWL, CRS, and LC-MS a multimodal analysis was performed to describe their effects on the
23
24 skin. This study highlights the efficacy and usefulness of multimodal SC analysis by utilizing the
25
26 synergies offered by the combination of TEWL, CRS, and LC-MS analysis. The combination of
27
28 three completely different methods proved to be a versatile approach in the characterization of an
29
30 emulsifier's impact on the skin barrier function. This will facilitate the characterization of the
31
32 impact of emulsifiers or other excipients of topical formulations in the future. Furthermore, these
33
34 detailed investigations lead to the finding that SEs, as w/o-emulsifiers, are skin-friendly substances
35
36 and can be used for dermal formulations, e.g., those commonly used for the treatment of skin
37
38 diseases, with a low skin barrier-impairing potential comparable to lecithin and cholesterol,
39
40 physiologically occurring substances that are known to be mild emulsifiers. As pegylated
41
42 emulsifiers in particular have come increasingly under fire amidst health and sustainability
43
44 concerns in the general public, the SEs present a, PEG-free and skin friendly alternative. The
45
46 multimodal approach to skin barrier impact characterization can easily be adapted to in-vivo
47
48 analysis. requiring Only minor modifications to the LC-MS-ceramide quantification methodology
49
50
51
52
53
54
55
56
57
58
59
60

1
2
3 would be necessary. Also, regarding the CRS system, options for measurements on human skin in
4
5 vivo, are available which are associated with only a minor loss of data quality. Together, this
6
7 method combination can facilitate an approach towards development of non-irritating and in the
8
9 best case, barrier restoring formulations. In the future, an in-vivo study will support this ex-vivo
10
11 approach and investigate ex-vivo – in-vivo - correlation.
12
13
14
15

16 Statement of ethics

17
18 Porcine ears were obtained from a local butcher. The ears were acquired after the animal's death.
19
20 Before the study, the Department of Pharmaceutical Technology was registered with the District
21
22 Office of Tuebingen to utilize animal products (registration number: DE 08 416 1052 21).
23
24
25
26
27

28 Conflicts of interest

29
30 The authors have no conflicts of interest to report.
31
32
33
34
35
36
37
38
39
40
41
42
43
44
45
46
47
48
49
50
51
52
53
54
55
56
57
58
59
60

ASSOCIATED CONTENT

Supporting material

Table S1. Supporting material: Overview of experimental and calculated saponification values of different SE variants.

Emulsifier name	batch	Nominal composition	SV calculated for 100% sorbitan monoesters	Specification for SV	SV measured (CoA)	SV calculated from peak area distribution (mono/di/tri)	% of measured SV
SE 40	#0001767384	sorbitan monopalmitate	139.4	140 - 155	148.0	173.1	117.0
SE 60	#0001616251	sorbitan monostearate	134.6	147 - 157	150.0	165.2	110.2
SE 80	#0001959128	sorbitan monooleate	131.4	145 - 160	155.0	160.3	103.4
SE 120	#0001949925	sorbitan monoisostearate	131.0	140 - 158	151.0	157.3	104.2

Mean: 108.7

%RSD: 5.8

Table S2. Overview of ceramides by precursor ion, product ion, collision energy, and retention time.

Ceramide Species Name	Precursor m/z	Product m/z	Collision Energy (volts)	Retention Time (Min)
NS16	538.51	264.4	-29	8.86
NDS16	540.5	284.4	-29	9.05
NS17	552.53	264.4	-29	9.16
NDS17	554.5	284.4	-29	9.35
NS18	566.54	264.4	-29	9.43
NDS18	568.6	284.4	-29	9.63
NDS19	582.6	284.4	-29	9.9
NS19	580.56	264.4	-29	9.72
NS20	594.17	264.4	-30	10
NS21	608.19	264.4	-30	10.28
NS22	622.41	264.4	-30	10.55
NS23	636.22	264.4	-30	10.85
NS24	650.34	264.4	-30	11.13
NS25	664.25	264.4	-30	11.42
NS26	678.37	264.4	-30	11.72
NS27	692.38	264.4	-30	12.03
NS28	706.4	264.4	-30	12.32

NDS20	596.6	284.4	-25	10.2
NDS21	610.6	284.4	-25	10.46
NDS22	624.6	284.4	-25	10.74
NDS23	638.6	284.4	-25	11.03
NDS24	652.6	284.4	-25	11.33
NDS25	666.6	284.4	-25	11.63
NDS26	680.7	284.4	-25	11.92
NDS27	694.7	284.4	-25	12.22
NDS28	708.7	284.4	-25	12.53
NS16:1	518.5	264.4	-25	8.64
NS24:1	630.6	264.4	-25	10.56
NS26:1	658.7	264.4	-25	11.13
NDS16:1	538.51	284.4	-29	8.93
NDS24:1	650.34	284.4	-30	10.91
NDS26:1	678.37	284.4	-30	11.35
EODS28	987	284.4	-49	13.77
EODS29	1001	284.4	-49	13.9
EODS30:1	1012.97	284.4	-49	13.77
EODS32:1	1041	284.4	-49	14
EODS30	1014.97	284.4	-49	14
EODS31	1028.99	284.4	-49	13.95

EODS32	1043	284.4	-49	14.04
EODS32:1	1041	284.4	-49	13.88
EODS33	1057	284.4	-49	14.1
EODS34	1071.1	284.4	-49	14.33
EODS34:1	1069.1	284.4	-49	13.74
EODS35	1085.1	284.4	-49	14.23
EOS28	984.94	264.4	-49	13.77
EOS29	998.96	264.4	-49	13.87
EOS30	1012.97	264.4	-49	13.96
EOS31	1026.99	264.4	-49	14.05
EOS32	1041	264.4	-49	14.13
EOS33	1055.02	264.4	-49	14.21
EOS34	1069.03	264.4	-49	14.29
EOS35	1083.05	264.4	-49	14.38
EOS30:1	1011	264.4	-49	13.77
EOS32:1	1039	264.4	-49	13.95
EOS34:1	1067.1	264.4	-49	14.12
AP16	572.6	300.4	-27	8.35
AP16:1	570.6	300.4	-27	7.64
AP17	586.6	300.4	-27	8.61
AP18	600.6	300.4	-27	8.88

AP19	614.6	300.4	-27	9.17
AP20	628.6	300.4	-33	9.44
AP21	642.6	300.4	-33	9.73
AP22	656.7	300.4	-33	10.06
AP23	670.7	300.4	-33	10.31
AP24	684.7	300.4	-33	10.62
AP25	698.7	300.4	-33	10.89
AP26	712.7	300.4	-33	11.18
AP24:1	682.7	300.4	-33	10.04
AP26:1	710.7	300.4	-33	10.59
AP27	726.7	300.4	-33	11.48
AP28	740.8	300.4	-33	11.78
NP16	556.6	300.4	-28	8.56
NP16:1	554.6	300.4	-28	7.76
NP17	570.6	300.4	-28	8.86
NP18	584.6	300.4	-28	9.12
NP19	598.6	300.4	-28	9.4
NP20	612.6	300.4	-31	9.68
NP21	626.6	300.4	-31	9.98
NP22	640.7	300.4	-31	10.26
NP23	654.7	300.4	-31	10.55

NP24	668.7	300.4	-31	10.84
NP25	682.7	300.4	-31	11.14
NP26	696.7	300.4	-31	11.44
NP24:1	666.7	300.4	-31	10.28
NP26:1	694.7	300.4	-31	10.85
NP27	710.7	300.4	-31	11.72
NP28	724.8	300.4	-31	12.05
EOP28	1003	300.4	-49	13.67
EOP29	1017	300.4	-49	13.78
EOP30	1031	300.4	-49	13.88
EOP30:1	1029	300.4	-49	13.67
EOP31	1045	300.4	-49	13.96
EOP32	1059	300.4	-49	14.05
EOP32:1	1057	300.4	-49	13.87
EOP34	1087.75	300.4	-49	14.38
EOP34:1	1085.1	300.4	-49	14.2
EOP33	1073	300.4	-49	14.3
EOP35	1101.1	300.4	-49	14.51
AS16	554.51	264.4	-28	8.67
AS17	568.52	264.4	-28	8.94
AS18	582.54	264.4	-28	9.2

AS19	596.55	264.4	-28	9.47
AS20	610.27	264.4	-32	9.75
AS21	624.49	264.4	-32	10.03
AS22	638.3	264.4	-32	10.31
AS23	652.22	264.4	-32	10.59
AS24	666.23	264.4	-32	10.83
AS25	680.35	264.4	-32	11.15
AS26	694.36	264.4	-32	11.44
AS27	708.38	264.4	-32	11.74
AS28	722.39	264.4	-32	12.03
AS16:1	552.5	264.4	-28	7.96
AS24:1	664.6	264.4	-32	10.31
AS26:1	692.7	264.4	-32	10.85
ADS16	556.5	284.4	-29	8.8
ADS17	570.5	284.4	-30	9.17
ADS18	584.6	284.4	-30	9.34
ADS19	598.6	284.4	-30	9.62
ADS20	612.6	284.4	-35	9.88
ADS21	626.6	284.4	-35	10.18
ADS22	640.6	284.4	-35	10.47
ADS23	654.6	284.4	-35	10.76

ADS24	668.6	284.4	-35	11.05
ADS25	682.6	284.4	-35	11.36
ADS26	696.7	284.4	-35	11.66
ADS27	710.7	284.4	-35	11.96
ADS28	724.7	284.4	-35	12.28
ADS16:1	554.51	284.4	-28	8.59
ADS24:1	666.23	284.4	-32	10.49
ADS26:1	694.36	284.4	-32	11.02

*Correspondence:

Dominique Jasmin Lunter, Department of Pharmaceutical Technology, Faculty of Science,
Eberhard Karls Universität Tübingen, Auf der Morgenstelle 8, 72076 Tuebingen, Germany

E-mail: dominique.lunter@uni-tuebingen.de

Tel: +49-7071-297-2462

Funding Sources

No funding was obtained.

References

- 1
2
3
4
5
6 (1) Tfaili, S.; Gobinet, C.; Josse, G.; Angiboust, J. F.; Manfait, M.; Piot, O. Confocal Raman
7 Microspectroscopy for Skin Characterization: A Comparative Study between Human Skin
8 and Pig Skin. *Analyst* **2012**, *137* (16), 3673–3682. <https://doi.org/10.1039/c2an16292j>.
- 9
10 (2) Jacobi, U.; Kaiser, M.; Toll, R.; Mangelsdorf, S.; Audring, H.; Otberg, N.; Sterry, W.;
11 Lademann, J. Porcine Ear Skin: An in Vitro Model for Human Skin. *Skin Research and*
12 *Technology* **2007**, *13* (1), 19–24. <https://doi.org/10.1111/j.1600-0846.2006.00179.x>.
- 13
14 (3) Pasparakis, M.; Haase, I.; Nestle, F. O. Mechanisms Regulating Skin Immunity and
15 Inflammation. *Nature Reviews Immunology*. Nature Publishing Group **2014**, pp 289–301.
16 <https://doi.org/10.1038/nri3646>.
- 17
18 (4) Bouwstra, J. A.; Helder, R. W. J.; El Ghalbzouri, A. Human Skin Equivalents: Impaired
19 Barrier Function in Relation to the Lipid and Protein Properties of the Stratum Corneum.
20 *Advanced Drug Delivery Reviews*. Elsevier B.V. August 1, **2021**.
21 <https://doi.org/10.1016/j.addr.2021.05.012>.
- 22
23 (5) Herbig, M. E.; Houdek, P.; Gorissen, S.; Zorn-Kruppa, M.; Wladykowski, E.; Volksdorf,
24 T.; Grzybowski, S.; Kolios, G.; Willers, C.; Mallwitz, H.; Moll, I.; Brandner, J. M. A
25 Custom Tailored Model to Investigate Skin Penetration in Porcine Skin and Its Comparison
26 with Human Skin. *European Journal of Pharmaceutics and Biopharmaceutics* **2015**, *95*,
27 99–109. <https://doi.org/10.1016/j.ejpb.2015.03.030>.
- 28
29 (6) Stella, A.; Bonnier, F.; Tfayli, A.; Yvergnaux, F.; Byrne, H. J.; Chourpa, I.; Munnier, E.;
30 Tauber, C. Raman Mapping Coupled to Self-Modelling MCR-ALS Analysis to Estimate
31 Active Cosmetic Ingredient Penetration Profile in Skin. *J Biophotonics* **2020**, *13*.
32 <https://doi.org/10.1002/jbio.202000136>.
- 33
34 (7) Kourbaj, G.; Gaiser, A.; Bielfeldt, S.; Lunter, D. Assessment of Penetration and Permeation
35 of Caffeine by Confocal Raman Spectroscopy in Vivo and Ex Vivo by Tape Stripping. *Int*
36 *J Cosmet Sci* **2023**, *45* (1), 14–28. <https://doi.org/10.1111/ICS.12820>.
- 37
38 (8) Krombholz, R.; Fressle, S.; Nikolić, I.; Pantelić, I.; Savić, S.; Sakač, M. C.; Lunter, D. Ex
39 Vivo–in Vivo Comparison of Drug Penetration Analysis by Confocal Raman
40 Microspectroscopy and Tape Stripping. *Exp Dermatol* **2022**, *31* (12), 1908–1919.
41 <https://doi.org/10.1111/EXD.14672>.
- 42
43 (9) Krombholz, R.; Fressle, S.; Lunter, D. Ex Vivo-In Vivo Correlation of Retinol Stratum
44 Corneum Penetration Studies by Confocal Raman Microspectroscopy and Tape Stripping.
45 *Int J Cosmet Sci* **2022**, *44*, 299–308. <https://doi.org/10.1111/ics.12775>.
- 46
47 (10) Vater, C.; Apanovic, A.; Riethmüller, C.; Litschauer, B.; Wolzt, M.; Valenta, C.; Klang, V.
48 Changes in Skin Barrier Function after Repeated Exposition to Phospholipid-Based
49 Surfactants and Sodium Dodecyl Sulfate in Vivo and Corneocyte Surface Analysis by
50 Atomic Force Microscopy. *Pharmaceutics* **2021**, *13* (4).
51 <https://doi.org/10.3390/pharmaceutics13040436>.
- 52
53
54
55
56
57
58
59
60

- 1
2
3 (11) Liu, Y.; Lunter, D. J. Systematic Investigation of the Effect of Non-Ionic Emulsifiers on
4 Skin by Confocal Raman Spectroscopy—a Comprehensive Lipid Analysis. *Pharmaceutics*
5 **2020**, *12* (3). <https://doi.org/10.3390/pharmaceutics12030223>.
6
7 (12) Kendall, A. C.; Kiezel-Tsugunova, M.; Brownbridge, L. C.; Harwood, J. L.; Nicolaou, A.
8 Lipid Functions in Skin: Differential Effects of n-3 Polyunsaturated Fatty Acids on
9 Cutaneous Ceramides, in a Human Skin Organ Culture Model. *Biochim Biophys Acta*
10 *Biomembr* **2017**, *1859* (9), 1679–1689. <https://doi.org/10.1016/j.bbamem.2017.03.016>.
11
12 (13) Vavrova, K.; Kovačik, A.; Opalka, L. Ceramides in the Skin Barrier. *European*
13 *Pharmaceutical Journal* **2017**, *64* (2), 28–35. <https://doi.org/10.1515/AFPUC-2017-0004>.
14
15 (14) Berkers, T.; Visscher, D.; Gooris, G. S.; Bouwstra, J. A. Topically Applied Ceramides
16 Interact with the Stratum Corneum Lipid Matrix in Compromised Ex Vivo Skin. *Pharm Res*
17 **2018**, *35* (48). <https://doi.org/10.1007/s11095-017-2288-y>.
18
19 (15) Beddoes, C. M.; Gooris, G. S.; Barlow, D. J.; Lawrence, M. J.; Dalglish, R. M.; Malfois,
20 M.; Demé, B.; Bouwstra, J. A. The Importance of Ceramide Headgroup for Lipid
21 Localisation in Skin Lipid Models. *BBA-Biomembranes* **2022**, *1864*, 183886.
22 <https://doi.org/10.1016/j.bbamem.2022.183886>.
23
24 (16) Ge, F.; Sun, K.; Hu, Z.; Dong, X. Role of Omega-Hydroxy Ceramides in Epidermis:
25 Biosynthesis, Barrier Integrity and Analyzing Method. *Int. J. Mol. Sci* **2023**, *2023*, 5035.
26 <https://doi.org/10.3390/ijms24055035>.
27
28 (17) Zhang, Z.; Lunter, D. J. Confocal Raman Microspectroscopy as an Alternative Method to
29 Investigate the Extraction of Lipids from Stratum Corneum by Emulsifiers and
30 Formulations. *European Journal of Pharmaceutics and Biopharmaceutics* **2018**, *127*, 61–
31 71. <https://doi.org/10.1016/j.ejpb.2018.02.006>.
32
33 (18) Liu, Y.; Ilić, T.; Pantelic, I.; Savić, S.; Lunter, D. J. Topically Applied Lipid-Containing
34 Emulsions Based on PEGylated Emulsifiers: Formulation, Characterization, and Evaluation
35 of Their Impact on Skin Properties Ex Vivo and in Vivo. *Int J Pharm* **2022**, *626*, 122202.
36 <https://doi.org/10.1016/j.ijpharm.2022.122202>.
37
38 (19) Mojumdar, E. H.; Kariman, Z.; Van Kerckhove, L.; Gooris, G. S.; Bouwstra, J. A. The Role
39 of Ceramide Chain Length Distribution on the Barrier Properties of the Skin Lipid
40 Membranes. *Biochim Biophys Acta Biomembr* **2014**, *1838* (10), 2473–2483.
41 <https://doi.org/10.1016/j.bbamem.2014.05.023>.
42
43 (20) Van Smeden, J.; Boiten, W. A.; Hankemeier, T.; Rissmann, R.; Bouwstra, J. A.; Vreeken,
44 R. J. Combined LC/MS-Platform for Analysis of All Major Stratum Corneum Lipids, and
45 the Profiling of Skin Substitutes. *Biochim Biophys Acta Mol Cell Biol Lipids* **2014**, *1841*
46 (1), 70–79. <https://doi.org/10.1016/j.bbalip.2013.10.002>.
47
48 (21) Ilić, T.; Savić, S.; Pantelić, I.; Marković, B.; Savić, S. Development of Suitable Working
49 Protocol for in Vitro Tape Stripping: A Case Study with Biocompatible Aceclofenac-
50 Loaded Topical Nanoemulsions. *Symposium on Pharmaceutical Engineering Research*
51 *SPhERe* **2019**, 25–27. <https://doi.org/10.24355/dbbs.084-202001221146-0>.
52
53
54
55
56
57
58
59
60

- 1
2
3 (22) Schoenfelder, H.; Liu, Y.; Lunter, D. J. Systematic Investigation of Factors, Such as the
4 Impact of Emulsifiers, Which Influence the Measurement of Skin Barrier Integrity by in-
5 Vitro Trans-Epidermal Water Loss (TEWL). *Int J Pharm* **2023**, *638*, 122930.
6 <https://doi.org/10.1016/J.IJPHARM.2023.122930>.
7
8
9 (23) Tfayli, A.; Guillard, E.; Manfait, M.; Baillet-Guffroy, A. Raman Spectroscopy: Feasibility
10 of in Vivo Survey of Stratum Corneum Lipids, Effect of Natural Aging. *European Journal*
11 *of Dermatology* **2012**, *22* (1), 36–41. <https://doi.org/10.1684/EJD.2011.1507>.
12
13 (24) Choe, C.; Lademann, J.; Darvin, M. E. A Depth-Dependent Profile of the Lipid
14 Conformation and Lateral Packing Order of the Stratum Corneum in Vivo Measured Using
15 Raman Microscopy. *Analyst* **2016**, *141* (6), 1981–1987.
16 <https://doi.org/10.1039/c5an02373d>.
17
18 (25) Zhang, Z.; Lunter, D. J. Confocal Raman Microspectroscopy as an Alternative to
19 Differential Scanning Calorimetry to Detect the Impact of Emulsifiers and Formulations on
20 Stratum Corneum Lipid Conformation. *European Journal of Pharmaceutical Sciences*
21 **2018**, *121*. <https://doi.org/10.1016/j.ejps.2018.05.013>.
22
23 (26) Lunter, D. J. Determination of Skin Penetration Profiles by Confocal Raman
24 Microspectroscopy: Statistical Evaluation of Optimal Microscope Configuration. *Journal*
25 *of Raman Spectroscopy* **2017**, *48* (2), 152–160. <https://doi.org/10.1002/jrs.5001>.
26
27 (27) Lunter, D. J. How Confocal Is Confocal Raman Microspectroscopy on the Skin? Impact of
28 Microscope Configuration and Sample Preparation on Penetration Depth Profiles. *Skin*
29 *Pharmacol Physiol* **2016**, *29* (2), 92–101. <https://doi.org/10.1159/000444806>.
30
31 (28) Liu, Y.; Lunter, D. J. Selective and Sensitive Spectral Signals on Confocal Raman
32 Spectroscopy for Detection of Ex Vivo Skin Lipid Properties. *Transl Biophotonics* **2020**,
33 1–9. <https://doi.org/10.1002/tbio.202000003>.
34
35 (29) Kligman, A. M. Preparation of Isolated Sheets of Human Stratum Corneum. *Arch Dermatol*
36 **1963**, *88* (6), 702. <https://doi.org/10.1001/archderm.1963.01590240026005>.
37
38 (30) Liu, Y.; Lunter, D. J. Optimal Configuration of Confocal Raman Spectroscopy for Precisely
39 Determining Stratum Corneum Thickness: Evaluation of the Effects of Polyoxyethylene
40 Stearyl Ethers on Skin. *Int J Pharm* **2021**, *597*.
41 <https://doi.org/10.1016/j.ijpharm.2021.120308>.
42
43 (31) Bridges, T. E.; Houlne, M. P.; Harris, J. M. Spatially Resolved Analysis of Small Particles
44 by Confocal Raman Microscopy: Depth Profiling and Optical Trapping. *Anal Chem* **2004**,
45 *76* (3), 576–584. <https://doi.org/10.1021/ac034969s>.
46
47 (32) Liu, Y.; Lunter, D. J. Selective and Sensitive Spectral Signals on Confocal Raman
48 Spectroscopy for Detection of Ex Vivo Skin Lipid Properties. *Transl Biophotonics* **2020**,
49 No. May, 1–9. <https://doi.org/10.1002/tbio.202000003>.
50
51
52
53
54
55
56
57
58
59
60

- 1
2
3 (33) Williams, A. C.; Edwards, H. G. M.; Barry, B. W. Raman Spectra of Human Keratotic
4 Biopolymers: Skin, Callus, Hair and Nail. *JOURNAL OF RAMAN SPECTROSCOPY* **1994**,
5 *25*, 95–98. <https://doi.org/10.1002/jrs.1250250113>.
6
7 (34) Snyder, R. G.; Hsut, S. L.; Krimm, S.; Randall, H. M. Vibrational Spectp in the C-H
8 Stretching Region and the Structure of the Polymethylene Chain. *Spectrochimica Acta*
9 **1978**, *34*, 395–406.
10
11 (35) Kawana, M.; Miyamoto, M.; Ohno, Y.; Kihara, A. Comparative Profiling and
12 Comprehensive Quantification of Stratum Corneum Ceramides in Humans and Mice by
13 LC/MS/MS. *J Lipid Res* **2020**, *61* (6), 884–895. <https://doi.org/10.1194/jlr.ra120000671>.
14
15 (36) Council of Europe. *European Pharmacopoeia, 11th Ed.*, 11.0.; Council of Europe:
16 Strasbourg, **2022**; Vol. Sorbitan stearate.
17
18 (37) Sheskey, P. J.; Hancock, B. C.; Moss, G. P.; Goldfarb, D. J. *Handbook of Pharmaceutical*
19 *Excipients*, 9th ed.; Pharmaceutical Press: London, England, **2020**.
20
21 (38) Medicines Agency, E. *Draft Guideline on Quality and Equivalence of Topical Products*;
22 **2018**. www.ema.europa.eu/contact.
23
24 (39) Törmä, H.; Lindberg, M.; Berne, B. Skin Barrier Disruption by Sodium Lauryl Sulfate-
25 Exposure Alters the Expressions of Involucrin, Transglutaminase 1, Profilaggrin, and
26 Kallikreins during the Repair Phase in Human Skin in Vivo. *Journal of Investigative*
27 *Dermatology* **2008**, *128* (5), 1212–1219. <https://doi.org/10.1038/sj.jid.5701170>.
28
29 (40) Liu, Y.; Lunter, D. J. Confocal Raman Spectroscopy at Different Laser Wavelengths in
30 Analyzing Stratum Corneum and Skin Penetration Properties of Mixed PEGylated
31 Emulsifier Systems. *Int J Pharm* **2022**, *616*, 121561.
32 <https://doi.org/10.1016/j.ijpharm.2022.121561>.
33
34 (41) Liu, Y.; Lunter, D. J. Profiling Skin Penetration Using PEGylated Emulsifiers as Penetration
35 Enhancers via Confocal Raman Spectroscopy and Fluorescence Spectroscopy. *European*
36 *Journal of Pharmaceutics and Biopharmaceutics* **2021**, *166*, 1–9.
37 <https://doi.org/10.1016/j.ejpb.2021.04.027>.
38
39 (42) Vater, C.; Bosch, L.; Mitter, A.; Göls, T.; Seiser, S.; Heiss, E.; Elbe-Bürger, A.; Wirth, M.;
40 Valenta, C.; Klang, V. Lecithin-Based Nanoemulsions of Traditional Herbal Wound
41 Healing Agents and Their Effect on Human Skin Cells. *European Journal of Pharmaceutics*
42 *and Biopharmaceutics* **2022**, *170*, 1–9. <https://doi.org/10.1016/j.ejpb.2021.11.004>.
43
44 (43) Vater, C.; Hlawaty, V.; Wardenits, P.; Cichoń, M. A.; Klang, V.; Elbe-Bürger, A.; Wirth,
45 M.; Valenta, C. Effects of Lecithin-Based Nanoemulsions on Skin: Short-Time Cytotoxicity
46 MTT and BrdU Studies, Skin Penetration of Surfactants and Additives and the Delivery of
47 Curcumin. *Int J Pharm* **2020**, *580*, 119209. <https://doi.org/10.1016/j.ijpharm.2020.119209>.
48
49 (44) Janssens, M.; Van Smeden, J.; Gooris, G. S.; Bras, W.; Portale, G.; Caspers, P. J.; Vreeken,
50 R. J.; Hankemeier, T.; Kezic, S.; Wolterbeek, R.; Lavrijsen, A. P.; Bouwstra, J. A. Increase
51 in Short-Chain Ceramides Correlates with an Altered Lipid Organization and Decreased
52
53
54
55
56
57
58
59
60

- Barrier Function in Atopic Eczema Patients. *J Lipid Res* **2012**, *53* (12), 2755–2766. <https://doi.org/10.1194/jlr.P030338>.
- (45) Liu, Y.; Binks, B. P. Fabrication of Stable Oleofoams with Sorbitan Ester Surfactants. *Langmuir* **2022**, *38* (48), 14779–14788. <https://doi.org/10.1021/acs.langmuir.2c02413>.
- (46) Fiume, M. M.; Bergfeld, W. F.; Belsito, D. V.; Hill, R. A.; Klaassen, C. D.; Liebler, D. C.; Marks, J. G.; Shank, R. C.; Slaga, T. J.; Snyder, P. W.; Gill, L. J.; Heldreth, B. Safety Assessment of Sorbitan Esters as Used in Cosmetics. *Int J Toxicol* **2019**, *38* (2_suppl), 60S–80S. <https://doi.org/10.1177/1091581819871877>.
- (47) Upadhyay, K. K.; Tiwari, C.; Khopade, A. J.; Bohidar, H. B.; Jain, S. K. Sorbitan Ester Organogels for Transdermal Delivery of Sumatriptan. <https://doi.org/10.1080/03639040701199266> **2008**, *33* (6), 617–625. <https://doi.org/10.1080/03639040701199266>.
- (48) Croda International Plc. https://www.crodapharma.com/en-gb/product-finder/product/5545-span_1_60_1_pharma#product-brochures-and-guides. https://www.crodapharma.com/en-gb/product-finder/product/5545-span_1_60_1_pharma#product-brochures-and-guides (accessed 2024-10-02).
- (49) United States Pharmacopeial Convention. *The United States Pharmacopeia, The National Formulary*, USP 43, NF 38.; United States Pharmacopeial Convention, **2019**; Vol. 1338–41–6.
- (50) Van Smeden, J.; Janssens, M.; Gooris, G. S.; Bouwstra, J. A. The Important Role of Stratum Corneum Lipids for the Cutaneous Barrier Function ☆. *BBA - Molecular and Cell Biology of Lipids* **2014**, *1841*, 295–313. <https://doi.org/10.1016/j.bbalip.2013.11.006>.
- (51) Bouwstra, J. A.; Ponc, M. The Skin Barrier in Healthy and Diseased State. *Biochimica et Biophysica Acta - Biomembranes*. December 2006, pp 2080–2095. <https://doi.org/10.1016/j.bbamem.2006.06.021>.
- (52) Moghadam, S. H.; Saliyaj, E.; Wettig, S. D.; Dong, C.; Ivanova, M. V.; Huzil, J. T.; Foldvari, M. Effect of Chemical Permeation Enhancers on Stratum Corneum Barrier Lipid Organizational Structure and Interferon Alpha Permeability. *Mol Pharm* **2013**, *10* (6), 2248–2260. <https://doi.org/10.1021/mp300441c>.
- (53) Takagi, Y.; Nakagawa, H.; Higuchi, K.; Imokawa, G. Characterization of Surfactant-Induced Skin Damage through Barrier Recovery Induced by Pseudoacylceramides. *Dermatology* **2005**, *211* (2), 128–134. <https://doi.org/10.1159/000086442>.
- (54) Imokawa, G. Surfactant-Induced Depletion of Ceramides and Other Intercellular Lipids: Implication for the Mechanism Leading to Dehydration of the Stratum Corneum. *Exogenous Dermatology* **2004**, *3* (2), 81–98. <https://doi.org/10.1159/000086158>.
- (55) Ananthapadmanabhan, K. P.; Mukherjee, S.; Chandar, P. Stratum Corneum Fatty Acids: Their Critical Role in Preserving Barrier Integrity during Cleansing. *International Journal of Cosmetic Science*. August **2013**, pp 337–345. <https://doi.org/10.1111/ics.12042>.

1
2
3
4
5
6
7
8
9
10
11
12
13
14
15
16
17
18
19
20
21
22
23
24
25
26
27
28
29
30
31
32
33
34
35
36
37
38
39
40
41
42
43
44
45
46
47
48
49
50
51
52
53
54
55
56
57
58
59
60